Arsenic Cellular Handling by Human Multidrug Resistance Protein 1 (MRP1/ABCC1) and MRP4 (ABCC4)

by

Brayden D. Whitlock

A thesis submitted in partial fulfillment of the requirements for the degree of

Doctor of Philosophy

Department of Physiology

University of Alberta

ABSTRACT

Arsenic is a proven human carcinogen to which hundreds of millions of people are chronically exposed at unsafe levels, primarily through contaminated drinking water. An environmentally ubiquitous metalloid, arsenic in different forms is currently being used therapeutically as an anti-cancer cytotoxic agent, and is in clinical trials to expand its uses. Understanding how the human body handles arsenic upon environmental and therapeutic exposures is thus crucial to both preventing and treating cancers. Arsenic is metabolized in cells to form methylated and other conjugated arsenicals. Multidrug resistance proteins, a group of membrane proteins belonging to the ATP-binding cassette transporter subfamily C (MRPs/ABCCs) have been demonstrated to transport these methyl and glutathione conjugated arsenicals, giving the proteins a potentially key role in the cellular efflux and eventual elimination of arsenic. Further, ABCC protein level correlates with cancer risk and chemotherapy outcomes. Studying the way ABCCs interact with arsenic can be done effectively *in vitro.* However, animal models are needed to understand their influence on toxicokinetics. In Chapter 3, this thesis examines species differences between mouse and human orthologues of ABCC4, a key urinary elimination pathway protein for arsenicals. First, the epitope of the M_4I-10 anti-ABCC4 antibody is mapped to determine that it can be used for inter-species work. Mouse Abcc4 is shown to not confer resistance to arsenicals in HEK293 cells and not transport DMA^V or $MMA(GS)_2$ in HEK293 membrane vesicles,

unlike its human counterpart ABCC4. However, mAbcc4 appears to be important in protecting mouse embryonic fibroblasts from arsenate, as MEFs with Abcc4 knocked out are more susceptible to arsenate toxicity. Understanding species differences allows for laboratory data developed in animal models to be more accurately and reliably translated to the clinic and to human populations exposed to arsenic at unsafe levels. Novel functions of ABCC1 are also reported and characterized in Chapters 4 and 5. In Chapter 4, ABCC1 is reported to both transport and confer resistance against the cytotoxicity of DMA^V in HEK293 but not HeLa cells. This cell line difference is not attributable to phosphorylation of Y920/S921 residues, unlike the HEK/HeLa cell line differences for $As(GS)_3$ transport. In Chapter 5, the protection from cytotoxicity of monomethylarsonic acid (MMA^V) conferred by ABCC1 in HEK293 cells but not HeLa cells is reported. Whole cell accumulation of MMA^V is characterized in HEK293 and HeLa cells stably transfected with ABCC1 and vector, showing that ABCC1 has a bigger impact in preventing accumulation of MMA^V in HEK cells, consistent with the cytotoxicity data. Using cytotoxicity, cellular accumulation, and vesicle transport experiments, this thesis advances the knowledge of how ABCC1 and ABCC4 proteins are involved in handling arsenic.

PREFACE

CHAPTER 1: INTRODUCTION

Chapter 1 uses portions of a book chapter published as: Whitlock, B. D., and Leslie, E. M. Efflux transporters in anti-cancer drug resistance: Molecular and functional identification and characterization of multidrug resistance proteins (MRPs/ABCCs). *Drug efflux Pumps in Cancer Resistance Pathways: From Molecular Recognition and Characterization to Possible Inhibition Strategies in Chemotherapy.* (15 November 2019) Elsevier. Permission from the publisher was obtained for the use of both the written portion and Figure 1.2.

CHAPTER 3: SPECIES DIFFERENCES FOR HUMAN AND MOUSE ABCC4/Abcc4

All experiments in Chapter three were conducted by the author with the following exceptions. Diane Swanlund made the stable HEK-mMrp4 cell lines (as referenced in Section 2.2.2) and completed some experiments contained in Table 3.1.

CHAPTER 4: MULTIDRUG RESISTANCE PROTEIN 1 (MRP1/*ABCC1*)-MEDIATED CELLULAR PROTECTION AND TRANSPORT OF METHYLATED ARSENIC METABOLITES DIFFERS BETWEEN HUMAN CELL LINES.

This chapter was published in Drug Metabolism and Disposition (August 2018, 46 (8) 1096-1105). Tables and figures have been renumbered to continue with the conventions of this thesis. BDW conducted experiments and contributed data only related to cytotoxicity studies, in Table 4.1 and Figure 1.4. Authorship attributions and acknowledgements are included at the end of the chapter, unchanged from the published form. Permission from the publisher was obtained for use in this thesis.

CHAPTER 5: CHARACTERIZATION OF ABCC1 CELLULAR PROTECTION AGAINST MMA^V

All experiments in Chapter 4 were conducted by the author with the exception of the HPLC-MS operation for the speciation studies, which was conducted by Xiufen Lu.

APPENDIX 1: INVESTIGATING BINDING SITES THROUGH INTERSPECIES CHIMERAS OF MOUSE/HUMAN ABCC4

All experiments in Appendix 1 were conducted by the author.

APPENDIX 2: RAT ABCC4: CYTOTOXICITY PROTECTION, TRANSPORT, AND BINDING SITE IMPLICATIONS

All experiments in Appendix 2 were conducted by the author. Diane Swanland screened clones for > 80% of cell populations expressing rMrp4 using FACS as referenced in section 2.2.2.

APPENDIX 3: ARSENIC SPECIES EFFLUXED FROM HEK293 CELLS AFTER EXPOSURE TO MMA^V

Appendix 3 contains the speciation data referred to in the Chapter 5 preface above. The experiments behind these data were all conducted by the author. Xiufen Lu contributed HPLC-MS expertise.

ACKNOWLEDGEMENTS

Some thanks are in order. My supervisor, Dr. Elaine Leslie, somehow dealt with a difficult and distracted PhD candidate by finding the perfect balance between flexibility and guidance. She was also the most thoughtful editor on earth and always extremely generous with her time. My supervisory committee, Dr. James Young and Dr. Xing-Zhen Chen, along with Elaine, gave me the special combination of guidance and freedom I needed to craft a scientific career that I love. I got lucky.

Dr. Mayukh Banerjee, Dr. Barbara Roggenbeck, Dr. Vanessa Marensi, Dr. Gurnit Kaur and Janet Zhou were as important and helpful to me while I was drinking tea as they were when I needed science help. Mayukh told me how I was wrong and how that was analogous to a behaviour observed in birds. Barb told me entertaining and relieving stories about how she was once far wronger. Vanessa told me how funny it was that I was wrong and then laughed with and at me. Gurnit told me that it was okay to be wrong and that it didn't make me a bad person. And Janet helped me appreciate that my wrongness isn't escapable and I might learn to live with it. Diane Swanlund, Xiufen Lu, and Dr. Denis Arutyunov solved more of my problems than I can count. Dr. Michael Carew kindly showed me my first cytotoxicity assay, and for that I will never forgive him. After considering the great contributions of these people to this work, I can hardly recall anything that I really added. Dr. X. Chris Le provided calm guidance that made my candidacy and chemistry more enjoyable than they had to be, and Dr. Andy Holt brought just the right amount of confrontational humour to my exam. Dr. Greg Funk provided equal parts great advice and great conversation in our far, far over-time meetings. These people made me a better scientist and person.

I doubt that Drs. Linda Chui, Xiaoli Lilly Pang, and Stephanie Smith appreciate how much impact their scientific and career guidance had on me during this degree program. I should send them a card. Michael Phair and Dr. Carolyn Sale forced me to become a more honest and uncompromising scholar with a series of conversations that I am sure they have forgotten but which meant the world to me, and which continue to inform my scientific practice today.

My other friends and my family put up with me and entertained my complaints and explanations. That they did not care about the answers didn't stop them from asking questions and waiting most patiently until I was finished answering. My mom was the first person in my family to write a thesis, so she lent me the support I didn't know I needed. My dad helped me profusely in countless ways. Matt Hodgson is owed particularly large thanks for doing both our jobs when I could do neither. So too are Kate, Kerri, Kyle, Maddy, Sia, Pam and Jeff for their terrific support, intellectual scrutiny, and listening. And, I could not have done this without Mike Myhovich.

Thank you.

TABLE OF CONTENTS

Contents

LIST OF ABBREVIATIONS

6-MP	6-mercaptopurine
ABC	ATP-binding cassette
ABCC	ATP-binding cassette, subfamily C; Multidrug Resistance Protein
ADP	Adenosine diphosphate
AQP	Aquaglyceroporin
As	Arsenic
As^{III}	Arsenite
As^{V}	Arsenate
As3MT	Arsenic (+3 oxidation state) methyltransferase
$As(GS)_3$	Arsenic triglutathione
ATP	Adenosine triphosphate
AZT	Azidothymidine
BCA	Bicinchoninic acid assay
BSA	Bovine serum albumin
BSO	Buthionine sulfoxamine
cAMP	Cyclic adenosine monophosphate
CFTR	Cystic fibrosis transmembrane regulator
cGMP	Cyclic guanosine monophosphate

CK	Creatine kinase
CL	Cytoplasmic loop
CP	Creatine phosphatase
DMA^{III}	Dimethylarsinous acid
DMA^{V}	Dimethylarsinic acid
DMDTA	Dimethyldithioarsinic acid
DMMTA	Dimethylmonothioarsinic acid
DMSO	Dimethyl sulfoxide
DNA	Deoxyribonucleic acid
$E_2$17βG	Estradiol-17β-glucuronide
ECL	Extracellular loop
EDTA	Ethylenediaminetetraacetic acid
FA	Folic acid
FACS	Fluorescence-activated cell sorting
FBS	Fetal bovine serum
G418	Geneticin
GLUT	Glucose transporter
$[GS2AsSe]^-$	Seleno-bis (S-glutathionyl) arsinium ion
GSSG	Glutathione disulfide
GSH	Glutathione

GST	Glutathione S-transferase
GSTO	Glutathione S-transferase omega
GSTP	Glutathione S-transferase pi
H69AR	Human small cell lung cancer, acquired resistance
HEK293	Human embryonic kidney
IARC	International Agency for Research on Cancer
ICP-MS	Inductively coupled plasma mass spectrometry
CL_0	N-terminus (cytosolic domain 1)
LTC_4	Leukotriene C_4
LTD_4	Leukotriene D_4
miRNA	micro RNA
MMA^{III}	Monomethylarsonous acid
MMA^{V}	Monomethylarsonic acid
$MMA(GS)_2$	Monomethylarsenic diglutathione
MMMTA	Monomethylmonothioarsonic acid
MOI	Multiplicity of infection
MRP	Multidrug resistance protein
MSD	Membrane spanning domain
MTS	(3-(4,5-dimethylthiazol-2yl)-5-(3-carboxymethoxyphenyl)-2-(4-sulfophenyl)-2Htetrazolium, inner salt
NADPH	Nicotinamide adenine dinucleotide

NBD	Nucleotide binding domain
PNP	Purine nucleoside phosphorylase
PMEA	9-(2-posphonylmethoxyethyl) adenine (adefovir)
RNS	Reactive nitrogen species
ROS	Reactive oxygen species
RR	Relative resistance: In cytotoxicity assays, the ratio of the concentrations of a substance that is required to kill 50% of cells in a cell line that does express the protein of interest vs a cell line that does not.
shRNA	Short hairpin RNA
siRNA	Small interfering RNA
SNP	Single nucleotide polymorphism
TM	Transmembrane helix
WHO	World Health Organization

LIST OF TABLES

4.2	Kinetic parameters of $MMA(GS)_2$ and DMA^V transport by MRP1 (and phosphorylation mutants)
5.1	Known arsenic-cytoprotective effects of ABCC1
5.2	Transport of Arsenic Species by ABCC1-enriched Membrane Vesicles Prepared from HEK293T or HeLa cells
5.3	Resistance of ABCC1- and vector- transfected HEK cells to inorganic and methylated arsenic species
A.2.1	Higher level rAbcc4 clone 1D4 confers resistance to As^V and MMA^V in stable HEK293 cells
A.2.2	Lower level rAbcc4 stable HEK293 clone 2D2 does not confer resistance to arsenicals.
A.2.3	Comparing cytotoxicity and transport data for human, rat, and mouse ABCC4/Abcc4.
A.2.4	All protein sequence differences between mAbcc4 and rAbcc4

LIST OF FIGURES

CHAPTER 1: INTRODUCTION

1.1 Arsenic

Approximately 94-220 million people worldwide are exposed to arsenic at levels above the World Health Organization limit of 10 ppb in their drinking water (Hubaux et al., 2013; Podgorski & Berg, 2020; WHO, 2012). A Group 1 (proven) human carcinogen, arsenic causes skin, lung, and bladder tumors (IARC, 2012). Arsenic poisoning of the population in Bangladesh has been called "the largest mass poisoning of a population in history" (Smith, Lingas and Rahman 2000). Arsenic is also associated with, among many other adverse health effects, infant mortality, impaired intellectual function, neuropathy, cardiovascular disease, endocrine dysregulation, and kidney and liver cancers (Naujokas et al. 2013). At more acute levels (0.15 mg/kg), arsenic is used to treat acute promyelocytic leukemia and is being investigated as a treatment for other cancers, including multiple myeloma and breast cancer (Duan et al., 2021; Hu et al., 2021; Khairul et al., 2017; Kritharis et al., 2013; Teva, 2018). As will be discussed in detail in Section 1.1.3, there are many mechanisms by which arsenic influences the cell, from direct protein binding and inhibition, to cell signaling interference, to cell damage through oxidative stress.

1.1.1 Arsenic exposure sources

Arsenic is an abundant element in the earth's crust, and is commonly present in complex with metals in rock formations all over the world (Garelick et al., 2008). When wells are dug to

find clean groundwater, the disruptive process can contribute to releasing arsenic from rock into the water. The levels in water are also dependent on complex factors like geothermal currents and volcanic activity (Garelick et al., 2008; Shankar et al., 2014). Mining is an anthropogenic source as it exposes workers and others nearby to arsenic that was previously buried, and other industrial sources of exposure can be found during coal-burning, wood preservation, glass-manufacturing, and electronics-manufacturing. Further, there are some foods that more readily bioaccumulate arsenic and can be significant exposure sources, including seafood and rice (IARC, 2012; Upadhyay et al., 2019; V et al., 2021).

1.1.2 Cellular influx of arsenic

Arsenic enters cells in the form of arsenate (As^{V}) through phosphate transporters, including the sodium/phosphate cotransporter Na^{+}/P_i-IIb (*SLC34A2*), and in the form of arsenite (As^{III}) through glucose transporters (GLUTs) and aquaglyceroporins (AQPs) (Mukhopadhyay et al., 2014; Roggenbeck et al., 2016; Villa-Bellosta & Sorribas, 2010). Important for tissue uptake after arsenic has been metabolized, methylated arsenic has been shown to enter cells through AQP9 (MMA^{III}, MMA^{V}, DMA^{V}) (Liu, 2010; McDermott et al., 2010); through GLUT1/*SLC2A1* (MMA^{III}) (Liu et al., 2006); and, through cysteine transporters xCT/*SLC7A11* and xAG/*SLC1A1* (DMA-Cys) (Garnier et al., 2014).

1.1.3 Arsenic toxicity and carcinogenicity

To get a sense of how arsenic can have harmful effects on the body, it is important to consider arsenic metabolism, and which chemical forms are prevalent. Although both As^{III} and

As^V can enter cells, most As^V is quickly reduced to As^{III} possibly with the help of purine nucleoside phosphorylase (PNP; reduces As^V *in vitro*), and/or glutathione transferase O1 (GSTO1; reduces As^V , MMA^V and DMA^V) (De Chaudhuri et al., 2008; Schläwicke Engström et al., 2007; Shi et al., 2004). Further *in vitro* evidence suggests that thiol-dependent reduction of As^V may be a common action of many enzymes via the creation of an arsenylated metabolite that is susceptible to reduction to As^{III} by a thiol such as glutathione (GSH), the ubiquitous cellular tripeptide γ-Glu-Cys-Gly (Gregus et al., 2009; Németi & Gregus, 2009a, 2009b). Arsenic (+3) methyltransferase (As3MT) facilitates the oxidative methylation of trivalent arsenic species into their corresponding pentavalent plus one methyl group. In rodents, and some bacteria and fungi, three methyl groups can be added, but humans only methylate to the dimethyl species except in the case of extremely high exposures (Koichi Kuroda et al., 2001; Li et al., 2018; Zhou & Xi, 2018). For a summary diagram see Fig. 1.1.

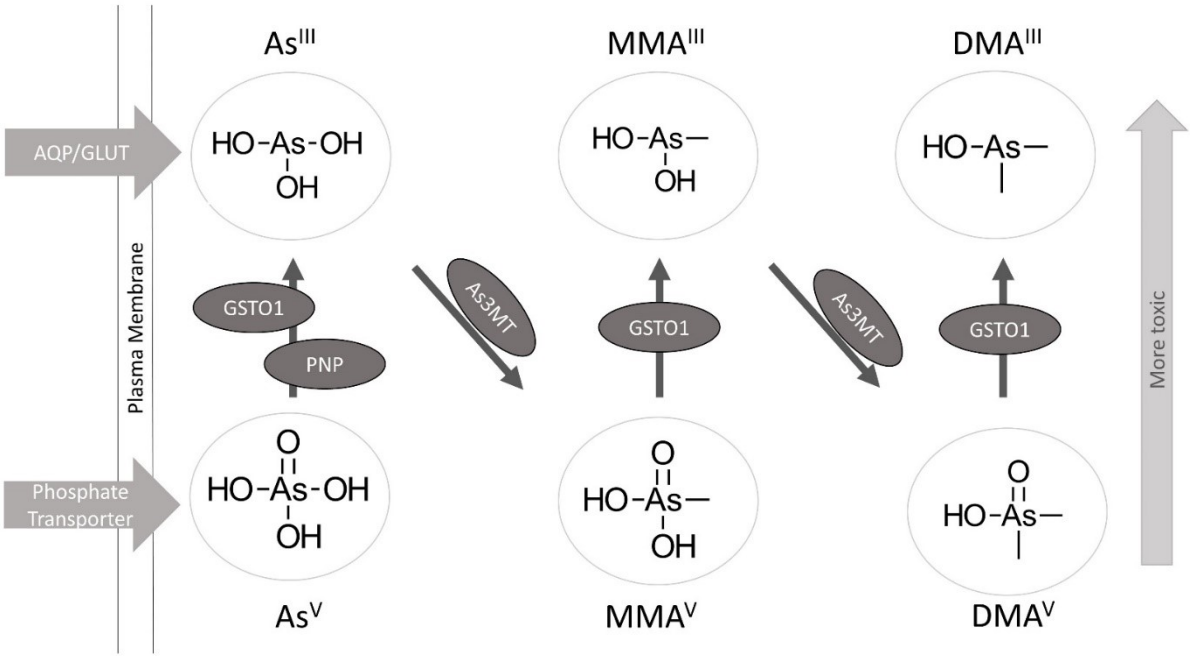

Figure 1.1. The uptake and metabolism of arsenic in mammalian cells. Reduction steps are done by glutathione transferase omega 1 (GSTO1) and purine nucleoside phosphorylase (PNP), and methylation is done by arsenite methyltransferase (As3MT).

In humans, arsenic is methylated inside cells via a multistep mechanism using predominantly one enzyme, AS3MT, to produce monomethylarsonous acid (MMA^{III}), monomethylarsonic acid (MMA^{V}), dimethylarsinous acid (DMA^{III}), and dimethylarsinic acid (DMA^{V}) (Cullen, 2014). Methylation of arsenic takes place primarily in the liver (Leslie 2012, Drobná et al. 2010). This is likely due to the first-pass nature of the hepatic circulation and the sheer size of the liver rather than the capacity of hepatocytes for methylation, as other tissue types (testes and kidney) show higher capacity per gram of tissue (Khairul et al., 2017).

Arsenic elimination occurs chiefly through the urine (60-80%), and most of this (~70%) is as DMA, with the remainder a mix of MMA and iAs (Loffredo et al. 2003, Vahter 2000). Further, the trivalent forms are more toxic than their pentavalent counterparts (Kligerman et al., 2003; Mass et al., 2001; Styblo et al., 2000).

Arsenate (As^{V})

Arsenate toxicity is largely due to its similarity to phosphate in a physiological context. Arsenate can replace phosphate and thereby interrupt a reaction in the process of ATP generation during glycolysis; it can also interfere with phosphate uptake, and generally inhibit phosphorylation through competition (Hughes 2002).

Other arsenicals

Aside from As^{v} effects, arsenic in its various forms generally causes toxicity in less direct ways, including through the formation of reactive oxygen species and reactive nitrogen species (ROS, RNS) during its metabolism, which are thought to be a major source of acute and

chronic toxicity including cancers (Shi, Shi and Liu 2004). The ROS are partially created by NADPH oxidase (Nox2), which is activated by As^{III} through a short signaling pathway, as part of what can be considered a stress-sensing system in cells. This has, among others, the ultimate effect of damaging the endothelium of vasculature and contributing to vascular disease (Ellinsworth 2015). The mechanism of arsenite neurotoxicity has also been established as at least partially reliant on oxidative stress, specifically through inhibiting the function of mitochondrial antioxidant enzymes (Prakash et al., 2016). Arsenic disulfide has been studied in mice and mouse cell lines, which showed that neurotoxicity was induced by arsenic-dependent activation of mitogen-activated protein kinases (Meng et al., 2021).

More generally, arsenic exposure has been found in numerous studies to cause an increase in ROS, majorly O_2^- and H_2O_2, in several mammalian and human cell systems (Shi et al. 2004). The diversity of arsenic-related maladies is likely at least partially rooted in the diversity of negative effects of ROS, which are well documented to cause damage to proteins, DNA, and lipids (Valko et al. 2007).

A more specific case of chronic toxicity is arsenic-induced carcinogenesis. The influence of arsenic on the development of cancer is still inadequately understood, but much has been learned in the last decade. Bustaffa et al. reviewed this area thoroughly in 2014 and have pointed out the complex and interconnected nature of the numerous ways in which arsenic leaves cells in a pro-cancer state. Arsenic's pro-cancer effects can be thought of as falling into four general categories:

Damage of large molecules

Arsenic readily binds to proteins largely due to its affinity for the sulfur found in cysteine, and this binding can alter the function of the proteins and even target them for degradation due to oligomerization and SUMOylation and/or ubiquitination (Liu et al., 2012; Shen et al., 2013). Arsenic also leads to the physical degradation of DNA and RNA molecules, which alone are often repairable, but in combination with other arsenic effects can be disease causing. The mechanism of DNA damage is largely through oxidative stress. Also, although arsenic is a poor mutagen, it has been shown to cause chromosomal mutations (Kligerman et al., 2003; Mandal, 2017; Mass et al., 2001) .

Inhibition of DNA repair

Arsenic can interfere with several proteins involved in DNA repair. The sensing of DNA damage relies on a protein that is inhibited by arsenic, thereby limiting the nucleotide excision repair (NER) pathway, and the ligation of DNA required for repair is also inhibited (Holcomb et al. 2017, Bustaffa et al. 2014(Ding et al., 2021).

Epigenetic promotion of tumor proliferation

Through modulating methylation and acetylation, arsenic can down-regulate tumor-suppression genes, and up-regulate oncogenes (Bustaffa et al., 2014). Arsenic can contribute to whole-body hypomethylation, by competing for methyltransferase enzymes and depleting S-adenosyl methionine (SAM), a cofactor that donates a methyl group for both arsenic methylation and DNA methylation (Bustaffa et al., 2014; Struck et al., 2012). Chronic arsenic exposure has also been linked to the hypermethylation with a putative overall pro-proliferation effect (Miao et al., 2015; Ren et al., 2011; Sage et al., 2017). The balance of these methylation

considerations and how they relate to arsenic carcinogenesis is currently being investigated and may partially depend on dose (Bustaffa et al. 2014, Sage et al. 2017).

Alteration of cell division mechanisms

Several effects of arsenic on the cell cycle have been discovered, and these could ostensibly increase the likelihood of cells becoming cancerous. Arsenic interferes with tubulin polymerization, a key process in mitosis, and influences telomere length, the maintenance of which is known to be a key way that tumour cells can become immortal (Bustaffa et al. 2014, Li et al. 2012).

1.2 Cellular Protection from Arsenic

Arsenicals are methylated as described above, but this does not fully explain the transformation that occurs to arsenic in the body. Thiolation and glutathione (GSH)-conjugation are also common. Upon exposure to inorganic arsenic, thiolated urinary metabolites have been found in animals, including humans (Wang et al., 2015). Raml et al. (2005, 2007) found thioarsenicals in human urine after people were exposed to arsenic in their drinking water, or to arsenic in the form of an arsenosugar (ribose derivative) which is a known form of dietary exposure (Raml et al., 2005; Raml et al., 2007). Thiolation does not seem to be a clear method of lowering the toxicity of arsenic, and indeed can increase the toxicity, but given its ability to affect tissue distribution, it may have a less direct protective effect (Naranmandura et al., 2011; Naranmandura et al., 2009; Wang et al., 2015).

Conjugation to GSH is another mechanism of arsenic handling that can affect its transport and toxicity. Trivalent arsenic, methylated or not, will readily form a conjugate with one or more GSH molecules (Leslie, 2012). However, while the GSH conjugate of DMA^{III} can be synthesized in vitro, it has never actually been found in biological samples. In contrast, $As(GS)_3$, $MMA(GS)_2$, and seleno-bis(S-glutathionyl) arsinium ion $[(GS)_2AsSe]^-$ have been identified in biological samples and are transported by membrane efflux transporters (described below), offering a clear explanation for how GSH can be involved in cellular protection(Cui et al., 2004; Gailer et al., 2002; Kala et al., 2004; Kala et al., 2000). Effluxing arsenic metabolites from the cell is another protective mechanism, in which a role is played by multidrug resistance proteins (ATP-binding cassette transporter, subfamily C; ABCCs) (Carew & Leslie, 2010; Carew et al., 2011; Leslie et al., 2004).

1.3 Multidrug Resistance Proteins (MRPs/ABCCs)

There are 48 members of the human ABC transporter superfamily divided into 7 subfamilies (A through G), based on their relative level of sequence homology (Dean, 2005). Many of these ABC transporters have been associated with resistance to multiple anti-cancer drugs in laboratory studies as well as correlative clinical studies. For example, ABCC1 overexpression is correlated with worse patient outcomes when treating neuroblastoma (Whitlock & Leslie, 2019). As mentioned above, several members of ABC subfamily C are established as transporters of multiple arsenic metabolites (Banerjee et al., 2014; Banerjee et al., 2018; Carew & Leslie, 2010; Carew et al., 2011; Kala et al., 2000; Roggenbeck et al., 2015).

In ABC subfamily C there are 12 functional protein members, including the cystic fibrosis transmembrane conductance regulator (CFTR/ABCC7) an ATP-dependent chloride channel, two sulfonylurea receptors (SUR1/ABCC8 and SUR2/ABCC9), and nine so-called multidrug resistance proteins (ABCC1-6,10-12). A thirteenth gene (ABCC13) was also identified, however, it does not encode a functional protein and is therefore considered a pseudogene (Annilo and Dean 2004).

The first identified and cloned "ABCC", ABCC1, was discovered in 1992 due to its overexpression in a doxorubicin selected small cell lung cancer cell line (H69AR) (Cole et al. 1992). The identification and cloning of ABCC1 facilitated the subsequent discovery and/or cloning of the other eight "ABCCs". ABCC2 was cloned in 1996 from rat liver, allowing the identification of the functionally well characterized "canalicular multi-specific organic anion transporter" deficient in the TR^- Wistar and Eisai hyperbilirubinemic rat (EHBR) Sprague Dawley rat strains, as well as humans with Dubin-Johnson syndrome (a mild form of conjugated hyperbilirubinemia) (Paulusma et al. 1996, Buchler et al. 1996). Partial sequences of ABCC3, ABCC4, and ABCC5 were reported in 1997, after mining of expressed sequence tag databases (Kool et al. 1997). ABCC6, ABCC10, ABCC11, and ABCC12 were cloned after identification in large scale human genome sequencing projects (Kool et al. 1999, Bera et al. 2001, Hopper et al. 2001, Tammur et al. 2001). Collectively, at least eight of these "ABCCs" are important in the cellular efflux of a chemically diverse array of endogenous and xenobiotic compounds, including anti-cancer drugs (Slot, Molinski and Cole 2011). The precise function of ABCC12 is still unclear, and it does not transport typical ABCC substrates (Ono et al., 2007). Recently,

ABCC12 has been found to play a role in bile duct formation and homeostasis (Pham et al., 2021).

1.3.1 Structure of ABCC proteins

Structurally, ABCCs can be divided into two classes, the "short" and the "long" (Figure 1.2.) The four "short" ABCCs (ABCC4, ABCC5, ABCC11, and ABCC12) have the typical mammalian ABC structure, with two polytopic membrane-spanning domains (MSD) (each composed of 6 transmembrane helices), and 2 cytosolic nucleotide binding domains (NBDs). The "long" ABCCs (ABCC1, ABCC2, ABCC3, ABCC6, and ABCC10) have a third MSD (MSD0) (composed of 5 transmembrane helices), the function of which is not fully understood, but has been implicated in dimerization and membrane trafficking (Yang, et al. 2010, Westlake et al. 2005, Bandler et al. 2008, Fernandez et al. 2002, Bakos et al. 2000).

The nucleotide binding domains are highly conserved throughout the ABC superfamily and consist of multiple motifs including the Walker A motif, which binds the α- and β-phosphates of ATP; a Walker B motif, responsible for supplying a glutamate residue critical for facilitating the nucleophilic attack of ATP by water; and an ATP-stabilizing ABC signature motif (Hollenstein, Dawson and Locher 2007, Locher 2016). The two NBDs are in close proximity, and arranged such that the Walker A motif from one NBD associates with the ABC signature motif from the other to form a functional unit (Hollenstein et al. 2007). In contrast with most ABC proteins, the two NBDs of ABCC proteins are functionally asymmetric, thus, the ATP-binding site in NBD1 has very low ATPase activity, but high ATP affinity, while

NBD2 has much higher ATPase activity (Jones and George 2014, Deeley et al. 2006, Hollenstein et al. 2007).

Here I will focus on two of these transporters, ABCC1 and ABCC4. ABCC1 is the major focus of Chapters 4 and 5 because of its substrate diversity and accompanying potential to affect toxicity of a variety of substances, especially its direct transport of methylated and GSH-conjugated arsenic. Thus, in learning about how ABCC1 performs its transport role and which substrates it interacts with, more can be understood about its implications in toxicity, carcinogenicity, and medical efficacy of a variety of drugs and compounds, including environmental and medicinal arsenic.

ABCC4 has been suggested as a key component of arsenic handling and elimination pathways (Banerjee 2014), and has growing evidence supporting clinical relevance to cancer biology, as discussed below. Less is known about substrate specificity and the potential corresponding clinical considerations than is known with ABCC1, but through work with knockout mice, *in vitro* transport assays, and some clinical expression-outcome correlation studies, the role of ABCC4 in detoxification at the cellular, tissue, and whole-body levels is becoming better understood.

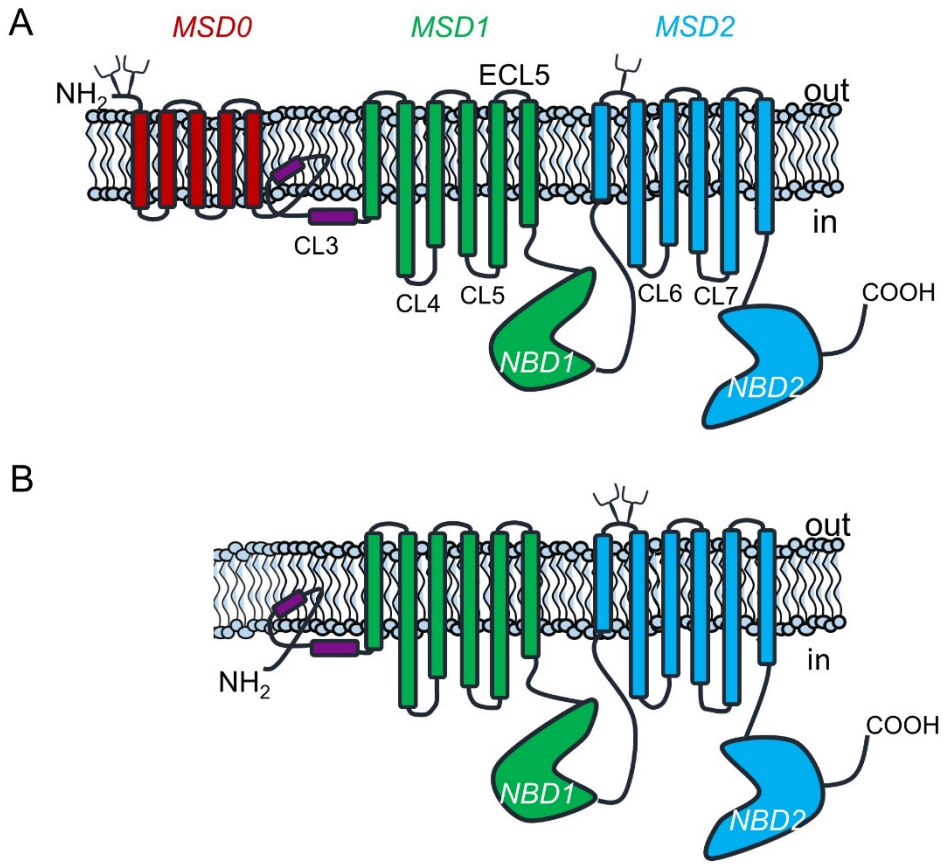

Figure 1.2. The topology of long and short ABCC proteins. A) ABCC1 with approximate helix length, which also represents the other "long" ABCCs: ABCC2, ABCC3, ABCC6, and ABCC10. (Johnson & Chen, 2018) B) ABCC4 with predicted helix length, which also represent the other "short" ABCCs: ABCC5, ABCC11, and ABCC12. *N*-glycosylation sites are shown on (A) for ABCC1 (N19, N23, and N1006), and on (B) for ABCC4 (N746 and N754). (Hipfner et al., 1997; Miah et al., 2016). CL: cytoplasmic loop. ECL: extracellular loop, MSD: membrane spanning domain, NBD: nucleotide binding domain. (from Whitlock and Leslie 2019, used with permission from publisher Elsevier)

1.3.2 Physiological ABCC1 Substrates

The current understanding of the physiological function of ABCC1 in humans is largely derived from *in vitro* experiments to determine endogenous molecules transported by human ABCC1, sometimes combined with *in vivo* evidence from investigations using *Abcc1*$^{-/-}$ mice. Much of the work has been reviewed (Cole 2014b, Cole 2014a). *In vitro*, ABCC1 can transport a chemically diverse array of endogenous molecules including lipid derived signaling molecules [e.g., leukotriene C_4 (LTC_4), prostaglandin (PG) E_2, GSH conjugates of PGA_2 and 15-deoxy-$\Delta(12,14)PGJ_2$ ($dPGJ_2$), lysophosphatidylinositol (LPI), sphingosine 1-phosphate (S1P)](de Waart et al., 2006; Evers et al., 1997; Leier et al., 1994; Paumi et al., 2003; Pineiro et al., 2011; Takabe et al., 2010). GSH conjugates of lipid peroxidation products (e.g., glutathione-4-hydroxy-2-nonenoic acid) (Renes et al. 2000), reduced and oxidized glutathione (GSH and GSSG) (Cole and Deeley 2006), conjugated steroids [e.g., 17β-estradiol 17-(β –D-glucuronide) ($E_2$17βG), estrone 3-sulfate ($E_1$3SO_4), dehydroepiandrostenedione] (Loe et al. 1996, Qian et al. 2001, Zelcer et al. 2003), unconjugated and glucuronide conjugated bilirubin (Rigato et al. 2004, Jedlitschky et al. 1997), folic acid (Zeng et al., 2001), vitamin B12 (cobalamin) (Beedholm-Ebsen et al., 2010), and nitric oxide (as GS-NO and possibly GS-Fe-NO) (Kovacevic et al., 2017).

Abcc1$^{-/-}$ mice are healthy and fertile and show no physical or histological differences compared to *Abcc1*$^{+/+}$ littermates, under normal conditions (Wijnholds et al., 1997). The pro-inflammatory mediator LTC_4 was identified as a high-affinity ABCC1 substrate using plasma membrane-enriched vesicle transport assays, shortly after the protein was discovered (Leier et

al. 1994). Consistent with a physiological role of ABCC1 as an LTC_4 transporter, *Abcc1*$^{-/-}$ mice had a reduced inflammatory response (Wijnholds et al. 1997). Furthermore, transport of LTC_4 by Abcc1 stimulates dendritic cell migration to lymph nodes in mice (Robbiani et al., 2000). LTC_4 highlights the best-characterized physiological substrate of ABCC1, although *in vitro* assays and studies with *Abcc1*$^{-/-}$ mice also provide evidence that Abcc1 plays an important role in cellular glutathione export and protecting tissues from anti-cancer drug and other chemical toxicity (Deng et al., 2015; Lorico et al., 1997; Tribull et al., 2003; Wijnholds et al., 1997; Zhang et al., 2015). Other investigations with Abcc1$^{-/-}$ mice suggest that Abcc1 could play a role in endothelial dysfunction during disease states such as diabetes and atherosclerosis (Jehle et al. 2017, Neuser et al. 2016).

1.3.3 ABCC1 and Glutathione

GSH is the most abundant cellular non-protein thiol, with cytosolic concentrations ranging from 0.1 to >10 mM (Meister, 1988). GSH is critical for cellular redox balance through its ability to neutralize free radicals. GSH can donate a reducing equivalent and form a disulfide bond with another oxidized GSH molecule (resulting in glutathione disulfide (GSSG) formation). GSH can also neutralize other electrophiles directly through GSH conjugate formation (GS-X) (Ballatori, Krance, Notenboom, et al., 2009). ABCC1 can export glutathione from cells in the form of GSH (by itself or in conjunction with other substrates), GSSG, and GS-X (Ballatori, Krance, Marchan, et al., 2009; Deeley & Cole, 2006). Export of GSSG and GS-X serves to reduce oxidized forms of glutathione in the cytosol and help maintain cellular redox balance. A balance between GSH synthesis, GSSG/GSH export, and enzymatic reduction

of GSSG in the cytosol exists, and excessive export of glutathione by ABCC1 can be detrimental to cell survival (Ballatori, Krance, Notenboom, et al., 2009; Mueller et al., 2005).

ABCC1 has at least three additional intriguing interactions with GSH. Firstly, certain compounds (e.g., the dietary flavonoid apigenin and the calcium channel antagonist verapamil) can markedly stimulate the transport of GSH, without being transported themselves (Leslie, et al. 2003, Loe et al. 2000). Secondly, GSH is required for (e.g., NNAL-O-glucuronide, dehydroepiandrostenedione) or enhances (e.g., estrone 3-sulfate, etoposide-glucuronide) the transport of certain conjugated compounds, without stimulation of GSH transport itself (Leslie, Deeley, et al., 2001; Peklak-Scott et al., 2005; Qian, Qiu, et al., 2001; Sakamoto et al., 1999; Zelcer et al., 2003). Lastly, GSH is required for the ABCC1-dependent cellular export of multiple anti-cancer drugs (e,g., vincristine, daunorubicin, and mitoxantrone) (Loe, 1998, Mao, 2000, Renes et al. 1999, Morrow et al. 2006). These drugs do not form GSH conjugates; however, they cause the stimulation of GSH export and thus a cross-stimulation or co-transport mechanism occurs (Cole 2014).

1.3.4 Localization and Expression of ABCC1

At the protein level, ABCC1 is found in specific cell types in most tissues with higher levels found in kidney, lung, blood-brain barrier, colon, placenta, skeletal muscle, skin, small/large intestine, and testes (Slot et al. 2011, Deeley et al. 2006). Notably, ABCC1 protein levels are usually not detected in healthy adult human hepatocytes, where the main ABCC transporter is ABCC2 (at the apical or canalicular surface) along with basolateral/sinusoidal

transporters ABCC3, ABCC4, and ABCC6 (Cole 2014b, Deeley et al. 2006, Keppler 2011, Keppler 2014).

In polarized epithelium, ABCC1 localizes almost exclusively to the basolateral (blood) surface while in capillary endothelium it has been found at both the luminal (e.g., capillaries of the blood brain barrier) and abluminal (e.g., capillaries of the placenta) membranes (Deeley et al. 2006, St.Pierre et al. 2000, Zhang et al. 2004, Nagashige et al. 2003, Grube, 2018).

1.3.5 Drug Substrates of ABCC1

Prior to the cloning of ABCC1 from the doxorubicin-selected small cell lung cancer cell line H69AR, H69AR cells were known to display high levels of resistance against multiple natural product type anti-cancer drugs relative to the unselected parental H69 cell line (Cole et al. 1992). These drugs included anthracyclines in addition to doxorubicin (e.g., daunomycin, epirubicin, menogaril, idarubicin), and the structurally related anthracenedione mitoxantrone (Mirski, Gerlach and Cole 1987, Cole 1990). Cross-resistance was also observed against the *Vinca* alkaloids vincristine and vinblastine, and the epipodophyllotoxin etoposide (Mirski et al. 1987). H69AR cells also displayed resistance to the antibiotic Gramicidin D, the γ-glutamyl transferase antagonist acivicin, and the toxic alkaloid colchicine (Mirski et al. 1987). In contrast, H69AR and H69 cells displayed equal levels of resistance against 5-fluorouracil, bleomycin, and platinum containing compounds (e.g., carboplatin) (Mirski et al. 1987).

Studies comparing cell line pairs stably transfected with ABCC1 cDNA and empty vector corroborated the direct involvement of ABCC1 in conferring resistance to the majority of the above-mentioned drugs (Cole et al. 1994, Grant et al. 1994, Morrow et al. 2006).

Furthermore, an additional drug-selected cell line and transfected pair revealed that ABCC1 was capable of conferring protection against camptothecin, CPT-11 (irinotecan, a water soluble camptothecin analog), and the CPT-11 activated metabolite SN-38 (Chen et al. 1999). This resistance was independent of GSH (Chen et al. 1999). ABCC1 has also been implicated in resistance to the camptothecin analog topotecan, although further corroboration and investigations of transport mechanism are required (Beretta et al. 2010, Jonsson et al. 1997).

ABCC1 confers resistance to the anti-cancer agent arsenic trioxide (arsenite under physiological conditions), and multiple methylated arsenic metabolites (Cole et al. 1994, Vernhet et al. 2001, Banerjee et al. 2018, Carew et al. 2011).

*In vitro t*ransport assays have shown that the anti-folate methotrexate is transported by ABCC1 (Hooijberg et al. 1999). Interestingly, ABCC1 only confers resistance to methotrexate during short term exposures due to the formation of polyglutamylated forms of methotrexate that are not transported by ABCC1 (Hooijberg et al. 1999, Zeng et al. 2001b). ABCC1 also transports the folate analogue leucovorin, which is administered either as an adjuvant to improve efficacy of 5-fluorouracil or to reduce bone marrow suppression by methotrexate (Zeng et al. 2001b).

The first-generation anti-androgen flutamide is used as part of a treatment regimen to inhibit androgen-dependent growth of prostate tumors (Crawford et al. 2018). ABCC1 reduced the accumulation of flutamide, and its active metabolite hydroxyflutamide, in cell lines over-expressing ABCC1 (after either drug selection or transfection) (Grzywacz et al. 2003). Prostate

tumors often become insensitive to anti-androgen therapy and increased levels of ABCC1 could contribute to this.

ABCC1 has been implicated in the resistance against "target-specific" therapeutics including tyrosine kinase inhibitors (Beretta et al. 2017). Furthermore, tyrosine kinase inhibitors have been shown to inhibit ABCC1 (along with other ABC transporters) and have been suggested as potential enhancers to conventional chemotherapeutic regimens (Beretta et al. 2017, Wu and Fu 2018). To date there is no direct evidence that ABCC1 directly transports tyrosine kinase inhibitors, however, multiple tyrosine kinase inhibitors (including imatinib, lapatinib, cediranib, ibrutinib, and vandetanib) have been shown to inhibit ABCC1-dependent efflux, resistance, and ATPase activity (Hegedus et al. 2002, Tao et al. 2009, Zheng et al. 2009, Zhang et al. 2014, Ma et al. 2014). Certain tyrosine kinase inhibitors have also been shown to shrink xenograft tumours derived from ABCC1-overexpressing cell lines when given in combination with conventional anti-cancer drugs (Zhang et al. 2014, Ma et al. 2014). The concentrations of tyrosine kinase inhibitor required to observe ABC transporter inhibition *in vitro* can be above clinically relevant levels, however, further investigations are warranted to determine if clinical benefits could be obtained through tyrosine kinase inhibitors combined with conventional therapy (Beretta et al. 2017, Wu and Fu 2018).

1.3.6 ABCC1 Structure

A combination of electron cryomicroscopy (cryo-EM) analysis of bovine Abcc1 (bAbcc1), and a variety of other techniques including cysteine-scanning mutagenesis and cross-linking analysis of human ABCC1 (hABCC1) have been used to deduce the *in vivo* 3-D

structure of hABCC1(Johnson & Chen, 2017; Trofimova & Deeley, 2018). hABCC1 is a 1531-amino-acid protein with 5 distinct domains: three MSDs, composed of 17 transmembrane helices (TM), and two NBDs. bAbcc1 has been structurally well characterized while bound to LTC_4, unbound, and bound to ATP, with a resolution of 3.3 Å and 3.5 Å, and 3.1 Å, respectively. These structures serve as the foundation of current models of hABCC1. The N-terminal MSD0 of bAbcc1, housing 5 of the 17 TMs, has very little interaction with the rest of the molecule, and comprises a linker region critical to the proper folding of the whole protein, known as the lasso motif. This motif is similar in function to the analogous motif in other ABC proteins, including other ABCCs and the structurally similar but functionally different CFTR channel (ABCC7). The rest of the protein conforms to the typical structure of ABC transporters and forms the transporter core (Johnson & Chen, 2017; Johnson & Chen, 2018; Zhang & Chen, 2016).

The transporter core structure is made of two transmembrane bundles, one consisting of TM 6, 7, 8, and 11 of MSD1 and TM 15 and 16 of MSD2 (TMB1); and the other consisting of TM 12, 13, 14, and 17 of MSD2 and TM 9 and 10 of MSD 1 (TMB2). The interaction of these two bundles form a pseudo-symmetrical transport domain and interacts with the two NBDs to control transport activity (Johnson & Chen, 2017). The NBDs similarly form two functional units as described above.

The binding site of bAbcc1 for LTC_4 contains two elements. The first is a positively charged site that coordinates with glutathione, called the P-pocket, the residues of which are

supplied by both TM bundles, TMB1 and TMB2. The second is a hydrophobic site that interacts with the lipid tail of LTC_4, the residues of which are supplied only by TMB2.

The structure predicts that the following residues are likely to be important in substrate specificity given their location in relation to the bipartite binding site: K332, H335, L381, F385, F694, Y440, R1196, and N1244 within the P-pocket, and W553, T550, M1092, Y1242, and W1245 within the H-pocket (Johnson & Chen, 2017).

Many findings from this cryo-EM study of bAbcc1 align with findings and predictions using other methods with hABCC1. The residues predicted to be important in substrate specificity are largely in agreement with earlier mutation-based studies which have mapped several of the key residues (Grant et al., 2008; Haimeur et al., 2002; Zhang et al., 2002; Zhang et al., 2006). Expressing bAbcc1 in human cells causes them to become resistant to multiple anticancer drugs (Taguchi et al., 2002). Kinetics of transport for GSSG and LTC_4 are similar (Johnson & Chen, 2017; Slot et al., 2011). Further, for both proteins, MSD0 is unnecessary for function as long as the rest of the protein is intact (Bakos et al., 1998), and the cryo-EM structure of bAbcc1 aligns closely with the structure of hABCC1 predicted using biochemical and sequence data. (Deeley & Cole, 2006; Slot et al., 2011) These similarities suggest that the structural data obtained for bAbcc1 can be relied upon as a reasonably close structural homologue of hABCC1 in many cases.

Some differences between hABCC1 and the bAbcc1 cryo-EM structure have also been found. Cysteine cross linking studies have shown that in hABCC1, TMs 8 and 15 within TMB1 are closer than predicted by the bAbcc1 structure, and the rotation and orientation of some other

TMs within the two TMBs are likely different between human and bovine isoforms (Trofimova & Deeley, 2018). The limits of the analogy between the two proteins is highlighted by the fact that bAbcc1 did not confer resistance against doxorubicin like its human counterpart (Taguchi et al., 2002), and the bAbcc1 structure does not predict or explain the estrogen-conjugate transport changes induced by H-pocket residue mutation in hABCC1 (Conseil et al., 2019).

In the next section, I will review another multidrug resistance protein of great relevance to arsenic handling, ABCC4.

1.3.7 Physiological Substrates of ABCC4

ABCC4 has a wide diversity of substrates which it can efflux from cells. Physiologically, ABCC4 can transport compounds that play a role in cell signaling, including ADP, cAMP, cGMP, eicosanoids, urate, and steroid hormones (Russel et al., 2008; Wen et al., 2015). ABCC4 transports LTC_4 and LTD_4 (GSH independent), LTB_4 (GSH dependent), and prostaglandins (GSH independent) with high affinity, which supports its putative role in the inflammatory response (Liu & Liu, 2021; Reid et al., 2003; Rius et al., 2008; Slot et al., 2011). ABCC4 also transports the bile salts cholytaurine, cholylglycine, and cholate in a GSH-dependent manner (Rius et al., 2003). This bile salt transport is reduced significantly or eliminated when GSH is absent (Rius et al., 2006). Urate, the estradiol metabolite $E_2$17βG, and the steroid sex hormone precursor DHEAS are also transported by ABCC4 (Chen et al., 2001; Van Aubel et al., 2005; Zelcer et al., 2003) There is some evidence that adenosine diphosphate (ADP) is transported by ABCC4 (Jedlitschky et al., 2004). Many insights into potential roles of ABCC4 in the physiological setting are drawn from studies with Abcc4 knock out mice. Whole

mice and tissue from KO mice have been used to investigate blood clotting, cAMP related signaling, bile salt and steroid hormone management, and inflammation and immune function. These studies and their findings are summarized in Table 1.1.

Table 1.1. The physiological function of Abcc4 as suggested by Abcc4-deficient mouse studies.

Role of ABCC4	Mechanism/method	Reference
Modulates clotting	Abcc4$^{-/-}$ mice have impaired platelet attachment and thrombus formation. Corroborated in human platelets	(Cheepala et al., 2015) (Decouture et al., 2015)
Maintains cAMP homeostasis	Abcc4 deficiency does not decrease overall cAMP levels in platelets, but redistributes it from dense granules to cytosol	(Decouture et al., 2015)
Participate in the elimination of steroid and bile salt sulfated metabolites	Abcc4$^{-/-}$ mice have downregulated sulfotransferase 2a1 (Sult2a1).	(Assem et al., 2004)
Involved in the development of pulmonary arterial hypertension	Abcc4$^{-/-}$ mice are less susceptible to hypertension developed from exposure to hypoxic conditions.	(Hara et al., 2011)
Involved in gametogenesis and testicular testosterone levels.	Abcc4$^{-/-}$ mice have lower testicular testosterone and impaired gametogenesis.	(Morgan et al., 2012)
Modulates the growth and contractility of cardiac tissue	Abcc4$^{-/-}$ mice have increased contractility and hypertrophy, and increased cAMP in myocytes.	(Sassi et al., 2012)
Modulate fibroblast migration.	Abcc4$^{-/-}$ mouse embryonic fibroblasts migrate more quickly.	(Sinha et al., 2013)
Modulates inflammatory pain	Abcc4$^{-/-}$ mice have an increased threshold for inflammatory pain, possibly due to changes in prostaglandin synthesis.	(Lin et al., 2008)
Lowers blood levels of kynurenic acid	Abcc4$^{-/-}$ mice have increased levels of kynurenic acid upon inducing hyperuricemia	(Dankers et al., 2013)

1.3.8 Drug Substrates of ABCC4

Experiments done on cells transfected with *ABCC4* have shown that antiviral agents, anticancer agents, diuretics, and other drugs interact with ABCC4, resulting in ABCC4 either conferring cellular resistance or facilitating transport (Wen et al., 2015). Direct transport has been shown for tenofovir, adefovir, (Lee et al., 2000; Ray et al., 2006); ceftizoxime, cefadroxil, cefazolin and cefmetazole (Ci et al., 2007); olmesartan, enalaprilat, edaravone glucuronide and p-aminohippurate (PAH) (Ferslew et al., 2014; Mizuno et al., 2007; Smeets et al., 2004; Yamada et al., 2007); methotrexate and leucovorin (Chen et al., 2002; El-Sheikh et al., 2007); and azidothymidine (AZT) (Abla et al., 2008).

Much study has been done on *Abcc4* knockout (*Abcc4*$^{-/-}$) mice and exogenous compounds. These mice typically change the accumulation of these compounds or lower the whole-body levels by changing urinary elimination. In some cases, Abcc4 deficiency can be compensated for by another protein. For example, either Abcc4 or breast cancer resistance protein (BCRP/Abcg2) must be present to avoid MTX accumulation in brain, and Abcg2 and P-glycoprotein (Abcb1) can compensate for Abcc4 deficiency in protecting the brain from camptothecin accumulation. These experiments are summarized in Table 1.2.

Table 1.2. Drug and toxicant handling in Abcc4 deficient mice.

Suggested Role of Abcc4	Mechanism/method	Reference
Sufficient but not necessary to protect brain from methotrexate	*Abcc4*$^{-/-}$ mice and *Abcg2*$^{-/-}$ mice both can avoid MTX accumulation in brain after 50 mg/kg dose, but the double KO cannot.	(Sane et al., 2014)
Increases systemic exposure to oral dasatinib	*Abcc4*$^{-/-}$ mice absorb less dasatinib orally, and this appears to be due to Abcc4 in the stomach.	(Furmanski et al., 2013)
Increases absorption of oral cefadroxil	Knocking out Abcc4 and Abcc3 lowers the intestinal absorption of cefadroxil, but either protein is sufficient.	(de Waart et al., 2012)
Increases sensitivity of neuroblastomas to irinotecan	Mice with allografted *Abcc4*$^{-/-}$ neuroblastomas survived longer than Mice with regular neuroblastomas upon treatment with irinotecan.	(Murray et al., 2017)
Sufficient but not necessary to protect the brain from camptothecin analogues	*Abcc4*$^{-/-}$ mice have increased brain concentrations of several camptothecin analogues but *Abcb1* and *Abcg2* can compensate. *Abcc4* alone appears sufficient for protection.	(Lin et al., 2013) (Leggas et al., 2004)
Protects retinal vascular development from forskolin	*Abcc4*$^{-/-}$ mice have impaired retinal vascular development when treated with forskolin	(Matsumiya et al., 2012)
Facilitates urinary excretion of adefovir and tenofovir	*Abcc4*$^{-/-}$ mice retain more adefovir and tenofovir in the kidneys.	(Imaoka et al., 2007)
Contributes to the renal clearance of an edaravone metabolite.	*Abcc4*$^{-/-}$ mice have lower, but not abolished, clearance of edaravone glucuronide.	(Mizuno et al., 2007)
Contributes to the efflux of sulfate-conjugated drug metabolites	*Abcc4*$^{-/-}$ livers transport less sulfate conjugated acetaminophen, harmol, and 4-methylumbelliferone in the perfusate of liver vasculature.	(Zamek-Gliszczynski et al., 2006)
Protects the brain from oseltamivir	*Abcc4*$^{-/-}$mice have more oseltamivir derivative in the brain.	(Ose et al., 2009)
Lowers the accumulation of thioguanine nucleotides upon mercaptopurine exposure	*Abcc4*$^{-/-}$mice have increased bone marrow accumulation of thioguanine, and this effect is even greater when thiopurine methyltransferase is also knocked out.	(Liu et al., 2017; Takenaka et al., 2007)

Increases urinary elimination of diuretics	*Abcc4*$^{-/-}$ mice have greatly reduced urinary clearance of furosemide and hydrochlorothiazide.	(Hasegawa et al., 2007)

1.3.9 ABCC4 structure

At the time of writing, no ABCC4 structure has been solved. Although it is functionally more similar to ABCC1, it is genetically more homologous to the cystic fibrosis transmembrane conductance regulator channel (CFTR), an ion channel with a very different function. ABCC4 lacks the MSD0 that ABCC1 has, as shown in Figure 1.2, and the two are only 31% identical in amino acid sequence (Slot et al., 2011). In contrast with other ABCC proteins, ABCC4 has two phenylalanine residues at position 368 and 369. It also has an arginine at residue 782, which gives it a positive charge at that position unique in the ABCCs to ABCC4, ABCC5, and CFTR (Russel et al., 2008). In 2008, a model of ABCC4 structure was built using the solved X-ray structures of Sav1866, a bacterial ABC transporter, and the NBD of ABCC1 (Dawson & Locher, 2006; Ramaen et al., 2006; Russel et al., 2008). In 2018, a model was made through advances in molecular dynamics modeling that accounted for the effects of the lipid bilayer (Chantemargue et al., 2018).

In the 2008 model, two units each comprising 6 TM helices that, at least in the ATP-bound state, come together to from a pore that serves as the presumed route of crossing the plasma membrane. Arginine 375 and 782 are inward pointing and line the pore. In the 2018 model, key residues previously reported to be important in substrate binding (Phe368, Phe369, Glu374, Arg375, Glu378, Trp995, Arg998) were found to be located in the pore, accessible to substrates (El-Sheikh et al., 2008; Russel et al., 2008; Wittgen et al., 2012).

1.3.10 ABCC4 SNPs and Mutations

As the structural knowledge of ABCC4 is still limited and developing, some known implications of certain amino acids can be used to inform the study of the protein's structure-function relationship. The *ABCC4* gene is highly polymorphic and at least 400 non-synonymous SNPs have been reported in humans (Banerjee et al., 2016). Several of these have been investigated due to being linked to a clinical outcome, and other variants, either found in humans or not, have been investigated based on predictions carried over from studies of ABCC1. A list of polymorphisms or mutations that have been associated with a reported clinical or in-vitro effect and their importance in transport of various substrates is assembled in Table 1.3.

Unsurprisingly, the residues of importance for this efflux transporter are either in transmembrane helices or in cytosolic portions of the protein. The one exception is E757, which was reported to be important for membrane trafficking, although this was not reproduced by the Leslie lab (Table 1.3). The most sensitive region of the protein for transport function appears to be transmembrane helix 6, where mutations in residues 368, 369, 374, 375, 378 all result in a severe change in protein function for several substrates (Table 1.3). Taken together, the experimental data on the variants in Table 1.3 suggest that TMs 1, 6, 8, 11, and 12 are the most important constituents of this transporter, at least for the transport of azidothymidine (AZT), 9-(2-posphonylmethoxyethyl) adenine (adefovir; PMEA), estradiol 17-β-D-glucuronide ($E_2$17βG), folic acid (FA), cGMP: cyclic guanosine monophosphate (cGMP), and methotrexate (MTX).

Table 1.3. ABCC4 mutations/polymorphisms and their effect on function.

AA change	Location	Effect on function	Reference
P78A*	CL_0	Decreased AZT transport	(Abla et al., 2008)
C171G*	TM1	Increased transport of $MMA(GS)_2$	(Banerjee et al., 2016)
G187W*	CL1	Decrease in AZT, PMEA, and $MMA(GS)_2$ transport	(Abla et al., 2008; Banerjee et al., 2016)
K304N*	CL2	Reduced transport of $MMA(GS)_2$ and DMA^V	(Banerjee et al., 2016)
F368A**	TM6	Loss of transport of $E_217\beta G$, MTX, FA and cGMP	(Wittgen et al., 2012)
F368Y**	TM6	Increased cGMP, decreased FA, MTX, $E_217\beta G$ transport	(Wittgen et al., 2012)
F368W**	TM6	Increased $E_217\beta G$, drastically decreased MTX, reduced FA transport	(Wittgen et al., 2012)
F368L**	TM6	Loss of function or decreased MTX, cGMP, $MMA(GS)_2$ and DMA^V transport	(Banerjee et al., 2016; El-Sheikh et al., 2008)
F369-**	TM6	Decreased MTX and cGMP transport	(El-Sheikh et al., 2008)
E374S**	TM6	Decreased MTX and cGMP transport	(El-Sheikh et al., 2008)

R375S**	TM6	Decreased MTX transport	(El-Sheikh et al., 2008)
R375E/A**	TM6	Loss of MTX and cGMP transport	(Abla et al., 2008; El-Sheikh et al., 2008)
E378Q	TM6	Loss of MTX and cGMP transport	(El-Sheikh et al., 2008)
P403L*	CL3	Decreased AZT transport	(Abla et al., 2008)
G487E*	NBD1	Decrease in AZT and PMEA transport	(Abla et al., 2008)
Y556C*	NBD1	Decreased protein expression, increased DMA^V transport	(Banerjee et al., 2016; Janke et al., 2008)
E757K*	ECL4	Impaired membrane trafficking.	(Janke et al., 2008; contradicted by Banerjee et al. 2016)
V776I*	TM8	Decreased 6-MP transport, impaired trafficking to PM	(Janke et al., 2008)
T796M	TM8	Impaired localization at PM	(Janke et al., 2008)
C956S*	TM11	Increased PMEA transport	(Abla et al., 2008)
W995F/Y/A**	TM12	Decreased $E_2$17βG, MTX, FA and cGMP transport	(Wittgen et al., 2012)
R998S/K/L/Y**	TM12	Drastically decreased of $E_2$17βG, MTX, FA and cGMP transport	(Wittgen et al., 2012)
R998A**	TM12	Decreased MTX, cGMP transport	(El-Sheikh et al., 2008)

T1142M*	NBD2	Increased PMEA transport, impaired localization at PM	(Janke et al., 2008)

*Variant chosen due to natural occurrence in humans.

**Variant chosen based on analogy to ABCC1 residues and/or predicted 3D location. AZT: azidothymidine, PMEA: 9-(2-posphonylmethoxyethyl) adenine (adefovir), $E_2$17βG: estradiol 17-β-D-glucuronide, FA: folic acid, cGMP: cyclic guanosine monophosphate. L_0 linker region before MSD1. CL: cytoplasmic loop, TM: transmembrane helix, ECL: extracellular loop, MSD: membrane spanning domain, NBD: nucleotide binding domain.

1.3.11 Localization and Expression of ABCC4

Similar to ABCC1, ABCC4 protein is widely expressed. It is expressed at the highest levels in the blood brain barrier, kidney, and lung, which also contain high levels of ABCC1 (Slot et al., 2011). ABCC4 can localize to either the apical or basolateral surface of polarized cells, and importantly, is basolateral in hepatocytes and apical in kidney proximal tubule cells (Hoque et al., 2009; Russel et al., 2008). This creates a suggested elimination pathway for several hepatic metabolites via the urine (Banerjee et al., 2014; Ci et al., 2007; Imaoka et al., 2007).

1.4 Species differences in ABCC1 and ABCC4

There are two excellent reasons for paying attention to species differences in the field of ABCCs. First, in order to translate medical science from laboratory animal models to humans in the clinic, the relevant differences expected in the different species' physiologies must be understood as completely as possible. Second, understanding species differences can provide us with an analytical tool. When we find that a protein acts differently if it is a human or a mouse orthologue, and the sequence differences are subtle, as is often the case, then nature has provided us with a good start at determining which parts of the protein are key to the function in question. Combining our knowledge of species differences in function and in sequence with 3D modelling and SNP/mutation studies, predictions can be made about the function of motifs and specific amino acids. This allows the design of experiments to understand how these proteins function.

This is all to say that the fruit is lower-hanging if we take advantage of species differences in structure/function studies.

1.4.1 Functional species differences in ABCC4/Abcc4

Studies using *Abcc4*$^{-/-}$ mice have provided key insights regarding the function of Abcc4 in mice, but there are not many instances of direct comparison between human ABCC4 and non-human Abcc4 protein function. In one example of clear species difference, human ABCC4 was found to be necessary for dendritic cell migration as part of a normal immune response, while Abcc4 was not important in either this migration or a successful immune response (van de Ven et al., 2009; van de Ven et al., 2008). Given the known function of ABCC4, including the transport of inflammatory mediators such as PGE_2 (Reid et al., 2003), this effect is likely due to a difference in substrate specificity, but that has not been tested directly. Human and mouse ABCC4/Abcc4 were examined head to head in the affinity for cGMP in vesicle transport studies, and mouse Abcc4 was found to have significantly lower affinity for the substrate (2.3 mM for mouse Abcc4 vs 10-180 μM for ABCC4) (Chen et al., 2001; de Wolf et al., 2007; Van Aubel et al., 2005).

1.4.2 Physiological context

Different animals handle, accumulate, and excrete xenobiotics differently in more ways than differences in the protein(s) they use for cellular efflux. For example, arsenic, which is exported from cells in several chemical forms by different ABCCs, is eliminated by rats at a much slower rate than mice. This has been explained by DMA^V accumulating in erythrocytes

in rats more than in mice (Vahter et al., 1984), and was further explained as a hemoglobin-binding proclivity of rat erythrocytes for inorganic, monomethyl, and dimethyl trivalent arsenic, confirmed *in vivo* with rats fed DMA^V (Lu et al., 2004). Conversely, MMA is preferentially accumulated in the kidney of the mouse, but not the rat (Kenyon et al., 2008). This difference in kidney accumulation in rodents may reflect a species difference in transporter function at the kidney, either in uptake or efflux, or it may be a result of the rat's increased accumulation of arsenic in the blood being a higher-affinity process which outcompetes that of kidney accumulation. The latter interpretation is fitting with the fact that rat red blood cells have a very high affinity for methylated arsenic (Lu et al., 2004)

Further, the methylation state of arsenic has a great impact on the ability of ABCCs to protect cells from arsenic (Banerjee et al., 2014; Banerjee et al., 2018; Carew et al., 2011); and methylation of arsenic is different across species, with rats and mice being more efficient at methylating from MMA^V to DMA^V, and thus having less MMA^V detected in their urine than humans have (Vahter, 2002). Dog, rat and rhesus monkey hepatocytes methylate As^{III} more efficiently than mouse, rabbit, or human hepatocytes (Drobná, Walton, Harmon, et al., 2010), but marmoset monkeys, chimpanzees, and guinea pigs do not methylate inorganic arsenic at all (Healy et al., 1999; Marafante et al., 1985; Vahter et al., 1995; Zakharyan et al., 1996). This shows that we cannot rely on genetic or evolutionary proximity as a predictor of analogy in arsenic-handling when choosing experimental models for human arsenic handling.

As a final example, mouse and rat models do not get cancer from arsenic at concentrations relevant to chronic exposure concentrations for humans; however, they do form

tumors at much higher exposure concentrations (reviewed in (Tokar et al., 2010)). This difference is likely due to some combination of uptake, metabolism, efflux, and other factors relevant to the formation of cancers such as DNA damage and repair mechanisms (Cohen et al., 2006).

Taken together, these data warn us about drawing conclusions that span across species, and force us to look at a whole-body context before we attribute certain outcomes to protein-specific effects.

1.5 Rationale, Hypotheses, and Objectives

This work was undertaken to learn more about how arsenic is handled by ABCCs by looking at how these proteins interact with arsenic. Two hypotheses drove the research: first, that there are species differences between human and mouse ABCC4/Abcc4 that have not yet been discovered, and second, that ABCC1 transports more inorganic arsenic metabolites than have been discovered.

Chapter 3:

The objectives of this work were to compare human and mouse ABCC4/Abcc4 in their ability to a) protect cells from arsenic, and b) transport arsenic out of cells. In order to do this, the protein levels had to be monitored, and thus the epitope of an ABCC4 antibody needed to be mapped to ensure cross-species utility. To better understand rodent models, a common tool in arsenic research, human and mouse orthologues of ABCC4/Abcc4 were compared in human and mouse cells, through cytotoxicity and transport experiments.

This work was continued with interspecies chimera ABCC4/Abcc4 studies presented in Appendix 1, with the goal of narrowing down the regions important to substrate binding and/or transport in ABCC4. Additional characterization of rat Abcc4 was conducted and reported in Appendix 2.

Chapter 4:

ABCC1 (MRP1) was investigated in HEK 293 cells in its ability to confer protection from cytotoxicity of arsenicals and in its ability to transport arsenic. Previously, Shukalek et al. (2016) showed cell line differences between HeLa and HEK293 cells for ABCC1 transport of

$As(GS)_3$, and that these differences in transport affinity and capacity were associated with the phosphorylation status of two amino acids Y920 and S921. Thus, this work sought to (1) look for additional cell line differences in the ability of ABCC1 to confer protection from cytotoxicity in HEK293 and HeLa cells, (2) investigate similar cell line differences in vesicle transport abilities, and (3) investigate the influence of Y920 and S921 phosphorylation on ABCC1 transport of other arsenicals. This chapter was published as Banerjee et al., 2018.

Chapter 5:

Given the growing data on the broad substrate specificity and clinical correlations of ABCC1, and the work leading to the discoveries in Chapter 4, the transport of methylated arsenic in the form of MMA^V was investigated. The objectives were to (1) determine whether ABCC1 conferred cellular protection to HEK293 cells, building on earlier work on cell line differences; (2) determine if ABCC1 directly transports MMA^V; and (3) investigate potential binding sites for transport. Objective (2) was pursued with direct transport experiments and by determining the effect of ABCC1 on whole cell accumulation. Objective (3) was pursued through competitive inhibition experiments, in which MMA^V was used as an attempted inhibitor of the transport of other ABCC1 substrates.

Chapter 2: Materials and Methods

1.6 Materials

1.6.1 Common reagents

Name	Source
6-mercaptopurine (6-MP)	Sigma-Aldrich (Oakville, ON, Canada)
Adenosine monophosphate (AMP)	Sigma-Aldrich (Oakville, ON, Canada)
Adenosine triphosphate (ATP)	Sigma-Aldrich (Oakville, ON, Canada)
Sodium (meta)arsenite (As^{III} sodium salt)	Sigma-Aldrich (Oakville, ON, Canada)
Bicinchoninic acid assay (BCA) kit	Pierce Chemicals (Rockford, IL)
Bradford protein assay solution	Bio-Rad Laboratories, Inc. (Hercules, CA)
Buthionine sulfoximine (BSO)	Sigma-Aldrich (Oakville, ON, Canada)
Calcium chloride ($CaCl_2$)	Thermo Fisher Scientific (Waltham, MA)
Creatine kinase (CK)	Roche Applied Science (Torrance, CA)
Creatine phosphate (CP)	Roche Applied Science (Torrance, CA)
Deoxynucleotides (dNTPs)	Thermo Fisher Scientific (Waltham, MA)
Diiodomethylarsine (MMA^{III})	Gift from Dr. X.Chris Le
Dimethylarsinic acid (DMA^{V})	Sigma-Aldrich (Oakville, ON, Canada)
Iododimethylarsine (DMA^{III})	Gift from Dr. X. Chris Le
Dimethyl sulfoxide (DMSO)	Thermo Fisher Scientific (Waltham, MA)
DNA polymerase (Pfu turbo)	Agilent Technologies (Santa Clara, CA)
DNA ladder (GeneRuler 1kb Plus)	Thermo Fisher Scientific (Waltham, MA)
Ethylenediamine tetraacetic acid (EDTA)	EMD Chemicals (Gibbstown, NJ)
G418 / Geneticin	Life Technologies (Carlsbad, CA)
GenElute ™ Plasmid Mini (Midi/Maxi) Prep Kit	Sigma-Aldrich (Oakville, ON, Canada)
Glass fiber filters (type A/E)	Pall Life Sciences (East Hills, NY)
Glucose ($C_6H_{12}O_6$)	Thermo Fisher Scientific (Waltham, MA)
Glutathione (GSH)	Sigma-Aldrich (Oakville, ON, Canada)
GSH reductase	Roche Applied Science (Torrance, CA)
Hexadimethrine bromide (polybrene)	Sigma-Aldrich (Oakville, ON, Canada)

HIV p24 ELISA assay	ZeptoMetrix Corporation (Buffalo, NY)
Iododimethylarsine (DMA^{III})	Gift from Dr. William Cullen
Lactate dehydrogenase (LDH) Cytotoxicity Detection Kit	Roche, Applied Sciences (Indianapolis, IN)
Magnesium sulfate ($MgSO_4$)	Thermo Fisher Scientific (Waltham, MA)
Mini PROTEAN ® TGX ™ gels	Bio-Rad (Hercules, CA)
Methotrexate	Sigma-Aldrich (Oakville, ON, Canada)
MISSION ® shRNA plasmid DNA glycerol stocks	Sigma-Aldrich (Oakville, ON, Canada)
MISSION ® shRNA plasmid packaging mix	Sigma-Aldrich (Oakville, ON, Canada)
Diiodomethylarsine (MMA^{III})	Gift from Dr. X. Chris Le
Monomethylarsonic acid (MMA^{V})	Sigma-Aldrich (Oakville, ON, Canada)
Nicotinamide adenine dinucleotide phosphate (NADPH)	Roche Applied Science (Torrance, CA)
Nitric acid	Thermo Fisher Scientific (Waltham, MA)
Phenylmethylsulfonyl fluoride	Bisho Canada Inc. (Burlington, Canada).
PhosSTOP phosphatase inhibitor cocktail (PIC) tablets	Roche Applied Science (Laval, Canada)
Potassium phosphate monobasic (K_2HPO_4)	Sigma-Aldrich (Oakville, ON, Canada)
Protease inhibitor cocktail tablets (Complete ™ mini EDTA-free)	Roche, Applied Sciences (Indianapolis, IN)
Protein ladder (Precision Plus Protein-Dual color standard (4-20%))	Bio-Rad (Hercules, CA)
Sodium arsenate dibasic heptahydrate (As^{V})	Sigma-Aldrich (Oakville, ON, Canada)
Sodium bicarbonate ($NaHCO_3$)	EMD Chemicals (Gibbstown, NJ)
Sodium choride (NaCl)	Thermo Fisher Scientific (Waltham, MA)
Sucrose ($C_{12}H_{22}O_{11}$)	Thermo Fisher Scientific (Waltham, MA)
SuperSignal ™ West Pico Chemiluminescent Substrate	Pierce Chemicals (Rockford, IL)
T4 DNA ligase	Promega Corporation (Madison, WI)
Tris base	Sigma-Aldrich (Oakville, ON, Canada)

1.6.2 Cell culture reagents

Name	Source
Dulbecco's modified Eagle's medium (DMEM)	Life Technologies (Carlsbad, CA)
Calf serum	Sigma-Aldrich (Oakville, ON, Canada)
Fetal bovine serum (FBS)	Sigma-Aldrich (Oakville, ON, Canada)
Roswell Park Memorial Institute (RPMI) -1640 medium	Life Technologies (Carlsbad, CA)

1.6.3 Buffers

Name	Composition
Homogenization Buffer	Tris-Sucrose Buffer- pH 7.4, 0.25 mM $CaCl_2$, protease inhibitor tablet /10ml
Laemmli Buffer (6X)	4ml of 1M Tris-pH 6.8, 3.2 ml glycerol, 3.2 g SDS, pinch bromophenol blue, 5.47 ml H_2O, dispense into 1 ml aliquots (Add 236 µl mercaptoethanol per ml prior to use)
Low Sucrose Buffer	50 mM Tris- pH 7.4, 50 mM sucrose
PBS (10X)	1.4 M NaCl, 30 mM KCl, 10 mM Na_2HPO_4-$7H_2O$, 14 mM KH_2PO_4
RIPA Buffer	0.1% SDS, 1% sodium deoxycholate, 1% Triton X-100, 10 mM Tris pH 8.0, 140 mM NaCl
Tank Buffer (10X)	250 mM Tris- pH 7.41, 92 M glycine, 1% SDS (Western blot)
TBS-Tween (10X)	100 mM Tris- HCl, 150 mM NaCl, 0.3% Tween® 20
Transfer Buffer (10X)	25 mM Tris, 192 mM glycine, 10% methanol (Western Blot)
Tris-Sucrose Buffer (TSB)	50 mM Tris- pH 7.4, 250 mM sucrose

1.6.4 shRNA knock down sequences

Clone	Region	Sequence
NT	N/A	CCGGCAACAAGATGAAGAGCACCAACTCGAGTTGGTGC TCTTCATCTTGTTGTTTTT (contained in TRC2 pLKO.1-puro vector)
5264	3'UTR	CCGGCCACCAGTTAAATGCCGTCTACTCGAGTAGACGGC ATTTAACTGGTGGTTTTT (contained in TRC1.5 pLKO.1-puro vector)
7334	CDS	CCGGGCCTTCTTTAACAAGAGCAATCTCGAGATTGCTCT TGTTAAAGAAGGCTTTTTG (contained in TRC2 pLKO.1-puro vector)

1.6.5 Antibodies

Name	Source	Application
ABCC1 [MRPr1] (monoclonal)	Novus Biologicals	Western Blotting (WB)
ABCC4 [M_4I-10] (monoclonal)	Abcam Inc	WB
ABCC4 [ALX-210-856] (polyclonal)	Enzo Life Sciences/Gift from Dr. Susan P.C. Cole	WB
Na^+/K^+ ATPase [H-300] (polyclonal)	Santa Cruz Biotechnology	WB

1.6.6 Radiochemicals

Name	Source
$^{73}As^V$ (158 Ci/mol)	Los Alamos Meson Production Facility (Los Alamos, NM)
[6,7- ^{3}H]17β-estradiol 17-(β-D-glucuronide) (E217βG) (47 Ci/mmol)	PerkinElmer Life and Analytical Sciences (Woodbridge, ON, Canada).
^{3}H-Leukotriene C_4 (170.2 Ci/mmol)	Custom Synthesis by PerkinElmer Life and Analytical Sciences (Woodbridge, ON, Canada). Gift from Dr. Susan P.C. Cole.

1.6.7 Cell lines

Cell line	Description	Source
HEK 293	Human embryonic kidney cells.	ATCC (CRL 11268)
HEK 293T	Human embryonic kidney cells transformed with simian virus 40 (SV40) large T antigen (www.atcc.org)	ATCC (CRL1573)
HEK-V	HEK-293 cells stably transfected with pcDNA 3.1(+)	Leslie lab (Banerjee et al., 2014)
HEK-ABCC4	HEK-293 cells stably expressing human ABCC4	Developed in Leslie lab using ABCC4 plasmid from Dr. Dietrich Keppler (German Cancer Research Center, Heidelberg, Germany)(Banerjee et al., 2014)
HEK-mAbcc4	HEK-293 cells stably expressing mouse Abcc4	Developed in Leslie lab using mAbcc4 plasmid from Dr. J. D. Schuetz.
HEK-rAbcc4	HEK-293 cells stably expressing rat Abcc4	Developed in Leslie lab using rAbcc4 plasmid from Dr. S. P. C. Cole
HEK-ABCC1	HEK-293 cells stably expressing ABCC1(ABCC1) (using pcDNA 3.1(-) vector)	S.P.C. Cole Lab (Conseil & Cole, 2013)
HeLa-V	HeLa cells stably transfected with pcDNA 3.1(-) vector	S.P.C. Cole lab (Ito et al., 2001)
HeLa-ABCC1	HeLa cells stably expressing ABCC1 (using pcDNA 3.1(-) vector)	S.P.C. Cole Lab (Leslie, Ito, et al., 2001)
MEF-Abcc4$^{+/+}$	Wild Type Mouse Embryonic Fibroblast Cells	(Sinha et al., 2013)
MEF-Abcc4$^{-/-}$	Mouse Embryonic Fibroblast cells with Abcc4 knocked out	(Sinha et al., 2013)

1.6.8 Sequencing primers for mAbcc4

Name	**Sequence** (5'-3')
mAbcc4_119r	TCCAGTCTCCGCTTATGACC
mAbcc4_760f	ATCGGGAAGCTGTTCTCGT
mAbcc4_1959f	CTTCTCCGAGGCCTCAATTT
mAbcc4_2142r	GATGAAGAACCAGGATGCG
mAbcc4_2448f	TCCAATCGGGAGGATTTTA
mAbcc4_3275r	GAGATGAGGGAGCTTTTCCC
mAbcc4_3765f	TGATGAGCCGTATGTCTTGC

1.6.9 Mutagenesis primers for ABCC4 restriction site introduction

Name	**Sequence** (5'-3')
hABCC4_T2073Gf	CTATCAGAGGAGAACCGGTCTGAAGGAAAAGTTGG
hABCC4_T2073Gr	CCAACTTTTCCTTCAGACCGGTTCTCCTCTGATAG
hABCC4_T1044Cf	GCAATGAGATTACAGCCAGCCACGTGTTTGTGGC
hABCC4_T1044Cr	GCCACAAACACGTGGCTGGCTGTAATCTCATTGC

1.6.10 PCR primers for amplifying mAbcc4 segments with restriction sites

Name	**Sequence** (5'-3')
hABCC4_T2073Gf	CAGTGCTAGCATGCTGCCGGTGCACACCGA
hABCC4_T2073Gr	TGACTACCGGTCGGAAGGGAGAATCGGCTTC
hABCC4_T1044Cf	TCAGTACCGGTTCTCCTCGGGTTGCACTGCC
hABCC4_T1044Cr	TGACTCTAGATCACAATGCTGTTTCAAATA

1.7 Methods

1.7.1 Cell culture

HEK293T cells were maintained in Dulbeco's modified Eagle's medium (DMEM) supplemented with 7.5% fetal bovine serum (FBS). HEK293 stably transfected cell lines (vector, ABCC1 and ABCC4/Abcc4) were grown in the same medium with the addition of 600 μg/ml geneticin (G418). All MEFs were grown in DMEM with 10% FBS and no selecting agent. All stably transfected HeLa cells were grown in Roswell Park Memorial Institute (RPMI)-1640 supplemented with 5% calf serum and 600 μg/ml G418.

1.7.2 Stably transfected cell lines

HEK293 cell lines stably expressing mAbcc4 (Chapter 3) and rAbcc4 (Appendix 2) were constructed as previously described (Ito et al., 2001; Leslie et al., 2003; Weigl, 2005). Cells were transfected with the appropriate abcc4, rat or mouse, using X-tremeGENE 9 transfection reagent according to the manufacturer's instructions. Cells were selected in Dulbecco's modified Eagle's medium containing 1 mg/ml G418 (Invitrogen) and 10% fetal bovine serum for 2 weeks. Surviving colonies were individually picked and subcultured in 96-well plates. Clones were screened by immunoblot for Abcc4 expression, and positive clones were evaluated by flow cytometry to determine the proportion of cells expressing Abcc4 (as described by Banerjee et al. 2014). Populations less than 80% positive for Abcc4 expression were further cloned by limiting dilution to obtain populations of 80% or greater. This resulted in the clones 1A6-37 (mouse), 1C1-1-3 (mouse), 1C1-2-62 (mouse), 2D2 (rat) and 1D4 (rat). All clones were

screened with flow cytometry to ensure that in all cases, at least 80% of cell populations were expressing the Abcc (Figure 2.1).

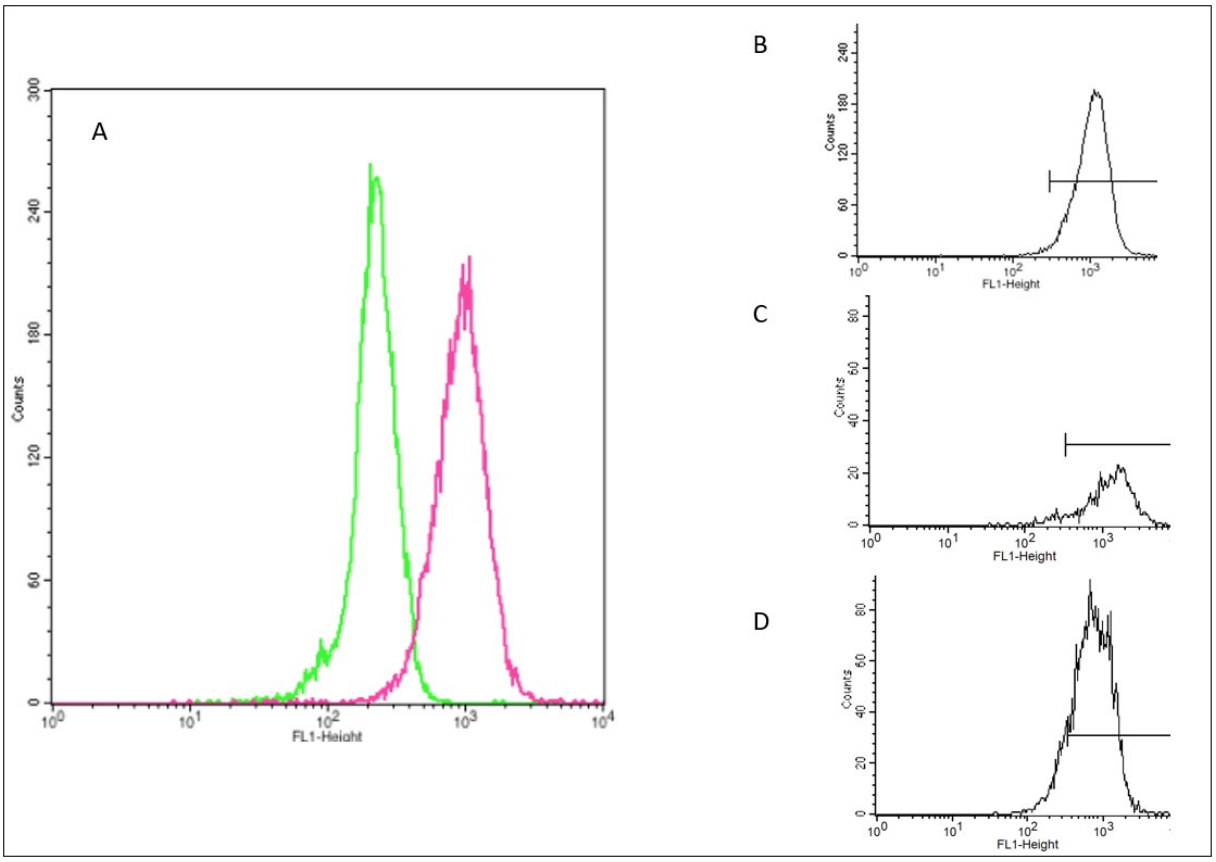

Figure 2.1. Fluorescence-activated cell sorting screening of stably transfected cell lines. (A) Flow cytometry was performed on HEK-V cells stained with secondary antibody alone (green) or anti-Abcc4 antibody (pink). This informed the construction of the gate shown in B-D (horizontal bars), inside of which shows Abcc4-expression, and outside of which shows cells not expressing Abcc4. The populations of cells expressing Abcc4 was above 85% in all clones: 99% for mMrp4 (B); 90% for rMrp4 (clone 1D4) (C); 87% for rMrp4 (clone 2D2) (D).

1.7.3 Production and immunoblotting of immobilized peptides for epitope mapping of the anti-hABCC4/mAbcc4 Mab M_4I-10

An immobilized peptide array was purchased from Kinexus (Vancouver, BC, Canada) on a trioxatridecanediamine (TOTD) cellulose membrane. Overlapping 6-mer or 10-mer peptides shifted by one amino acid were synthesized to cover the human ABCC4 sequence against which the M_4I-10 antibody was originally raised ((Leggas et al., 2004); Abcam Inc.) (AIERVSEAIVSIRRAQTFLLLDEISQRNRQLPSDGKKMVHVQDFTAFWDKASE TPLQGL; amino acids 372-431). The membranes were wet with 100% methanol for 10 minutes, and then washed three times with Tris-buffered saline (TBS). The membranes were blocked with 4% BSA and 5% sucrose solution in Tris-buffered saline with 0.05% Tween 20 (TBS-T), for two hours at room temperature and then washed again with TBS-T. The membranes were then probed with the anti-ABCC4 rat MAb M_4I-10 (1:1000) in blocking buffer at 4˚C overnight, and washed three times with TBS-T. The membranes were then incubated in horseradish peroxidase-labeled goat anti-rat secondary antibody at 0.1 µg/ml in blocking buffer for two hours at room temperature, washed three times with TBS-T, and then washed in TBS. The membranes were incubated in SuperSignal™ West Pico Chemiluminescent Substrate for 5 minutes and used for X-ray film exposure.

1.7.4 Peptide competition of MAb binding

The epitope peptide (HVQDFTAF; amino acids 411-418 in human ABCC4) was synthesized (Institute for Biomolecular Design, University of Alberta) and used for peptide competition to

corroborate the immobilized peptide results. Identical ABCC4-enriched membrane vesicle samples (0.5 ug protein) were resolved by 6% SDS-PAGE and transferred to a PVDF membrane. The PVDF membrane was cut into strips with one sample per strip and subjected to various immunoblotting conditions. The synthesized epitope peptide was preincubated in various concentrations (0, 5, 10, 20, 50 µg/ml) with the M_4I-10 MAb (1:30,000) at room temperature for 1 hour to determine if the synthetic epitope would bind the antibody and render it saturated and unable to bind the sample on the membrane. This mixture was used to probe the membrane strips overnight at 4˚C. A different anti-ABCC4 antibody was used alongside M_4I-10 with the same preincubation with synthetic peptide as a control to ensure that the peptide binding was specific for M_4I-10 (ALX-210-856, polyclonal rabbit antibody raised against synthetic peptide S^{1249}GRLKEYDEPYVLLQNKESL^{1268} from hABCC4 (Schuetz et al., 1999), at 1:1000 dilution). After these primary antibody incubations, the membranes were probed with secondary antibody and visualized as described in the previous section.

1.7.5 Cytotoxicity assay

The CellTiter 96® tetrazolium-based cell proliferation assay (MTS) was used to measure the toxicity of As^{III}, As^{V}, MMA^{III}, MMA^{V}, DMA^{III}, and DMA^{V} in HEK293 cells stably expressing empty vector, ABCC1, ABCC4 or mAbcc4; and in MEF *abcc4*$^{(+/+)}$ and MEF *abcc4*$^{(-/-)}$ cells according to the manufacturer's instructions and previously published work (Banerjee et al., 2014; Banerjee et al., 2018). Briefly, cells were seeded at 10,000 or 3,000 cells per well for HEK and MEF cells, respectively, in 96-well plates. Cells were then exposed to As^{III} (0.1-100 µM), As^{V} (0.001-3 mM), MMA^{III} (0.1-100 µM), MMA^{V} (0.3-100 mM), DMA^{III} (0.1-100 µM),

or DMA^V (0.001-100 mM). The pH of MMA^V and DMA^V were adjusted to 7.4 before being applied to cells. The positive control for MRP4, 6-mercaptopurine (6-MP) (0.1-100 uM), was used in parallel with all arsenic species. In the BSO treated conditions for GSH depletion, cells were in their regular media with 100 µM BSO added at the time of seeding, and for the rest of the experiment. After 72 h of exposure to arsenic or control, cell viability was determined. EC_{50} values were determined using the sigmoidal dose-response equation in GraphPad Prism (GraphPad Software, La Jolla, CA). Ratios of EC_{50} values between the ABCC/Abcc expressing line and the vector-transfected (HEK) or knockout (MEF) line were calculated and compared (relative resistance, RR).

1.7.6 Lentivirus production

For the delivery of shRNA sequences referenced in Table 2.1.4 to knock down endogenous human ABCC4: The Mission shRNA protocol by Sigma was followed and viral particles were concentrated as previously described (Tiscornia et al., 2006), with some modifications. Briefly, HEK293T cells were seeded in T75 flasks at 1.8 million cells per flask. Cells were grown in DMEM with 10% FBS until they were approximately 50% confluent (approximately 24 hours). They were then transfected with MISSION shRNA packaging mix and shRNA transfer vector at a 10:1 ratio (34 µl : 3.4 µl per flask), using 21 ul XtremeGene9 transfection reagent. After 24 hours, the media was removed and replaced. At 48 hours and 72 hours post-transfection, the media was collected, and in the case of the first harvest, replaced. These two aliquots of harvested media were kept at 4°C and pooled, then filtered through a 0.45 µm membrane into centrifuge tubes. To concentrate the harvested virus, the filtered media was centrifuged at

98,000*g* for 2 hours at 20°C. The supernatant was then removed, and the pellet was resuspended in 50 µl of phenol red free DMEM. This concentrated virus suspension was stored at -80°C until needed for knock down experiments. The number of viral particles was determined using the ZeptoMetrix HIV p24 ELISA assay, following the manufacturer's protocol. The number of viral particles required to knock down ABCC4 was determined by repeated experiments with increasing multiplicity of infection (MOI; number of viral particles per cell) until ABCC4 protein was undetectable.

1.7.7 shRNA knock down

UTR shRNA sequence (Table 2.1.4) was used to knock down endogenous ABCC4 in HEK293 cells. Non-target sequence was used as a negative control to activate the RNA-induced silencing complex without targeting it to interfere with any protein translation. Viral particles were produced per the manufacturer's instructions (as described in 2.2.7). HEK293 cells were infected 10 days prior to experiments with lentiviral particles containing shRNA in Table 2.1.4 at 500 viral particles per cell seeded, or untreated. Two hours after seeding 270,000 cells in a 6-well plate well, virus was added and the cells were left to grow for approximately 72 hours. After 72 hours, cells were harvested from the 6-well plate and 100% reseeded in a T75 flask. Cells were then cultured as usual and used for cytotoxicity experiments described in s 2.2.6. Cells from the time of seeding and the end of each experiment were lysed and immunoblotted to determine the extent of knockdown.

1.7.8 Transient transfection and vesicle preparation

Cells were transfected using the calcium phosphate method, with a medium change 24 hours after transfection, as previously described (Carew and Leslie, 2010). Cells were harvested 72 hours after transfection by scraping into homogenization buffer (Table 2.1.3) and pelleted by centrifugation at 800 x *g* for 10 minutes and then stored at -80ºC until vesicle preparation. Plasma membrane-enriched vesicles were prepared from pellets using the nitrogen cavitation method described previously (Carew 2010). ABCC1, ABCC4 and mAbcc4 levels were verified by immunoblot using the MRPr1 antibody of the rat anti-ABCC4/Abcc4 antibody M_4I-10 (1:10,000). Bands were visualized after incubation with primary antibody as in section 2.2.3. In the case of comparison of MRP1 levels between the two different cell lines (the Na^+/K^+-ATPase level was found to be different). Thus, blots were stained with Coomassie blue and normalized to total protein levels in each lane. Relative levels of MRP1 were quantified using ImageJ Software (National Institutes of Health, Bethesda, MD) and/or ImageLab Software (Bio-Rad, Hercules, CA).

1.7.9 $As(GS)_3$, $MMA(GS)_2$, DMA^V, and 17-β Estradiol 17-β-D-glucuronide vesicle transport

Chapters 3 and 5: $MMA(GS)_2$ was synthesized as described previously, and both $MMA(GS)_2$ and DMA^V were tested in triplicate with methods described in Carew (2011) ($MMA(GS)_2$) and Banerjee (2014) (DMA^V) and used at a final concentration of 1 μM. [^{3}H]-$E_2$17βG was used at 400 nM, 80 nCi/reaction. Membrane vesicles were incubated with $MMA(GS)_2$-, DMA^V-, or [^{3}H]-$E_2$17βG-containing reaction mix at 37 ˚C for 3, 5, or 1.5 minutes, respectively. For

$MMA(GS)_2$ and DMA^V, time points were chosen to be at the initial rates of uptake for hABCC4 as described previously (Banerjee et al., 2014). Transport was stopped by rapid dilution in 800 µl of ice-cold Tris-sucrose buffer. In the case of $MMA(GS)_2$ or DMA^V, vesicles were then centrifuged at 100,000 x *g* to pellet, washed twice with ice cold Tris-sucrose buffer, then digested for 48 hours with 250 µl of nitric acid. After digestion, dissolved vesicles were diluted 1:1 with deionized water and filtered with 0.45-µm syringe filters. Arsenic was quantified by inductively coupled plasma mass spectrometry (ICP-MS) using the standard addition method with an Agilent 7500ce (Carew et al, 2011; Kalivas et al., 1987). In the case of [^{3}H]-$E_2$17βG, the stopped reaction mix was vacuum filtered over Perkin Elmer Unifilter GF/B filter plates, washed three times with cold TSB, and counted with a PerkinElmer Microbeta^2 liquid scintillation counter. The ATP-dependent transport was determined by subtracting transport in the presence of AMP from that in the presence of ATP.

Chapter 4: Reduction of arsenate [$^{73}As^V$] into arsenite [$^{73}As^{III}$] and subsequent synthesis of $^{73}As(GS)_3$ from $^{73}As^{III}$ and GSH, were carried out as described previously (Reay & Asher, 1977; Shukalek et al., 2016). $MMA(GS)_2$ was synthesized from MMA^{III} and GSH as described above. Vesicular transport was carried out in triplicate for each substrate, employing previously described methods (M. Banerjee et al., 2014; M. W. Carew et al., 2011; Shukalek et al., 2016). Time points were chosen to be in the linear range of uptake based on time courses previously published (Carew et al. 2011) or shown in Figure 4.2. The amount of $^{73}As(GS)_3$ transported was quantified using liquid scintillation counting, as described previously (Leslie et al., 2004;

Shukalek et al., 2016). The amount of $MMA(GS)_2$ and DMA^V transported was quantified by inductively coupled plasma mass spectrometry (ICP-MS) described above. ATP-dependent transport was calculated as described above.

The linear range of DMA^V transport was determined by incubating the HEK-WT-MRP1 or HEK-vector membrane vesicles with DMA^V (1μM) in transport buffer at 37°C for the indicated time points. Kinetic parameters were determined by measuring the initial rate of DMA^V and $MMA(GS)_2$ transport at eight different substrate concentrations [0.1–2.5 μM for DMA^V and 1–200 μM for $MMA(GS)_2$] at 20 sec and 1 min, respectively. Curve fitting was done by nonlinear regression analysis using GraphPad Prism® 6 software (La Jolla, CA).

The ability of DMA^V and $MMA(GS)_2$ to inhibit $^{73}As(GS)_3$ transport was first characterized by using a fixed concentration of $^{73}As(GS)_3$ (1 μM, 40 nCi) in the presence of increasing concentrations of DMA^V (0.04 and 1000 μM) or $MMA(GS)_2$ (0.01-300 μM). The conditions for the synthesis of $As(GS)_3$ resulted in the presence of 3 mM GSH in transport reactions (Leslie et al., 2004). Thus, $As(GS)_3$ inhibition experiments were completed under plus GSH conditions. This is important because the *in vitro* inhibition of MRP1 by certain compounds can be enhanced by physiological concentrations of GSH (Cole & Deeley, 2006). IC_{50} values were calculated for $MMA(GS)_2$ inhibition using GraphPad Prism® 6 Software [nonlinear regression log(inhibitor) vs response variable slope (four parameters)]. To determine the mode of inhibition of $^{73}As(GS)_3$ by $MMA(GS)_2$, the K_i of $MMA(GS)_2$ was determined by performing $^{73}As(GS)_3$ (0.1-20 μM, 40-100 nCi) transport in the presence of three different $MMA(GS)_2$ concentrations (5, 10, and 15 μM), as described previously (Leslie et al., 2004).

All transport data were normalized as needed to correct for any difference in level of HeLa-WT-MRP1 or mutant MRP1 expressed in HEK cells relative to HEK-WT-MRP1 as determined by immunoblotting of each membrane vesicle preparation. Positive control transport experiments using $MMA(GS)_2$ or $As(GS)_3$ were run for each vesicle preparation, as described above and previously (M. W. Carew et al., 2011; Leslie et al., 2004).

1.7.10 Site-Directed Mutagenesis

Mutants of MRP1 (S905A-, S915A-, S916A-, S917A-, Y920F-, S921A-, Y920F/S921A-, Y920E/S921E-, and T931A-MRP1) were generated previously (Shukalek et al., 2016). In addition, several new potential phosphorylation mutants (S916E-, S918A-, S919A-, and S919E-MRP1) were generated using the QuikChange II XL site-directed mutagenesis kit (Stratagene, Agilent Technologies, Santa Clara, CA). pcDNA3.1(-)-MRP1 was used as the PCR template and mutagenesis was carried out according to the manufacturer's instructions using mutagenic primers from Integrated DNA Technology (Coralville, IA), sequences are available upon request. The incorporation of desired mutations was confirmed by DNA sequencing (Molecular Biology Servicing Unit, University of Alberta, Edmonton, Canada).

1.7.11 Arsenic speciation

HEK293 cells stably expressing transfected with ABCC1 or vector were exposed to MMA^V (200 μM)-supplemented media, or media without arsenic, for 24 hours. After arsenic exposure was complete, media was collected for analysis. After media collection, a parallel set of cells were washed twice with media and had fresh media added back, and were then incubated in the fresh media for an additional 2 hours. The media from these cells was then collected and the cells were washed and processed as above. Collected media was filtered through a 3000 Da centrifugal filter to remove large molecules. What passed through the filter was analyzed for different species of arsenic.

The arsenic speciation analyses were carried out using high performance liquid chromatography (HPLC) separation coupled with inductively coupled plasma mass spectrometer (ICP-MS). An Agilent 1100 HPLC composed of a binary pump, auto-sampler, column, and solvent degasser was used. The arsenic species separation was based on anion exchange chromatography using a PRP-X100, 150 mm x 4.1 mm, 5 μm, column (Hamilton, Reno, NV, USA). The mobile phase was 35 mM NH_4HCO_3, 5% methanol, pH 8.25; the HPLC flow rate was 0.8 mL/min for 4 min, and 1.5 mL/min for 46 min; and the injection volume was 50 μL. The following standards were run for every experiment: MMA^V, DMA^V, monomethylmonothiolarsonic acid (MMMTA), Dimethylmonothioarsinic acid (DMMTA), and Dimethyldithioarsinic acid (DMDTA).

The species detection was conducted on the Agilent 7500ce ICP-MS system with an octopole reaction cell (Agilent Technologies, Japan). The instrument was operated at radio frequency 1550 W, the carrier gas flow rate was 0.95 L/min, and m/z 75 was monitored for arsenic. To eliminate polyatomic ion ArCl interference on ^{75}As, helium mode was used with a gas flow rate at 3.5 mL/min.

1.7.12 Whole cell uptake and ICP-MS measurement

HEK and HeLa stables were maintained as described above. Cells were seeded in 150 mm tissue culture plates with two million cells per plate in 20 ml media. Cells were allowed to grow for 24 hours, and then their media was replaced with media containing 100 μM MMA^V for 24 hours. After 24-hour drug exposure, cells were harvested, counted and centrifuged at 5000*g* for 10 minutes. The supernatant was removed and the cells were washed with PBS. The pellets were then dissolved in 200 μl of 65% nitric acid by shaking in an orbital shaking incubator at 180 rpm for 45 minutes. The dissolved pellets were then filtered and analyzed using the ICP-MS standard addition method described above.

1.7.13 Mouse/human Abcc4/ABCC4 chimera construction

A mouse human chimera was designed to be approximately half hABCC4 and half mAbcc4. mABCC4 in pcDNA3.1(+) was used as the template, and restriction site digests were performed with either *Nhe*I and *Age*I, or *Age*I and *Xba*I, per the manufacturer's instructions. This removed

either the front half of the DNA sequence encoding the protein (nucleotides 0-2109) or the back half (nucleotides 2109-3975). The products of these digestions were resolved on an agarose gel and the product corresponding to the half remaining ABCC4 protein in the vector was excised from the gel, dissolved, and column purified.

PCR primers were constructed to amplify the two corresponding halves of mAbcc4. The primers were constructed with restriction sites so that the products of PCR could be digested to match the products of the ABCC4 digest. This PCR reaction used 50 µl water, 5 µl 10X *Pfu* buffer, 10 µM dinucleotide mix, 500 ng of template DNA (mAbcc4 construct), 3 units of *Pfu* polymerase. The PCR thermocycling protocol was:

1) 95°C for 2 min
2) 95°C for 30 sec
3) 56°C for 30 sec
4) 72°C for 9 min
5) Go to step 2 for 38 cycles
6) 72°C for 10 minutes
7) Hold at 4°C until ready to purify.

The PCR amplified half of Abcc4 was then ligated into the products of restriction digests and gel extraction/purification. The ligation reaction used 5 fmol of the vector/ABCC4 half and 40 fmol of the Abcc4 half and used T4 DNA Ligase for 16 hours at room temperature. The ligation products were then transformed into DH5 alpha cells for DNA amplification per manufacturer's instructions.

The chimera DNA was collected and used for transient transfection as in the transient transfection protocol and then vesicles were prepared as described in Section 2.2.9.

CHAPTER 3: Species differences between human and mouse ABCC4/Abcc4 function.

1.8 Introduction

Arsenic is a proven human carcinogen (IARC, 2012), to which it is estimated that 94-220 million people worldwide are exposed at levels above the World Health Organization limit of 10 ppb (Hubaux et al., 2013; Podgorski & Berg, 2020; WHO, 2012). While arsenic has been causally linked to skin, lung, and bladder tumors (IARC, 2012), it has also been associated with prostate, liver and kidney cancers (Naujokas et al., 2013), and numerous other deleterious health effects of the immune, vascular, respiratory, reproductive, neurological, and endocrine systems (Hunt et al., 2014).

For most human populations, the primary exposure source of arsenic is the consumption of contaminated ground water, which contains arsenic leached from its complex with other minerals (Cui & Jing, 2019). Other exposures of concern can occur from anthropogenic sources, including in mining, coal-burning, wood-preservation, glass-manufacturing, and electronics-manufacturing industries (Upadhyay et al., 2019).

Arsenic can enter cells *in vitro* in the form of arsenate (As^{V}) through several phosphate transporters, including the sodium/phosphate cotransporter Na^{+}/P_i-IIb (*SLC34A2*)., and in the form of As^{III} through glucose transporter GLUT1 (*SLC2A1*) and aquaglyceroporins (AQPs) 3, 7, 9, and 10 (Kaur et al., 2020; Mukhopadhyay et al., 2014; Roggenbeck et al., 2016; Villa-Bellosta & Sorribas, 2010). In the cells, arsenic is metabolized by the processes of methylation, thiolation, and conjugation with reduced glutathione (GSH, γ-Glu-Cys-Gly) (Roggenbeck et al., 2016; Thomas et al., 2007; Wang et al., 2015). Uptake of the monomethylated trivalent species

monomethylarsonous acid (MMA^{III}) by GLUT1 has been shown (Liu et al., 2006). In addition, AQP9 has been shown to allow permeation of MMA^{III}, the pentavalent monomethylarsonic acid (MMA^{V}), and the pentavalent dimethylarsinic acid (DMA^{V}) (Liu, Boles, et al., 2004; Liu, Carbrey, et al., 2004; McDermott et al., 2010).

Multidrug resistance proteins (MRPs/ABCCs) are members of the ATP-binding cassette (ABC) protein family and export substrates from the cytosol across the plasma membrane (Whitlock & Leslie, 2019). Once inside the cell, arsenic metabolites are known to be pumped out by ABCCs including ABCC1, ABCC2, and ABCC4 (Roggenbeck et al., 2016). ABCC4 transports a wide range of substrates, including hormones, cell signaling molecules, and drugs (Wen et al., 2015). ABCC4 is found in the kidney, liver, erythrocytes, pancreas, platelets, brain, adrenal glands, and cardiomyocytes, with mRNA detected in other tissues (Jedlitschky et al., 2004; Klokouzas et al., 2003; Konig et al., 2005; Nies et al., 2004; Rius et al., 2003; Sassi, 2019; van Aubel et al., 2002; Zelcer et al., 2003).

ABCC4 has several potential physiological functions. It helps modulate cellular cAMP levels through efflux, making it potentially relevant in many cell signaling pathways (Sassi et al., 2008; Whitlock & Leslie, 2019). ABCC4 transport of bile salts and urate has also been observed (Rius et al., 2006; Van Aubel et al., 2005). Further, ABCC4 transports prostaglandins E_1, E_2 and $F_{2\alpha}$, thromboxane B_2, conjugated steroids estradiol 17-β-D-glucuronide ($E_2$17βG) and dehydroepiandrosterone sulfate (DHEAS), and sphingosine-1-phosphate (Chen et al., 2001; Reid et al., 2003; Rius et al., 2005; Vogt et al., 2018; Zelcer et al., 2003).

In addition to important physiological roles, ABCC4 has important roles in defense against xenobiotics. Through the use of *Abcc4*$^{(-/-)}$ mice, Abcc4 has been shown to be important for limiting the level of the anti-cancer drug topotecan in the brain, which, together with its presence in human brain tissue suggests a role in blood brain barrier function (Kanamitsu et al., 2017; Leggas et al., 2004; Nies et al., 2004). ABCC4 is localized to the basolateral surface of hepatocytes, and the apical surface of kidney proximal tubule cells, placing it in a position to be relevant in the urinary elimination of hepatic metabolites. Since arsenic is predominantly metabolized in the liver and eliminated in the urine, human ABCC4 (hABCC4)[1] was investigated in vitro as an arsenic transporter, where it was found to transport arsenic in the forms of $MMA(GS)_2$ and DMA^V, forming a complete efflux pathway for urinary elimination of hepatic arsenic metabolites (Banerjee et al., 2014). Several single nucleotide polymorphisms (SNPs) of hABCC4 are responsible for changes in arsenic transport capabilities in vitro, and this has been proposed as a potential contributing factor to inter-individual risk of developing arsenic-induced disease (Banerjee et al., 2016).

After identification of hABCC4 as a transporter of DMA^V and $MMA(GS)_2$ it was a natural next step to explore the role of hABCC4/mAbcc4 in arsenic toxicokinetics using an *in vivo* model, such as comparing the handling of arsenic species by *Abcc4*$^{(-/-)}$ with *Abcc4*$^{(+/+)}$ mice. The hABCC4 and mAbcc4 orthologues have an amino acid similarity and identity of 92% and 87%, respectively (Fig. 3.1). There are some documented examples of species differences

[1] Conventionally, human ABC transporters are referred to with all capital letters, while other species are referred to with only the first letter capitalized. For clarity, from this point forward, human, mouse and rat ABCC4/Abcc4 will be referred to as hABCC4, mAbcc4, and rAbcc4.

between hABCC4 and mAbcc4; for example, hABCC4 was found to be necessary for dendritic cell migration important for a normal immune response, while knock-out of mAbcc4 had no influence on this process (van de Ven et al., 2009; van de Ven et al., 2008). Another difference between hABCC4 and mAbcc4 is in their affinities for cGMP, with mAbcc4 having a 100-fold higher K_m than hABCC4 (de Wolf et al., 2007). Given these mAbcc4/hABCC4 differences it was important to characterize the ability of mAbcc4 to transport and protect cells from inorganic arsenic metabolites, prior to *in vivo* studies.

The first objective of this study was to map the epitope of the anti-ABCC4 antibody M_4I-10 to determine whether it could be used to quantify relative levels of hABCC4, mAbcc4, and Abcc4 from other species. The second objective was to compare cellular protection conferred by mAbcc4 and hABCC4 against inorganic and methylated arsenic metabolites. The third was to characterize any differences in cytotoxicity profiles by measuring transport of arsenic metabolites using mAbcc4/hABCC4-enriched membrane vesicles. The findings in this chapter serve as a foundation for better understanding hABCC4/mAbcc4 function in arsenic detoxification, and how this function differs between mouse and human, while giving us insight on the usefulness of mouse models for investigation of mAbcc4 influence on whole-body arsenic handling. Further work on this topic extends in Appendix 1 to the construction of an interspecies chimeric mAbcc4/hABCC4 and the investigation of substrate transport by the chimera in HEK293 vesicles; and, in Appendix 2 to the characterization of rAbcc4 using similar methods as within this chapter.

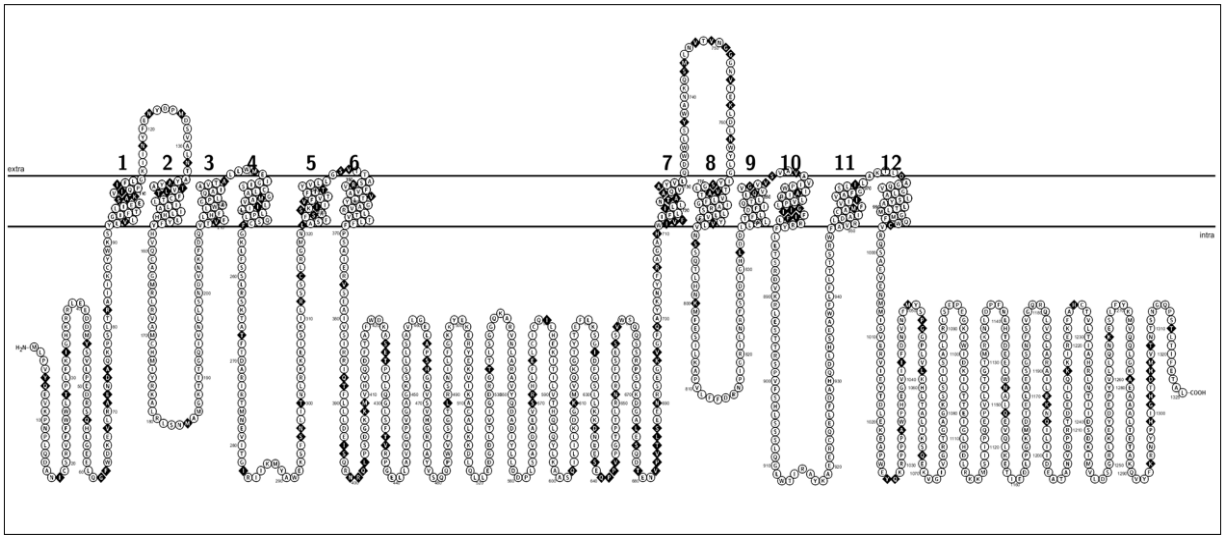

Figure 3.1. The predicted secondary structure of hABCC4 with amino acids that differ in mAbcc4 indicated in black. Made with software from (Omasits, 2013).

1.9 Results

1.9.1 Epitope Mapping

The rat mAb M_4I-10 is known to cross-react with mAbcc4, hABCC4, and rAbcc4 and was raised against the hABCC4 peptide (amino acids 372-431) fused to maltose binding protein (Leggas et al., 2004). In order to use the M_4I-10 antibody to compare hABCC4 and mAbcc4 levels, its epitope within hABCC4 and mAbcc4 needs to be identical. Thus, the M_4I-10 antibody epitope was mapped and the sequences between mAbcc4 and hABCC4 compared. Two cellulose membrane arrays, one of 55 hexapeptides and one of 53 decapeptides were probed with M_4I-10 MAb (Fig 3.2A). The peptides covered the entire sequence of the segment of hABCC4 against which the antibody was raised, and shifted by one amino acid each (Fig 3.2A). The synthesized peptides corresponding to amino acids 410-423 of hABCC4 interacted with M_4I-10, with any 6 amino acids of ^{410}VHVQDFTAF^{418} being sufficient for binding. The "sufficient" window is defined as the window within which any peptide at the highest resolution used in this study (hexapeptide) would have detectable binding (Figure 3.2 A, B). Further, amino acids ^{414}DF^{415} were necessary for binding but not sufficient, and amino acids ^{412}VQDFTAFWDK^{421} gave maximal binding (Fig. 3.2A,B).

The octapeptide, ^{411}HVQDFTAF^{418}, that contained both the necessary and sufficient region was constructed and used in a competitive immunoassay to verify the location and specificity of the mapped M_4I-10 epitope. The octapeptide completely inhibited the M_4I-10 antibody binding to ABCC4 at 50 µg/ml (Figure 3.2C). This assay was run in parallel with a negative control, the ABCC4 antibody (ALX 210-856), raised against a synthetic peptide

containing hABCC4 amino acids 1249-1268, and as expected, ^{411}HVQDFTAF^{418} did not outcompete this antibody (Fig. 3.2C). These data reveal that the M_4I-10 epitope is located in a region that is 100% conserved between mAbcc4 and hABCC4 (Fig. 3.2C). M_4I-10 can therefore be used to accurately compare relative hABCC4 and mAbcc4 protein levels.

A)

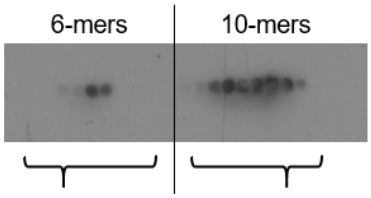

#	Hexapeptide	Reactivity
38	MVHVQD	-
39	VHVQDF	+
40	HVQDFT	+
41	VQDFTA	+++
42	QDFTAF	++
43	DFTAFW	-

#	Decapeptide	Reactivity
35	DGKKMVHVQD	-
36	GKKMVHVQDF	+
37	KKMVHVQDFT	+
38	KMVHVQDFTA	++
39	MVHVQDFTAF	+++
40	VHVQDFTAFW	++++
41	HVQDFTAFWD	++++
42	VQDFTAFWDK	+++++
43	QDFTAFWDKA	++++
44	DFTAFWDKAS	++
45	FTAFWDKASE	-

B)

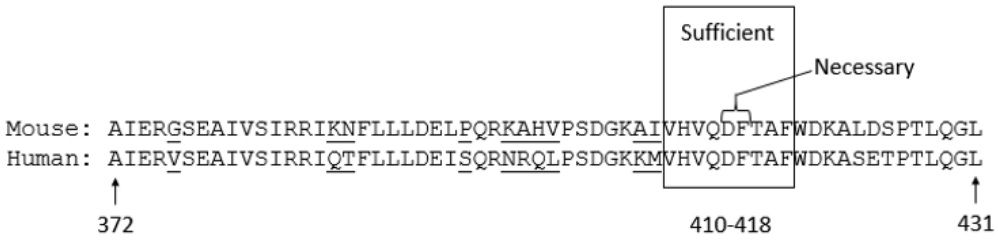

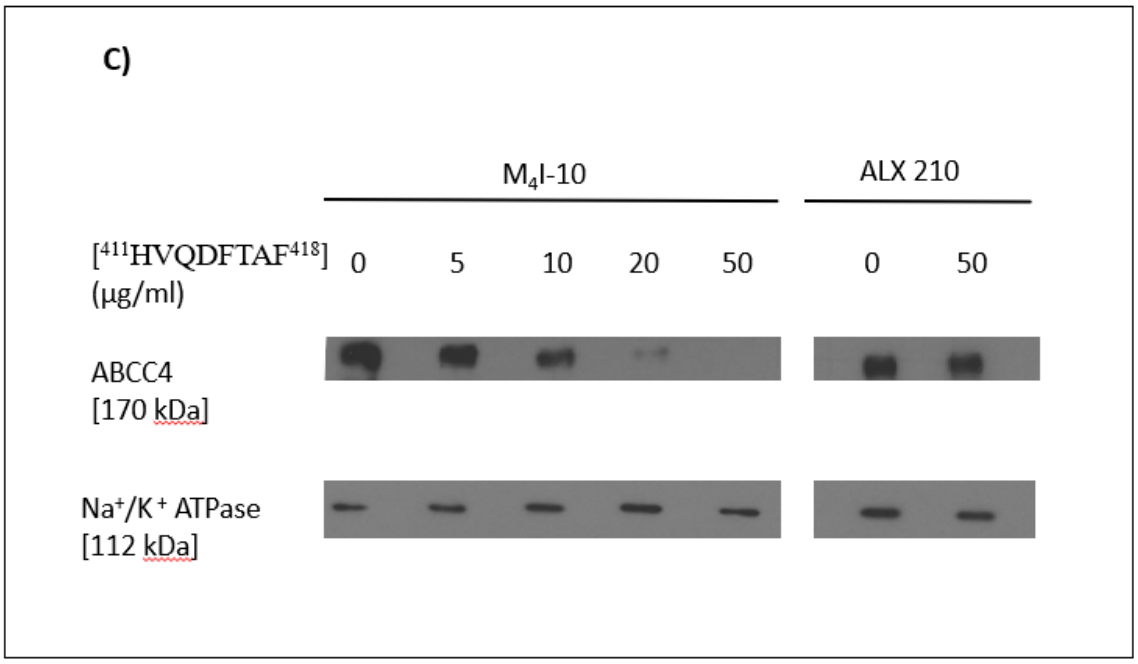

Figure 3.2. Epitope mapping for the rat monoclonal anti-hABCC4 (M_4I-10) antibody. A) The peptide array was created as a series of 6-mers and 10-mers that spanned across the entire sequence against which the antibody was raised (amino acids 372-431), shifting by one amino acid. Immunoblotting with M_4I-10 (1:1000) showed the peptides that interact most strongly with the antibody. B) The epitope region of ABCC4 is 100% conserved between hABCC4 and mAbcc4. Residues ^{411}HVQDFTAF^{418} are labelled as the determined epitope, with ^{414}D and ^{415}F as necessary for M_4I-10 binding. C) hAbcc4 samples were blotted and probed with antibody M_4I-10 (1:30 000 dilution) that had been preincubated with different concentrations of the peptide determined to be the epitope to verify that it could fully saturate the antibody. An antibody raised against a different fusion protein (ALX 210; 1:15,000 dilution) was used in a parallel attempt at inhibition. D) 10 µg of total protein in the form of whole cell lysates of HEK cell lines stably expressing hABCC4, mAbcc4, or vector transfected, were resolved by SDS-PAGE and probed with a 1:10,000 dilution of M_4I-10.

1.9.2 mAbcc4 does not confer resistance to arsenicals in HEK cells

HEK 293 cell lines stably expressing mAbcc4 (HEK-mAbcc4) and empty vector (HEK-V) were generated and treated with varying concentrations of inorganic arsenic and methylated metabolites (As^{III}, As^{V}, MMA^{III}, MMA^{V}, DMA^{III}, and DMA^{V}) and 6-MP as a positive control (Chen et al., 2001). The EC_{50} value for each arsenic species and 6-MP was determined, and the relative resistance was calculated from the ratio of the EC_{50} values for HEK-mAbcc4 and HEK-V. Table 3.1 summarizes the relative resistance of HEK-mAbcc4 against the arsenicals, and no differences between HEK-mAbcc4 and HEK-V were found. This contrasts with HEK-hABCC4 stable cell lines, which are resistant relative to vector controls to all of the arsenicals tested above except arsenite (Banerjee et al., 2014). Although mAbcc4 conferred no resistance to any arsenical, it conferred a 45-fold resistance to 6-MP (Table 3.1). This resistance to 6-MP was roughly 9-fold higher than the resistance to 6-MP conferred by hABCC4 (Banerjee et al., 2014). These results were repeated in two additional independently derived HEK-mAbcc4 cell clones.

Previously, hABCC4 was shown to confer significantly higher levels of resistance against DMA^{III}, MMA^{V} and DMA^{V} after GSH depletion of cells with BSO (Banerjee, Carew et al., 2014). To determine if GSH-depletion of cells might influence the ability of mAbcc4 to confer resistance against these three arsenicals, cells were depleted of GSH prior to treatment. Consistent with GSH-containing conditions, mAbcc4 did not confer resistance to DMA^{III}, MMA^{V}, or DMA^{V} after BSO treatment (Table 3.1).

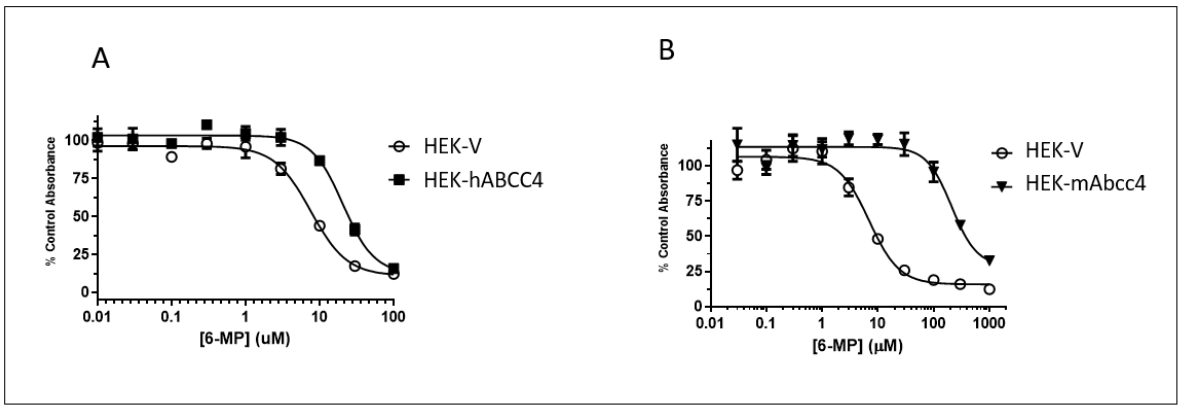

Figure 3.3. Representative cytotoxicity experiments in stably transfected HEK293 cells. HEK293 cells stably expressing hABCC4 (A) or mAbcc4 (B) were compared with vector-transfected cells in their ability to survive a range of concentrations of 6-MP for 3 days using the MTS cytotoxicity assay. Each point shows the mean of 4 absorbance readings (4 wells of a 96-well plate per condition) at each point with SD error bars. Relative resistance is calculated from the curve shift at 50% control absorbance (EC_{50}). Graphs are representative experiments and mean values from multiple experiments are summarized in Table 3.1.

TABLE 3.1. Resistance of mAbcc4 transfected HEK293 cells to inorganic and methylated arsenic species compared with hABCC4

	EC_{50} (± S.D.) (μM)		RR	RR
	HEK-V	HEK-mAbcc4-1A6-37[b]	Mouse	Human[c]
As^{III} (*n = 4)*	6.4 ± 1.5	5.5 ± 3.6	0.9	0.7
As^{V} *(n = 4)*	57 ± 22	43 ± 18	0.7	2.9*
MMA^{III} *(n = 5)*	2.8 ± 0.5	2.3 ± 0.8	0.8	1.7*
MMA^{V} *(n = 3)*	8602 ± 795	9847 ± 517	1.1	1.5*
MMA^{V} + BSO *(n = 2)*	3325, 3017	2597, 2690	0.8	2.0*
DMA^{III} (n = 7)	2.3 ± 2.1	2.3 ± 1.5	1.0	2.0*
DMA^{III} + BSO *(n = 3)*	4.5 ± 1.9	3.3 ± 0.3	0.7	2.9*
DMA^{V} *(n = 5)*	1356 ± 386	1221 ± 339	0.9	1.6*
DMA^{V} + BSO *(n = 5)*	5616 ± 2067	4589 ± 1338	0.8	2.5*
6-MP *(n = 7)*	3.4 ± 1.6	156 ± 88	45*	5.4*

*EC_{50} for HEK-mAbcc4 or HEK-hAbcc4 is significantly different from HEK-V, $P < 0.05$ (Student's *t* test).

[a]Ratio of EC_{50}HEK-mAbcc4/ EC_{50} HEK-Vector

[b]Similar results were obtained for two additional clones (HEK-mAbcc4-1C1-1-3 and –mAbcc4-1C1-2-62)

[c](Banerjee et al., 2014). Similar results were obtained with one additional independently derived hABCC4 stable cell clone.

1.9.3 Mouse Abcc4 does not transport DMA^V or $MMA(GS)_2$ in HEK vesicles

Transport studies were conducted with mAbcc4- and hABCC4-enriched HEK293 membrane vesicles made from cells transiently transfected with mAbcc4 along with an empty vector transfected control. The prototypical hABCC4 substrate $E_2$17βG was run as a positive control on the same membrane vesicle preparations, and mAbcc4 and hABCC4 vesicle preparations both had activity significantly higher than empty vector expressing controls (Fig. 3.4B). Similar to the higher resistance of mAbcc4 than hABCC4 to 6-MP, mAbcc4 also transports $E_2$17βG with over two-fold higher activity than hABCC4 does ($p < 0.01$, Student's t-test). While hABCC4 showed expected transport activity for its previously described substrates, DMA^V and $MMA(GS)_2$, (Banerjee et al., 2014) consistent with cytotoxicity results, mAbcc4 showed no transport activity for either (Figure 3.4 C, D).

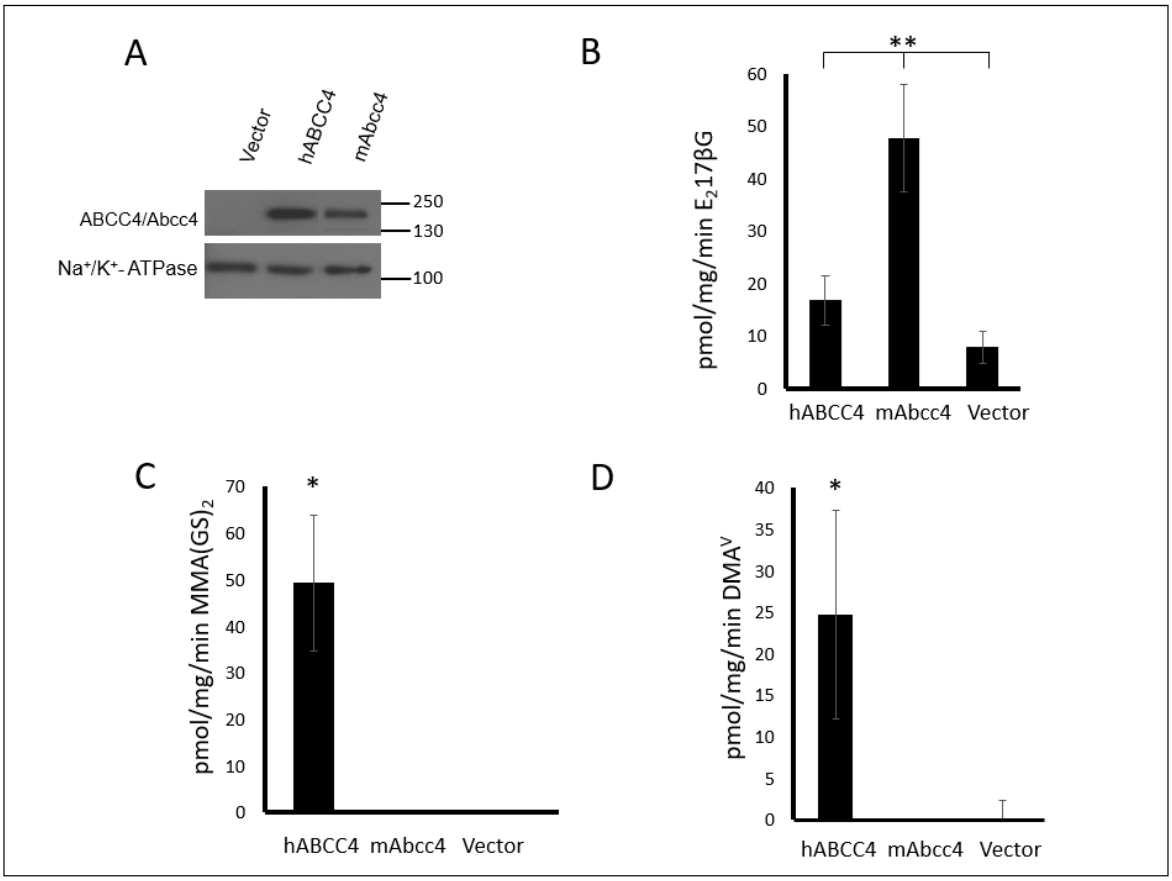

Figure 3.4. The transport of $E_2$17βG, $MMA(GS)_2$, and DMA^V by hABCC4- and mAbcc4-enriched membrane vesicles prepared from transiently transfected HEK293 cells. (A) ABCC4/Abcc4 protein levels were determined by resolving 1 µg of total protein from membrane vesicles prepared from HEK293 cells expressing pcDNA3.1(+)-neomycin (vector), pcDNA3.1(+)-hABCC4, or pcDNA3.1(+)-mAbcc4 and immunoblotting with M_4I-10 antibody. Blots were then stripped and reprobed for Na^+/K^+-ATPase as a loading control. (B) Vesicles (5 µg protein per experiment) were incubated with $E_2$17βG (400 nM, 40 nCi) for 1.5 minutes. The transport was stopped by dilution in ice-cold tris-sucrose buffer (TSB), the vesicles were filtered and washed, and the $E_2$17βG was quantified by liquid scintillation counting. (C,D) Arsenic

transport was measured using the same membrane vesicle preparations as in (B) (20 μg protein per experiment) by incubating them with (C) $MMA(GS)_2$ for 3 minutes or (D) DMA^V for 5 minutes (both at 1 μM). Transport was stopped by diluting in ice-cold TSB and the vesicles were pelleted and processed for arsenic quantification by inductively coupled plasma mass spectrometry. Bars represent mean determinations of three independent experiments with standard deviation (SD). All incubations were at 37ºC. * Significantly different from vector by student's t-test ($p < 0.01$). **All pairs significantly different (one way ANOVA with Bonferroni post hoc correction).

1.9.4 Influence of endogenous hABCC4 knock-down on mAbcc4 resistance to arsenic

Previously reported cellular protection against arsenicals in HEK cells conferred by hABCC4 relative to vector were low (1.5 to 3-fold) (Banerjee et al. 2014). Thus, the low but detectable levels of endogenous hABCC4 in HEK-vector cells could mask the possibly less substantial effects of transfected mAbcc4 on arsenicals by raising baseline resistance to arsenicals. To test this possibility, endogenous hABCC4 levels in HEK293 cells were reduced through shRNA knockdown, and the effect on arsenical toxicity was measured. Two shRNA sequences (7334 and 5264) targeting hABCC4 were found to substantially knock down hABCC4, while 9334 was less effective (Fig 3.5A). The 5264 sequence was chosen as the most effective and used for further knockdown experiments. A non-target shRNA sequence was delivered as a negative control to activate the same RNA-induced silencing complex (RISC) without hABCC4 knock down. Endogenous levels of hABCC4 were compared with overexpression levels in stably transfected HEK293 cells expressing hABCC4 and mAbcc4 (Fig. 3.5B). The endogenous level of hABCC4 in HEK cells is markedly lower than the transfected counterparts, and only detected upon over-exposure. Knockdown of endogenous hABCC4 in the cell lines was measured before and after the cytotoxicity experiments and it was found that knockdown was consistent and stable (representative blot from pre-experiment Fig. 3.5C). HEK-V cells were subjected to three conditions: untreated (UT) with shRNA, treated with nontarget (NT) shRNA, or treated with ABCC4-targeted shRNA resulting in endogenous ABCC4 being knocked down (KD). The EC_{50} values for NT and KD conditions were each compared to that of the UT condition to obtain a fold-difference. Almost complete knock-down

of endogenous hABCC4 in the HEK-V cell line did not result in a significant difference (in fold-difference from UT condition) in resistance against As^{III}, As^{V}, MMA^{III}, or DMA^{V} compared to the non-target shRNA control (Fig. 3.5 D-G). This result suggests that endogenous hABCC4 levels are not masking a low level of resistance conferred by mAbcc4 in the HEK-mAbcc4 cell line.

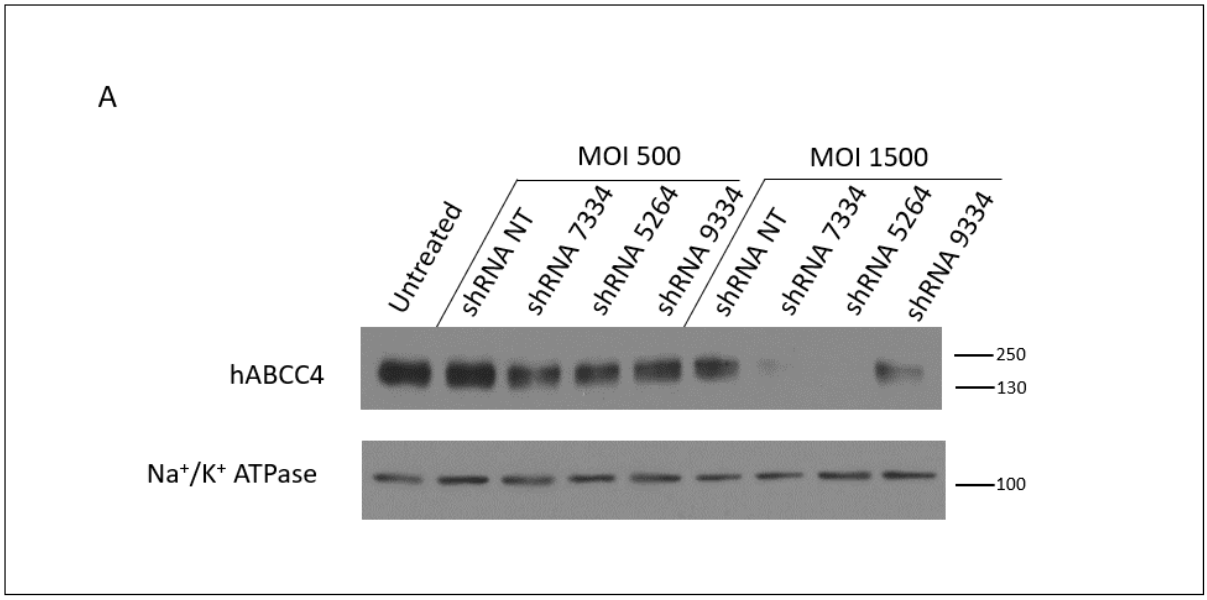
A
MOI 500
MOI 1500
Untreated
shRNA NT
shRNA 7334
shRNA 5264
shRNA 9334
shRNA NT
shRNA 7334
shRNA 5264
shRNA 9334
hABCC4
Na+/K+ ATPase
250
130
100

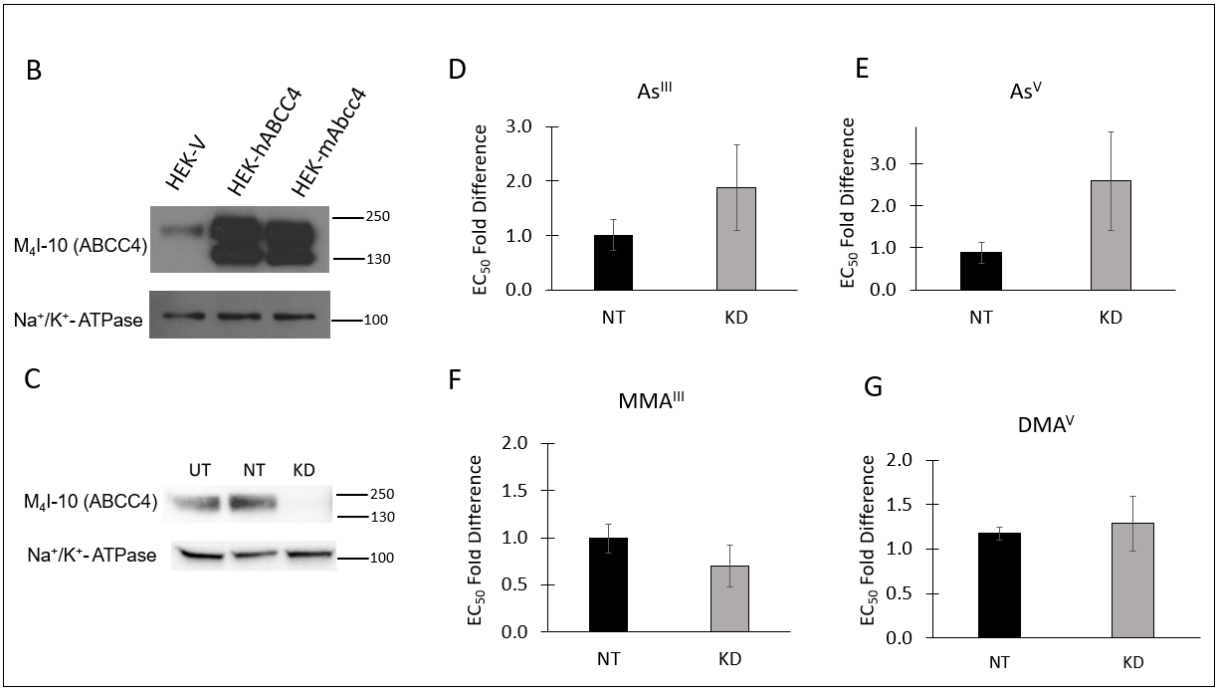
B
HEK-V
HEK-hABCC4
HEK-mAbcc4
M4I-10 (ABCC4)
Na+/K+-ATPase
250
130
100
C
UT
NT
KD
M4I-10 (ABCC4)
Na+/K+-ATPase
250
130
100
D
AsIII
EC50 Fold Difference
3.0
2.0
1.0
0.0
NT
KD
E
AsV
EC50 Fold Difference
3.0
2.0
1.0
0.0
NT
KD
F
MMAIII
EC50 Fold Difference
2.0
1.5
1.0
0.5
0.0
NT
KD
G
DMAV
EC50 Fold Difference
2.0
1.5
1.0
0.5
0.0
NT
KD

Figure 3.5. Lentiviral knock-down of endogenous hABCC4 in HEK293-V cells and cytotoxicity. (A) Three shRNA sequences specific for hABCC4 (7334, 5264, 9334) and one non-target (NT) negative control shRNA were introduced to HEK293 cells expressing pcDNA3.1(+)-hABCC4 (human ABCC4) via lentiviral particles at a ratio of either 500 or 1500 viral particles per cell (MOI) to determine which shRNA molecules achieved the greatest knockdown. B) Endogenous hABCC4 levels were compared with overexpressed hABCC4 levels and mAbcc4 levels in HEK293 cells expressing pcDNA3.1(+)-neomycin (vector), pcDNA3.1(+)-hABCC4 (hABCC4), or pcDNA3.1(+)-mAbcc4 (mAbcc4) by resolving 10 µg of total protein from whole cell lysates with SDS-PAGE and immunoblotting with M_4I-10 antibody. (C) hABCC4 level monitoring of cells at the beginning of the 5-day cytotoxicity experiment. Protein levels were determined 3 days after shRNA knock down by shRNA 5264 (MOI 1500) (KD) and a negative control non-target treatment (1500 MOI) (NT) alongside cells not treated with shRNA (UT) by resolving 10 µg of total protein from whole cell lysates of HEK293 cells expressing pcDNA3.1(+)-neomycin (vector) and immunoblotting with M_4I-10 antibody. Cytotoxicity of arsenicals was measured in the cells after knockdown of endogenous hABCC4 (KD) or after treatment with negative control non-target shRNA (NT). The EC_{50} of As^{III} (D), As^{V} (E), MMA^{III} (F), or DMA^{V} (G) were measured for the two conditions and compared to cells not treated with shRNA. The Y-axis shows the fold difference in the concentration required to kill half the cells (EC_{50}) between either NT and shRNA-untreated or KD and shRNA-untreated. Bars show the mean of three independent experiments, each with 4 replicate determinations. No significant differences were detected between knock-down and non-target control conditions (Student's t-test).

1.9.5 *Abcc4*$^{+/+}$ MEFs confer higher levels of resistance to arsenate than *Abcc4*$^{-/-}$ MEFs

HEK-mAbcc4 6-MP resistance levels (Table 3.1) were well above HEK-V (suggesting that mAbcc4 was fully functional), and endogenous hABCC4 in HEK293 cells does not seem to be contributing to masking the ability of mAbcc4 to confer resistance to arsenicals (Figure 3.5). A remaining possibility was that mAbcc4 required expression in a mouse cellular environment in order to specifically confer resistance to arsenicals. Thus, the EC_{50} toxicity values of the 6 arsenic species in wild-type mouse embryonic fibroblasts (MEFs) (*Abcc4*$^{+/+}$) were compared with mAbcc4 knock out (*Abcc4*$^{-/-}$) MEFs using the tetrazolium based MTS cytotoxicity assay, as was done with the HEK stable cell lines (Figure 3.6). In contrast with mAbcc4 expressed in HEK293 cells, MEF-*Abcc4*$^{+/+}$ cells conferred a significant level of resistance to arsenate (2.7-fold) relative to MEF-*mAbcc4*$^{-/-}$ (Table 3.2). There was no other significant resistance against other arsenic species.

This result was somewhat surprising because mAbcc4 was functional in HEK293 cells using multiple assays, just not in the transport of or resistance against the arsenic species tested. Thus, differences, in addition to mAbcc4 levels, could exist between the MEF-Abcc4$^{-/-}$ and MEF-Abcc4$^{+/+}$ cell lines. One obvious protein difference to explore was mouse Abcc1, well characterized to confer cellular protection against inorganic arsenic (Stride et al., 1997). Membrane vesicles were prepared from the cell lines as described above, and protein was resolved by SDS-PAGE and immunoblotted with the MRPr1 antibody. After correcting for the amount of protein loaded using Na^+/K^+ ATPase as a loading control, the Abcc4$^{-/-}$ MEFs did not

have significantly higher levels of Abcc1 (*Abcc4*$^{-/-}$ MEFs : *Abcc4*$^{+/+}$ MEFs ABCC1 levels ratio = 1.04, SD 0.18, n=5, Figure 3.6(C)).

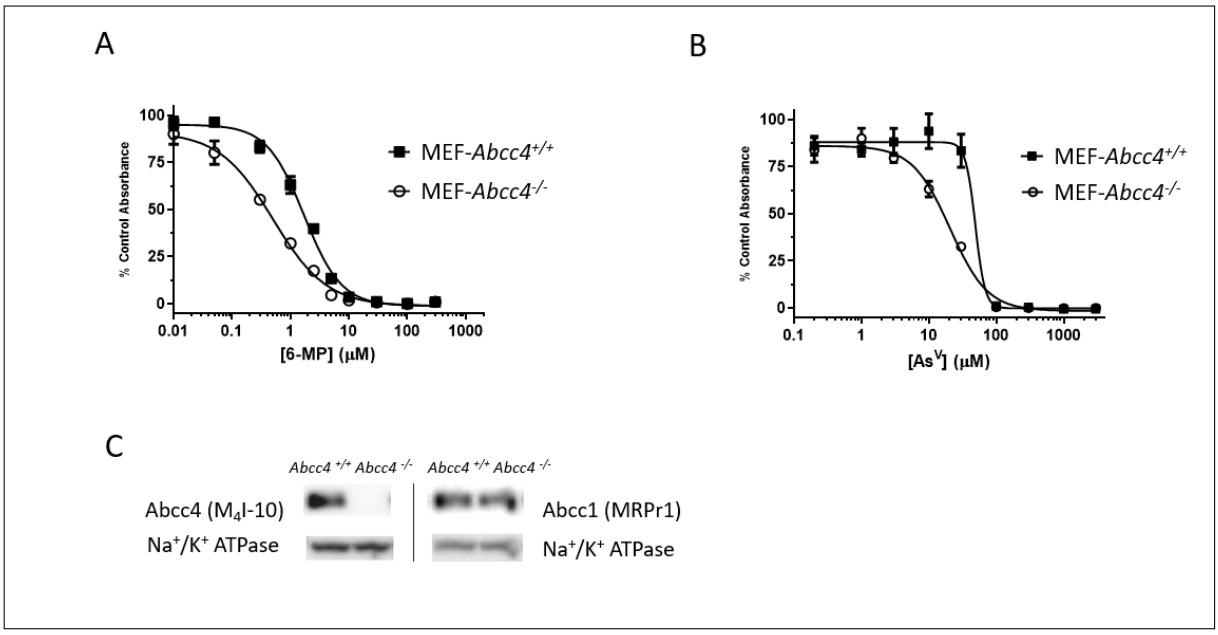

Figure 3.6. Representative cytotoxicity experiments in MEF cells. MEF cells with endogenous mAbcc4 (MEF-*Abcc4*$^{+/+}$) were compared to MEF cells with Abcc4 knocked out (MEF-*Abcc4*$^{-/-}$) in their ability to survive a range of concentrations of (A) 6-MP or (B) arsenate for 3 days using the MTS cytotoxicity assay. Each point represents the mean of 4 absorbance readings (4 wells of a 96-well plate per condition) ±SD. Graphs are representative experiments and mean values from multiple experiments are summarized in Table 3.2.(C) Representative immunoblot comparing Mrp4 and Mrp1 levels between the MEF cell lines. 10 µg of total protein from whole

cell lysates were resolved by 6% PAGE, transferred to a PVDF membrane and probed with either M_4I-10 or MRPr1 antibody (1:10,000 dilution), and visualized per section 2.2.3.

TABLE 3.2. Resistance of MEF-*Abcc4*$^{+/+}$ and MEF-*Abcc4*$^{-/-}$ cells to inorganic and methylated arsenic species

	EC_{50} (± S.D.) (μM)		Relative Resistance[a]
	MEF-*Abcc4*$^{-/-}$	MEF-*Abcc4*$^{+/+}$	
As^{III} (*n = 4)*	1.9 ± 0.9	5.1 ± 2.3	2.7
As^{V} *(n = 4)*	16 ± 2.7	43 ± 1.0*	2.7
MMA^{III} *(n = 3)*	1.8 ± 1.4	1.8 ± 0.8	1.0
MMA^{V} *(n = 3)*	939 ± 508	1059 ± 230	1.1
DMA^{III} *(n = 3)*	1.3 ± 1.1	1.5 ± 1.3	1.1
DMA^{V} *(n = 3)*	1798 ± 444	919 ± 405	0.5
6-MP *(n = 5)*	1.0 ± 0.5	3.0 ± 1.6*	3.1

*EC_{50} for MEF-*Abcc4*$^{+/+}$ is significantly different from MEF-*Abcc4*$^{-/-}$, $P < 0.05$ (paired *t*- test).
[a]Ratio of EC_{50}(MEF-*Abcc4*$^{+/+}$) / EC_{50} (MEF-*Abcc4*$^{-/-}$)

1.10 Discussion

Arsenic is both an environmental carcinogen and a chemotherapeutic agent. To study arsenic toxicokinetics, intact mouse models provide a potential tool. On the whole, there are major differences in the outcomes of arsenic exposure in humans and mice, making mice a poor model for human arsenic handling (Whitlock, 2021). Nevertheless, in developing arsenic-containing anticancer agents for humans, mice are used in both efficacy and toxicity experiments (Bureta et al., 2019; Hao et al., 2016; Liu et al., 2020; Xin et al., 2018). Further, mice have been used extensively in arsenic carcinogenicity studies (Tokar et al., 2010). To understand how analogous to humans these mouse models are, and interpret the data from these studies, we need to understand the difference between mouse and human orthologues of arsenic-relevant proteins.

In the current study, differences in the ability of mAbcc4 and hABCC4 to confer cellular protection against and transport multiple chemical forms of arsenic were explored. To begin with, the epitope of the M_4I-10 antibody, reported to cross react with hABCC4, mAbcc4, and rAbcc4 was mapped to a region conserved between hABCC4 and mAbcc4, allowing the use of this antibody to compare their relative levels. Using the mapped epitope sequence (Figure 3.1A), the ability of this antibody to react with other Abcc4 species can be predicted. In Table 3.3, the amino acid sequences of ABCC4/Abcc4 in select species are compared to the mapped epitope. M_4I-10 should react with equal affinity to human (*sapiens*), rat (*norvegicus*), mouse (*musculus*), wild pig (*scrofa*), rhesus monkey (*mulatta*), and chimpanzee (*troglodytes*) ABCC4/Abcc4. M_4I-

10 will likely react with but have lower affinity for Abcc4 of rabbit (*cuniculus*) and guinea pig (*porcellus*), which differ by one amino acid. In contrast, frog (*laevis*), zebrafish (*rerio*), fruit fly (*melanogaster*), and worm (*elegans*) Abcc4 have significantly or completely different sequences at the epitope site.

TABLE 3.3. Sequence alignment of ABCC4/Abcc4 of various species with the epitope sequence of the M_4I-10 antibody.

M_4I-10 Epitope:	**VHVQDFTAF**
H. sapiens:	VHVQDFTAF
M. musculus:	VHVQDFTAF
R. norvegicus:	VHVQDFTAF
P. troglodytes:	VHVQDFTAF
M. mulatta:	VHVQDFTAF
S. scrofa:	VHVQDFTAF
C. porcellus:	VDVQDFTAF
O. cuniculus:	VHVQDFTAS
X. laevis:	VQIQDLTCY
D. rerio:	VEMQDLICY
D. melanogaster:	IEFSQFQAR
C. elegans:	ICLKEACLS

All sequences downloaded from UniProt Knowledgebase at https://www.uniprot.org/uniprot.

Differences in the ability of hABCC4 and mAbcc4 to confer resistance to inorganic and methylated arsenic species when stably expressed in HEK293 cells were explored. Unlike hABCC4, when mAbcc4 was stably expressed in HEK293 cells, it did not confer protection against any of the arsenic chemical forms tested. In experiments run at the same time, HEK-mAbcc4 cells had a 45-fold higher EC_{50} value than HEK-V for the positive control 6-MP, showing that the cell lines (and mAbcc4) were functioning properly. To test if this lack of resistance could be an artifact of the stable cell clone, two independently derived HEK-mAbcc4 stable cell clones were tested, and similar results were obtained. Consistent with the cytotoxicity data, transport of $MMA(GS)_2$ and DMA^V (well characterized hABCC4 substrates) by mAbcc4-enriched HEK293 membrane vesicles was not detected under the conditions tested. Transport experiments were carefully controlled for with hABCC4-enriched vesicles used as a positive experimental control. Furthermore, mAbcc4-enriched membrane vesicle preparations were functional, as determined by $E_2$17βG transport assays.

HEK293 cells are known to have low levels of endogenous hABCC4. To rule out the possible masking of mAbcc4 protection from arsenicals by this endogenous hABCC4 level, shRNA knockdown studies were performed. When HEK293 cells with hABCC4 knocked down were compared with non-target shRNA controls (relative to shRNA free controls), no significant difference was observed, suggesting that endogenous hABCC4 is not high enough to influence the cytotoxicity of these arsenic species.

Overall, the HEK293-mAbcc4 cytotoxicity and mAbcc4-enriched membrane vesicle transport data provided strong evidence that mAbcc4 is not protective against the six arsenicals tested. This is in contrast with previously published hABCC4 data (Banerjee et al., 2014), the striking differences between mAbcc4 and hABCC4 laid the foundation for using a chimera approach to narrow down the hABCC4 DMA^V and $MMA(GS)_2$ binding site, as described in Appendix 1.

Surprisingly, the lack of resistance to arsenic in the presence of mAbcc4 was only partially true in the native mouse cell environment of MEF cells. MEF cells expressing endogenous levels of mAbcc4 (MEF-*Abcc4*$^{+/+}$) and cells with no detectable mAbcc4 (MEF-*Abcc4*$^{-/-}$) were tested. As expected, MEF-mAbcc4$^{+/+}$ cells were more resistant to the positive control 6-MP, though it was lower than that conferred by mAbcc4 in HEK cells reported in section 3.2.2 (Banerjee et al., 2014; Chen et al., 2001). The resistance to As^V in MEF-*Abcc4*$^{+/+}$ compared to MEF- *Abcc4*$^{-/-}$ cells was a surprise. Given that in HEK293 cells mAbcc4 conferred an 8-fold higher level of resistance to 6-MP, and mAbcc4-enriched vesicles prepared from HEK293 cells transported $E_2$17βG at a 3-fold higher activity than hABCC4, cell environment was not expected to have a major impact. In the vesicle preparation, virtually all cytoplasm components are removed, and added back are only the bare necessities of transport, including osmolarity and pH adjusters and ATP. This suggests that the protein is not particularly sensitive to being in a native cytosolic environment, and that it only needs a few factors in order to conduct its transporter function.

If cellular environment is important, a potential explanation for the difference in Abcc4 function in different cell lines is that Abcc4 has different post-translational modifications in the different cell lines, perhaps via differential phosphorylation by mouse vs human kinases. This would fit with our growing knowledge of the effect of phosphorylation on ABCCs (Banerjee et al., 2018; Shukalek et al., 2016).

An alternative explanation for our observation that MEF-mAbcc4$^{+/+}$ cells have higher resistance to As^{V} than MEF-Abcc4$^{-/-}$ and HEK-mAbcc4 cells are no different than HEK-V cells is that a compensatory mechanism may exist to make up for the lack of Abcc4, possibly with cell line differences. Several examples of Abcc4 having another ABC protein that can compensate for it are known. For example, the ABC efflux transporter breast cancer resistance protein (mBcrp/mAbcg2) can compensate during Abcc4 knockout to lower methotrexate accumulation, mAbcc3 can compensate for Abcc4 knockout in cefadroxil absorption, and both ABC efflux transporters P-glycoprotein (Abcb1) and Abcg2 can compensate for Abcc4 knockout in reducing brain accumulation of camptothecin analogues (de Waart et al., 2012; Lin et al., 2013; Sane et al., 2014). Further, given that the measured end point in this study was toxicity, this could be explained equally well by some unknown difference in uptake or metabolism pathway that occurs in response to Abcc4 knockdown. In order to fully understand the extent to which Abcc4 is responsible for the arsenic resistance seen in MEF cells, further study will be needed to include other proteins that may form yet to be discovered synergistic and/or compensatory mechanisms with Abcc4 for arsenicals.

The most obvious export pathway to check for differential levels between the MEF-Abcc4$^{+/+}$ and MEF-Abcc4$^{-/-}$ cells was Abcc1. The level of Abcc1 was similar between the MEF-Abcc4$^{+/+}$ and -Abcc4$^{-/-}$ cell lines, and therefore is unlikely to contribute to the As^V resistance observed. Current studies underway in the Leslie lab are investigating whole cell accumulation in the MEF cell line pair and using the Abcc4 inhibitor ceefourin-1 in cytotoxicity experiments to look further into the potential role of Abcc4 in the resistance to As^V seen in MEFs

If arsenic exposure induced expression of other proteins, this should have happened equally in the mAbcc4 $^{-/-}$ and $^{+/+}$ cell lines. Thus, the differences observed likely either are due to a change that was induced by the knockout, such as compensation by another protein, or indeed show that mAbcc4 acts differently in different cells. If hABCC4 and mAbcc4 have different functions, and/or if the proteins can behave differently in different cells, this should affect study design when, for example, using rodents as human models, expressing human proteins in rodent cells, transplanting human tissues in rodent bodies, and any other work which may expose a protein to an environment different from its physiological one.

The differences we find in the orthologue proteins between humans and other species may help explain why they handle arsenic differently. For example, rats are much slower at eliminating oral DMA^V than mice are. This has been explained by arsenic accumulating in erythrocytes in rats more than in mice (Vahter et al., 1984), and was further explained as a hemoglobin-binding proclivity of rat erythrocytes specifically (Lu et al., 2004). Conversely, MMA is preferentially accumulated in the kidney of the mouse, but not the rat (Kenyon et al., 2008). This difference in kidney accumulation in rodents may reflect a species difference in

transporter function at the kidney, either in uptake or efflux, or it may be a result of the rat's better accumulation of arsenic in the blood being a higher-affinity process which outcompetes that of kidney accumulation.

Further, methylation of arsenic strongly influences the ability of hABCC4 to transport and confer cellular protection against arsenic (Banerjee et al., 2014; Banerjee et al., 2018); and methylation is different between species, with rats being more efficient at methylating from MMA^V to DMA^V, and thus having less MMA^V detected in their urine than humans have (Vahter, 2002). Importantly, regarding finding animal models for humans, we cannot rely on genetic or evolutionary proximity as a predictor of analogy to arsenic handling in humans, as arsenic is not methylated at all in chimpanzees or marmoset monkeys (Vahter, 2002).

There is much to be discovered about how the ABC proteins of humans and other species differ. Here it was reported that in HEK cells, mAbcc4 did not have the same arsenic transport abilities as hABCC4 does, but had a greater ability to transport $E_2$17βG and conferred greater protection against 6-MP. Some evidence of the importance of the cellular environment in Abcc4 function is also presented. That the activity of the mouse orthologue can be higher or lower than its human counterpart, depending on the experiment/substrate, adds to the complexity and emphasizes the warning when looking across species in experimental work. Learning more about these species differences builds the foundation for better animal models and better interspecies experiments, better drug development, and a stronger understanding of how human populations will be affected by the substances these proteins handle.

Chapter 4: Multidrug Resistance Protein 1 (MRP1/*ABCC1*)-mediated cellular protection and transport of methylated arsenic metabolites differs between human cell lines.

This chapter was published in Drug Metabolism and Disposition (August 2018, 46 (8) 1096-1105). The authors were: Mayukh Banerjee, Gurnit Kaur, Brayden D. Whitlock, Michael W. Carew, X. Chris Le, and Elaine M. Leslie

BDW conducted experiments and contributed data only related to cytotoxicity studies, in Table 4.1 and Figure 4.1. Authorship attributions and acknowledgements are included at the end, unchanged from the published form.

1.11 Introduction

Arsenic is a proven human carcinogen, causing lung, skin, and bladder tumors (IARC, 2012). Chronic arsenic exposure is associated with increased incidences of kidney and liver tumors, and a myriad of non-cancerous adverse health effects (IARC, 2012; Naujokas et al., 2013; Platanias, 2009). Millions of people world-wide are exposed to levels of arsenic above the World Health Organization acceptable level of 10 µg/l, predominantly through the consumption of groundwater naturally contaminated with inorganic arsenic [arsenite (As^{III}) and arsenate (As^{V})] (Rahman et al., 2009). In addition to environmental exposures, arsenic trioxide is used clinically in the treatment of acute promyelocytic leukemia and is in clinical trials for the treatment of other hematological and solid tumors (Ally et al., 2016; Cicconi & Lo-Coco, 2016; Falchi et al., 2016; Kritharis et al., 2013). Other arsenic compounds are also in clinical trials for the treatment of various cancers (Khairul et al., 2017). Thus, understanding the cellular handling of arsenic is critical for the development of therapeutics to treat chronic arsenic exposure, and to maximize the clinical effectiveness of arsenic based drugs.

Cellular uptake of arsenic has been recently reviewed (Mukhopadhyay et al., 2014; Roggenbeck et al., 2016). Once inside most mammalian cells, arsenic undergoes extensive methylation (Drobná, Walton, Paul, et al., 2010; Vahter, 1999). In humans, the four major methylation products are monomethylarsonic acid (MMA^{V}), monomethylarsonous acid (MMA^{III}), dimethylarsinic acid (DMA^{V}), and dimethylarsinous acid (DMA^{III}) (Thomas et al., 2007). Arsenic methylation has a significant impact on its toxicity, tissue distribution, and retention (Thomas et al., 2007; Thomas et al., 2004; Wang et al., 2015). Although arsenic

methylation results in an increased rate of arsenic whole body clearance (Drobna et al., 2009; Drobná, Walton, Harmon, et al., 2010; Hughes et al., 2010), and reduces susceptibility to acute arsenic toxicity (Yokohira et al., 2010, 2011), trivalent methylated forms of arsenic (MMA^{III} and DMA^{III}) are considered bioactivation products because they are more reactive metabolites than As^{III} (Kligerman et al., 2003; Mass et al., 2001; Moe et al., 2016; Petrick et al., 2000; Styblo et al., 2000).

In addition to methylation, arsenic can be conjugated with reduced glutathione (GSH/GS) (Leslie, 2012). Arsenic triglutathione [$As(GS)_3$] and the diglutathione conjugate of the highly toxic MMA^{III} [$MMA(GS)_2$], have been isolated from rat bile and mouse urine, thus, these two As-GSH complexes are formed physiologically, and account for a major fraction of arsenic in urine and bile (Bu et al., 2011; Cui et al., 2004; Kala et al., 2004; Kala et al., 2000; Suzuki et al., 2001). The ATP-binding cassette (ABC) transporter Multidrug Resistance Protein 1 (MRP1/ABCC1), along with the related MRP2 and MRP4 (ABCC2 and ABCC4, respectively) mediate the cellular export of multiple methylated and/or glutathionylated metabolites of arsenic (Banerjee et al., 2014; Carew & Leslie, 2010; Carew et al., 2011; Kala et al., 2004; Kala et al., 2000; Leslie et al., 2004; Shukalek et al., 2016).

ABCC11 is a 190 kDa phosphoglycoprotein with three polytopic membrane spanning domains (MSDs) and two nucleotide binding domains (NBDs) arranged as MSD0-MSD1-NBD1-MSD2-NBD2 (Cole, 2014). ABCC1 confers resistance to a chemically diverse array of anti-cancer drugs and is involved in the cellular export of physiological compounds including GSH, glutathione disulphide, 17β-estradiol 17-(β-D-glucuronide) ($E_2$17βG), and leukotriene C_4

(LTC_4) (Cole, 2014). Furthermore, ABCC1 transports a variety of xenobiotics often conjugated to GSH, glucuronate, or sulphate (Jedlitschky et al., 1996; Leslie et al., 2005; Loe, Almquist, Cole, et al., 1996; Loe, Almquist, Deeley, et al., 1996). Included in this list are the arsenic metabolites $As(GS)_3$ and $MMA(GS)_2$, the glutathionylated forms of inorganic arsenic (As^{III} and As^{V}) and MMA^{III}, respectively (Carew et al., 2011; Leslie et al., 2004).

Interestingly, $As(GS)_3$ is transported by ABCC1 expressed in HEK293 cells with markedly different kinetics than by ABCC11 expressed in HeLa cells (Shukalek et al., 2016). Further investigation revealed that ABCC1 affinity and capacity for $As(GS)_3$ was associated with the phosphorylation status of two residues in the linker region between NBD1 and MSD2 (Y920 and S921). Furthermore, the glycosylation status of two residues in the amino-terminus (N19 and N23) influenced the stability of Y920 and/or S921 phosphorylation (Shukalek et al., 2016). Given this cell line difference, the first objective of the current study was to determine differences in arsenical cytotoxicity between the HEK-ABCC1 and HeLa-ABCC1 cell lines. The second objective was to use ABCC1-enriched membrane vesicles isolated from HEK and HeLa cells to determine the cell line differences in ABCC1 transport function. The third objective was to investigate the influence of Y920/S921 phosphorylation on the ability of HEK-ABCC1-enriched membrane vesicles to transport arsenic metabolites in addition to $As(GS)_3$.

1.12 Results

1.12.1 ABCC1 expressed in HEK293 cells decreases the cytotoxicity of As^{III}, As^{V}, MMA^{III}, and DMA^{V}.

Previously we have shown that ABCC1 stably expressed in HeLa cells reduced the toxicity of As^{III}, As^{V}, and MMA^{III}, but not MMA^{V}, DMA^{III}, or DMA^{V} relative to HeLa cells expressing empty vector alone (Carew et al., 2011). Given that we have recently reported substantial differences in the transport of $As(GS)_3$ between ABCC1-enriched membrane vesicles isolated from HEK293 and HeLa cells (Shukalek et al., 2016), differences in arsenical cytotoxicity between the two cell lines were investigated. Thus, the cytotoxicity of five of these arsenicals (As^{III}, As^{V}, MMA^{III}, DMA^{III}, and DMA^{V}) in HEK-ABCC1 and HEK-vector cell lines were determined in parallel with HeLa-ABCC1 and HeLa-vector for comparison [Figure 4.1, Table 4.1, and (Carew et al., 2011)].

The arsenic compounds that HEK-ABCC1 cells conferred resistance to (relative to HEK-vector) were the same as the HeLa cell line pair (Figure 4.1A-C and Table 4.1), except that HEK-ABCC1 conferred a significantly increased level of resistance against DMA^{V} (relative resistance value of 1.4, $P < 0.05$) [Figure 4.1D, Table 4.1, and (Carew et al., 2011)]. In addition, HEK-ABCC1 cells had a relative resistance of 9.2 against As^{V} (Table 4.1 and Figure 4.1B), while HeLa-ABCC1 cells had a relative resistance of only 2.1 [Table 4.1 and (Carew et al., 2011)]. These results led us to characterize the cell line differences for DMA^{V} and As^{V} transport using ABCC1-enriched membrane vesicles. Furthermore, although resistance to MMA^{III} was conferred by both HEK-ABCC1 and HeLa-ABCC1 cell lines [Figure 4.1C, Table 4.1 and

(Carew et al., 2011)], differences in transport characteristics between membrane vesicles prepared from these cell lines were also investigated for $MMA(GS)_2$.

1.12.2 Transport of DMA^V by ABCC1-enriched membrane vesicles.

To test if differences in cytotoxicity were due at least in part to differences in ATP-dependent cellular efflux, DMA^V transport by HEK- and HeLa-WT-ABCC1 membrane vesicles was measured at 0.05 and 1 μM of DMA^V (Figure 4.2A). ABCC1-enriched vesicles prepared from transiently transfected HEK293T cells transported DMA^V (101 ± 15 pmol mg^{-1} protein min^{-1} at 0.05 μM and 264 ± 42 pmol mg^{-1} protein min^{-1} at 1 μM). In contrast, DMA^V transport was not detected for HeLa-WT-ABCC1 vesicles (Figure 4.2A), despite the fact that the same vesicle preparations were functional for $MMA(GS)_2$ transport (Figure 4.4A), and comparable levels of ABCC1 were present (Figure 4.3). Thus, we report for the first time that ABCC1 is capable of transporting this important methylated arsenic metabolite, at least under certain conditions.

Table 4.1

Resistance of ABCC1-transfected HEK293 and HeLa cells to inorganic and methylated arsenic species.

	IC_{50} (± S.D.)			IC_{50} (± S.D.)		
	HEK-vector	HEK-ABCC1	Relative Resistance	HeLa-vector	HeLa-ABCC1	Relative Resistance
As^{III}	4.9 ± 1.0	25.5 ± 4.2	**5.3 ± 0.9******	7.0 ± 1.2	17.5 ± 2.4	**2.5±0.3*****
As^{V}	26 ± 6.7	221 ± 62	**9.2 ± 3.6*****	156±55	303±51	**2.1 ± 0.5****
MMA^{III}	1.7 ± 0.12	3.9 ± 0.5	**2.3 ± 0.2*****	5.0 ± 1.2	7.6 ± 1.3	**1.5 ± 0.2***
DMA^{III}	1.2 ± 1	1.6 ± 1.6	**1.2 ± 0.2**	6 ± 0.5[b]	7 ± 2.3 [b]	**1.2 ± 0.4** [b]
DMA^{V}	1090 ± 290	1500 ± 250	**1.4 ± 0.2***	690 ± 430	680 ± 450	**1.0 ± 0.13**

[a] The resistance of HEK293 and HeLa cell lines expressing wild-type ABCC1 was determined using an MTS assay and relative resistance factors calculated by dividing the IC_{50} values obtained for the ABCC1-expressing cell line by the IC_{50} values obtained for empty vector expressing cell line. Values shown are the mean (± S.D.) obtained from at least three independent experiments.

[b]Previously published in (M. W. Carew et al., 2011) but done in parallel experiments with unpublished HEK data.

The IC_{50} values for the ABCC1 expressing cell lines were compared with the IC_{50} values for the empty vector control cell lines using a Student's t-test (* $P < 0.05$, ** $P < 0.01$, *** $P < 0.001$, **** $P < 0.0001$).

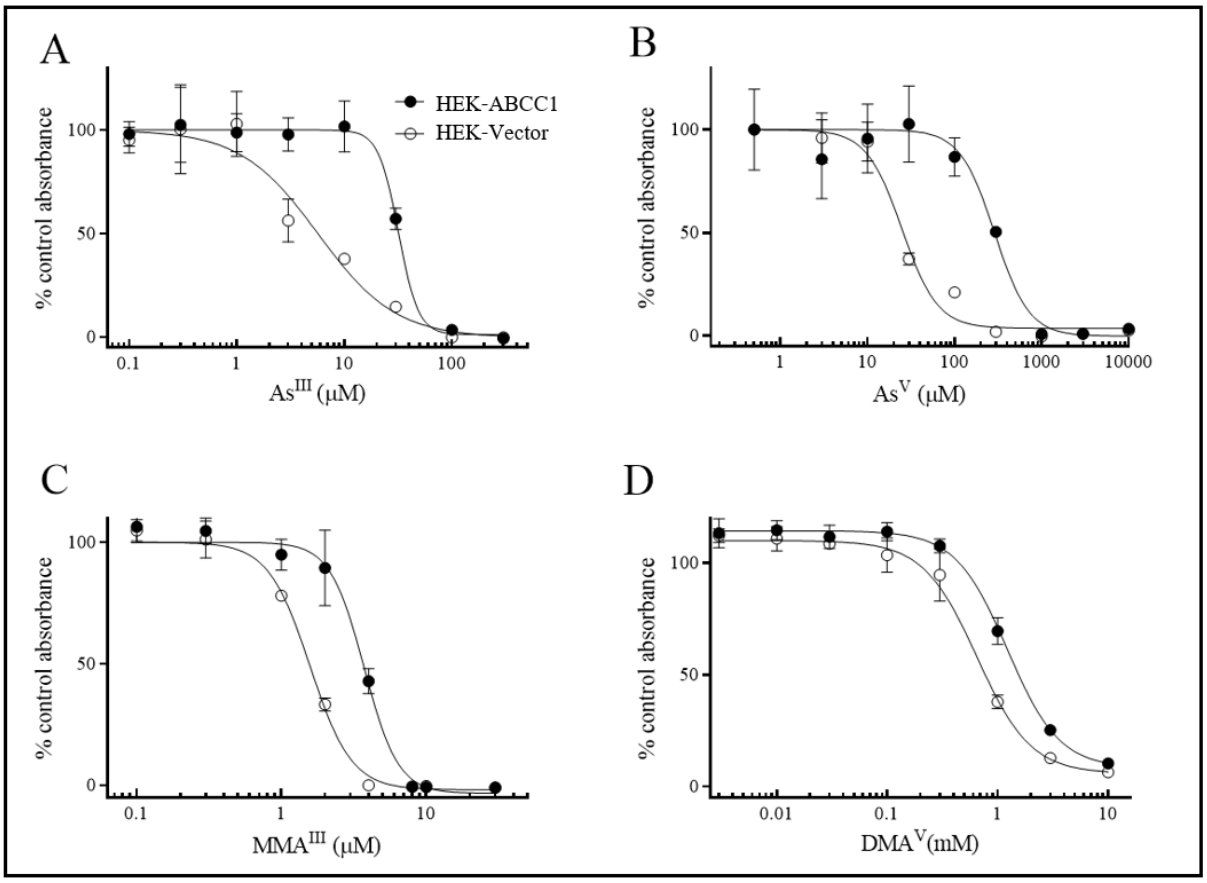

Figure 4.1: Effect of selected arsenic compounds on the viability of HEK293 cells stably expressing human ABCC1. Cells expressing empty vector (HEK-vector) (○) and ABCC1 (HEK-ABCC1) (●) were incubated in the presence of (A) As^{III}, (B) As^{V}, (C) MMA^{III}, or (D) DMA^{V} for 72 h. Cell viability was determined using a tetrazolium-based cytotoxicity assay. Data points are means (± S.D.) of quadruplicate determinations in a representative experiment; similar results were obtained in at least two additional experiments (mean relative resistance data from independent experiments are shown in Table 4.1).

1.12.3 Kinetic analysis of ABCC1-mediated DMA^V transport.

Transport of DMA^V by HEK-WT-ABCC1 membrane vesicles was then further characterized. The linear range of DMA^V (1 μM) transport versus time was measured for HEK-WT-ABCC1 and HEK-vector control membrane vesicles (Figure 4.2B). Transport by HEK-WT-ABCC1 was linear for up to 30 sec and reached a maximal activity of 138 ± 24 pmol mg^{-1} protein at 30 sec. ATP-dependent transport of DMA^V by HEK-vector was very low and similar to transport observed in the presence of AMP. HEK-WT-ABCC1 membrane vesicle transport of DMA^V was characterized kinetically by determining the initial rates of transport over several concentrations of DMA^V (Figure 4.2C and Table 4.2). HEK-ABCC1 was found to transport DMA^V with high apparent affinity and capacity (K_m of 0.19 ± 0.06 μM and V_{max} of 342 ± 37 pmol mg^{-1} protein min^{-1}).

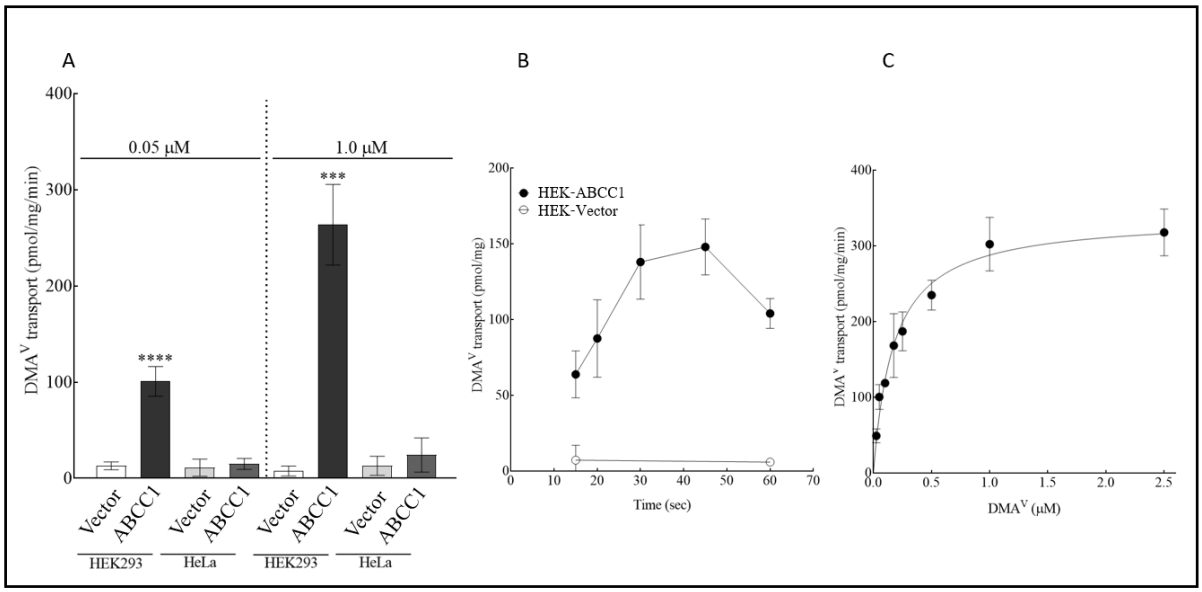

Figure 4.2: ATP-dependent transport of DMA^V by ABCC1-enriched membrane vesicles. Transport experiments were done with membrane vesicles (20 µg of protein) prepared from HEK293T cells transiently transfected with WT-ABCC1 (black bars or symbols) or empty pcDNA3.1(-) (vector) (white bars or symbols) or HeLa cells stably transfected with WT-ABCC1 (dark gray bars) or empty vector (light gray bars). For individual experiments, transport was done in triplicate, and then reactions were pooled for analysis by ICP-MS. Bars and symbols represent the means (± S.D.) of three independent experiments. (A) Vesicles were incubated for 20 sec at 37°C in transport buffer with DMA^V (0.05 or 1 µM). Statistically significant differences in DMA^V transport were determined using a one way ANOVA followed by a Dunnett's multiple comparisons post hoc test with HEK-Vector as the control group (***$p < 0.001$; ****$p < 0.0001$). (B) Time course of ATP-dependent DMA^V transport was determined by incubating membrane vesicles with DMA^V (1 µM) in transport buffer at 37°C for the indicated time points. (C) HEK-WT-ABCC1 membrane vesicles were incubated for 20 sec at 37°C with increasing concentrations of DMA^V (0.025–2.5 µM). Data were fitted using a one-site Michaelis-Menten kinetic model with GraphPad Prism®6.

Table 4.2. Kinetic parameters of $MMA(GS)_2$ and DMA^V transport by ABCC1 (and phosphorylation mutants)

			Kinetic parameter		
Compound	**Cell Line**	**Variant**	***n***	***K_m*** (μM)	***V_{max}***[a]
DMA^V	HEK293T	WT	3	0.19 ± 0.06	342 ± 37[b]
$MMA(GS)_2$	HEK293T	WT	3	23 ± 2.2	4.9 ± 0.5
		Y920F/S921A	4	24 ± 5.5	5.3 ± 2.2
		Y920E/S921E	2	29, 18	5.8, 5.0
	HeLa	WT	3	33 ± 24	16.8 ± 5.3**

[a]V_{max} values are in nmol mg^{-1} protein min^{-1} unless otherwise indicated and were corrected for ABCC1-level relative to HEK-WT-ABCC1 as described in Materials and Methods.

[b]pmol mg^{-1} protein min^{-1}

**significantly different from HEK293-ABCC1 ($P<0.01$ One way ANOVA with Tukey's multiple comparisons post-hoc test).

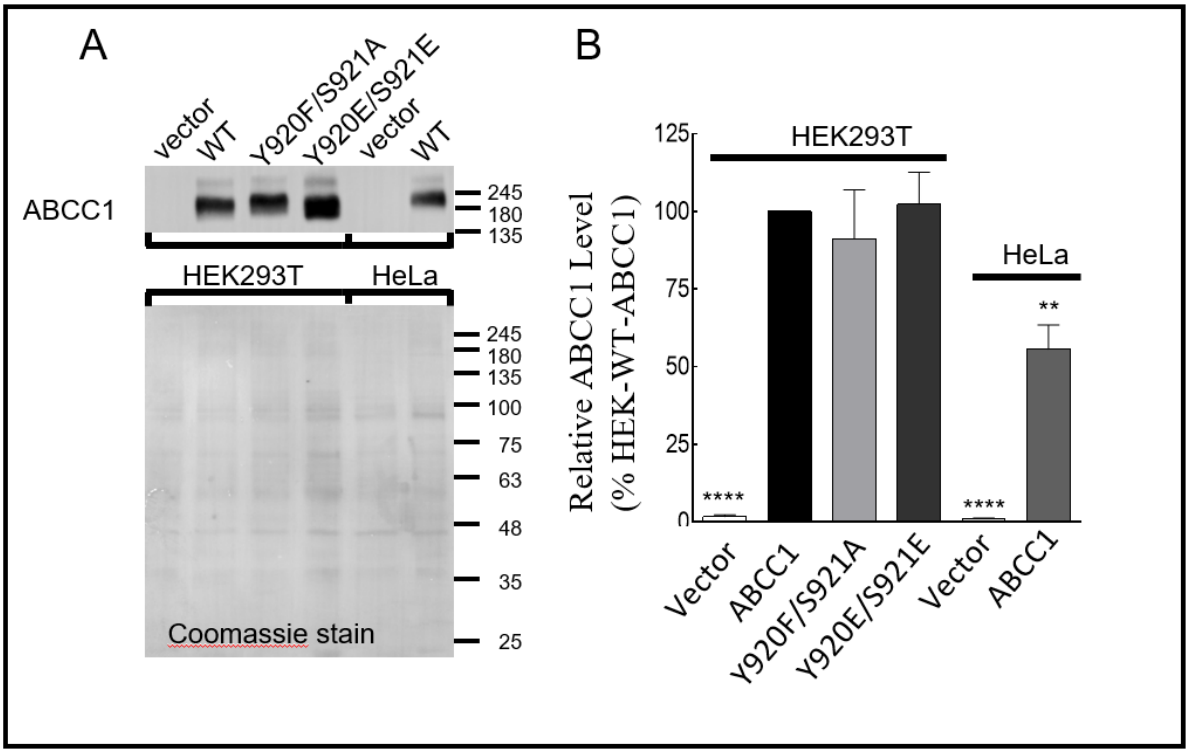

Figure 4.3: Relative protein levels of ABCC1 in membrane vesicles prepared from HeLa and HEK293T cells. (A) Membrane vesicles (0.5 µg protein per lane) prepared from HEK293T cells (transiently expressing empty pcDNA3.1 vector (vector), WT-, Y920F/S921A, or Y920E/S921E-ABCC1) or HeLa cells (stably expressing vector or WT-ABCC1) were resolved by 7% SDS-PAGE and immunoblotted with the ABCC1-specifc MAb MRPr1 (1:10,000) (top panel). Blots were then stained with Coomassie blue for total protein levels (bottom panel). (B) Densitometry on the ABCC1 and Coomassie stained blots was performed using ImageJ software. Vector control, WT- and mutant-ABCC1 levels were normalized for protein loading as needed based on the entire corresponding lane of the Coomassie stained blot and then plotted as a % HEK-WT-ABCC1 level. Bars represent the mean (± S.D.) values obtained from three independent vesicle preparations. ** $p < 0.01$, ****$p < 0.0001$ (one way ANOVA followed by a Dunnett's multiple comparisons post hoc test).

1.12.4 Analysis of DMA^V transport by HEK-ABCC1 phosphorylation mutants.

Due to the complete lack of DMA^V transport by HeLa-WT-ABCC1 and substantial transport by HEK-WT-ABCC1 membrane vesicles, this cell line difference was further explored. We have previously shown that HEK293 and HeLa cell line differences in $As(GS)_3$ transport by ABCC1 were associated with differences in phosphorylation at Y920/S921 (Shukalek et al., 2016). In order to determine if phosphorylation differences at these sites were responsible for the difference in DMA^V transport by ABCC1 between the two cell lines, DMA^V transport by ABCC1-Y920/S921 dephosphorylation- and phosphorylation-mimicking mutants was investigated.

Dephosphorylation-mimicking HEK-Y920F/S921A-ABCC1 membrane vesicles exhibited a complete loss of DMA^V transport (Figure 4.4A), suggesting these sites are critical for the cell line difference. However, the phosphorylation-mimicking HEK-Y920E/S921E-ABCC1, which we expected would restore DMA^V transport, also completely lacked DMA^V transport (Figure 4.4A). Mutant membrane vesicle preparations had ABCC1 levels similar to HEK-WT-ABCC1 (Figure 3), and were functional for $MMA(GS)_2$ (Figure 4.5B, Table 4.2) and/or $As(GS)_3$ (Figure 4.6A) transport.

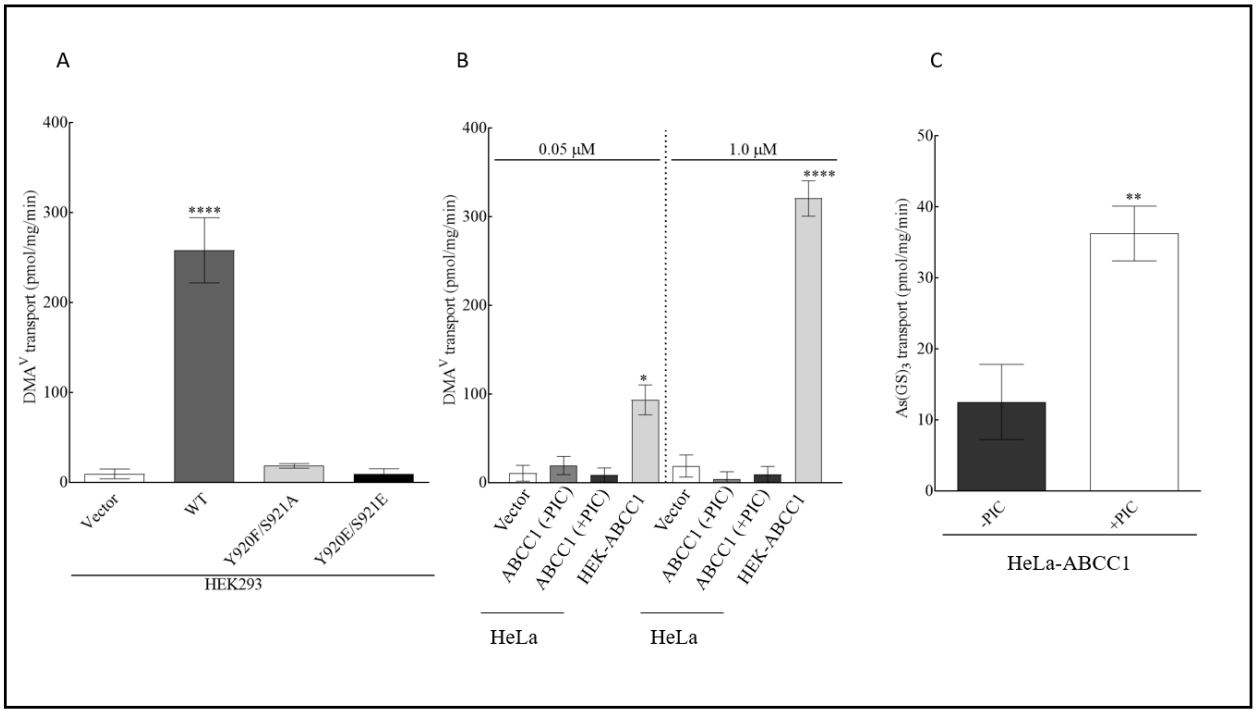

Figure 4.4: Effect of Y920/S921-ABCC1 mutation and/or phosphatase inhibitors on ATP-dependent transport of DMA^V or $As(GS)_3$ by ABCC1-enriched membrane vesicles. Transport experiments were done with membrane vesicles (20 µg of protein) prepared from HEK293T cells transiently transfected with WT-ABCC1, Y920F/S921A-ABCC1, Y920E/S921E-ABCC1, or empty pcDNA3.1 (-) (vector) or from HeLa cells stably transfected with WT-ABCC1 or empty vector. Bars and symbols represent the means (± S.D.) of three independent experiments. (A) Membrane vesicles from HEK293T cells transiently transfected with WT-ABCC1 (dark gray bars), Y920F/S921A-ABCC1 (light gray bars), Y920E/S921E-ABCC1 (black bars), or vector (white bars) were incubated for 20 sec at 37°C with DMA^V (1 µM). For individual experiments, transport was done in triplicate, and then reactions were pooled for analysis by ICP-MS. Statistically significant differences in DMA^V transport were determined using a one way ANOVA followed by a Dunnett's multiple comparisons post hoc test using HEK-Vector as the control group (****$p < 0.0001$). (B) Membrane vesicles from HeLa cells stably transfected with vector (light gray bars), or WT-ABCC1 prepared in the presence (white bars) or absence (black bars) of a PIC were incubated for 20 sec at 37°C with DMA^V (0.05 or 1 µM). HEK-WT-ABCC1 membrane vesicles

were used as a positive control. For individual experiments, transport was done in triplicate, and then reactions were pooled for analysis by ICP-MS. Statistically significant differences in DMA^V transport were determined using a one way ANOVA followed by a Dunnett's multiple comparisons post hoc test using HeLa-Vector as the control group (*$p < 0.05$; ****$p < 0.0001$). (C) ATP-dependent transport of $As(GS)_3$ by ABCC1-enriched membrane vesicles from stably transfected HeLa cells prepared with (white bar) or without (black bar) PIC. The membrane vesicles were incubated for 3 min at 37°C with $As(GS)_3$ (1 μM). Statistically significant differences in $As(GS)_3$ transport were determined using an unpaired two-tailed t-test (**$p < 0.01$).

1.12.5 Analysis of DMA^V transport by HeLa-WT-ABCC1 in the presence of phosphatase inhibitors.

The possible modulation of DMA^V transport by ABCC1 through phosphorylation was also investigated by studying the transport in ABCC1-enriched vesicles prepared from HeLa cells in the presence or absence of a phosphatase inhibitor cocktail (PIC) at two different substrate concentrations (0.05 and 1 μM) (Figure 4.4B). We have previously shown for $As(GS)_3$ that HeLa-WT-ABCC1 membrane vesicles prepared in the presence of a PIC have a 19- and 12-fold increase in K_m and V_{max}, respectively, compared to HeLa-WT-ABCC1 prepared in the absence of a PIC (Shukalek et al., 2016). In contrast, the inclusion of a PIC did not influence DMA^V transport by HeLa-WT-ABCC1 at either concentration (Figure 4.4B). To ensure that the HeLa-WT-ABCC1 ± PIC membrane vesicles used in the DMA^V transport assays were functional, and the PIC active, $As(GS)_3$ transport experiments were completed on the same vesicle preparations (Figure 4.4C). Consistent with our previous report (Shukalek et al., 2016), $As(GS)_3$ transport by HeLa-WT-ABCC1 vesicles, prepared in the presence of a PIC, was significantly higher than for HeLa-WT-ABCC1 vesicles prepared in the absence of a PIC. These results could suggest that mechanisms other than phosphorylation are likely responsible for the cell line difference observed in DMA^V transport by HEK-WT-ABCC1 compared to HeLa-WT-ABCC1. Alternatively, a differential phosphorylation site that remains stable in the absence of PIC could be involved.

The lack of DMA^V transport by all mutants of Y920/S921 could also be due to the disruption of phosphorylation/dephosphorylation of neighboring sites that are critical for DMA^V

transport. We screened the influence of seven additional putative phosphorylation sites in the linker region (S905-, S915-, S916-, S917-, S918-, S919-, T931-ABCC1) by mutating them to phospho-mimicking and/or dephospho-mimicking residues in full length ABCC1, expressing them in HEK293 cells, preparing membrane vesicles, and measuring DMA^V transport. Surprisingly, all mutants lacked DMA^V transport activity, despite the fact that they were comparable to HEK-WT-ABCC1 for $As(GS)_3$ transport and ABCC1 level (Figure 4.6).

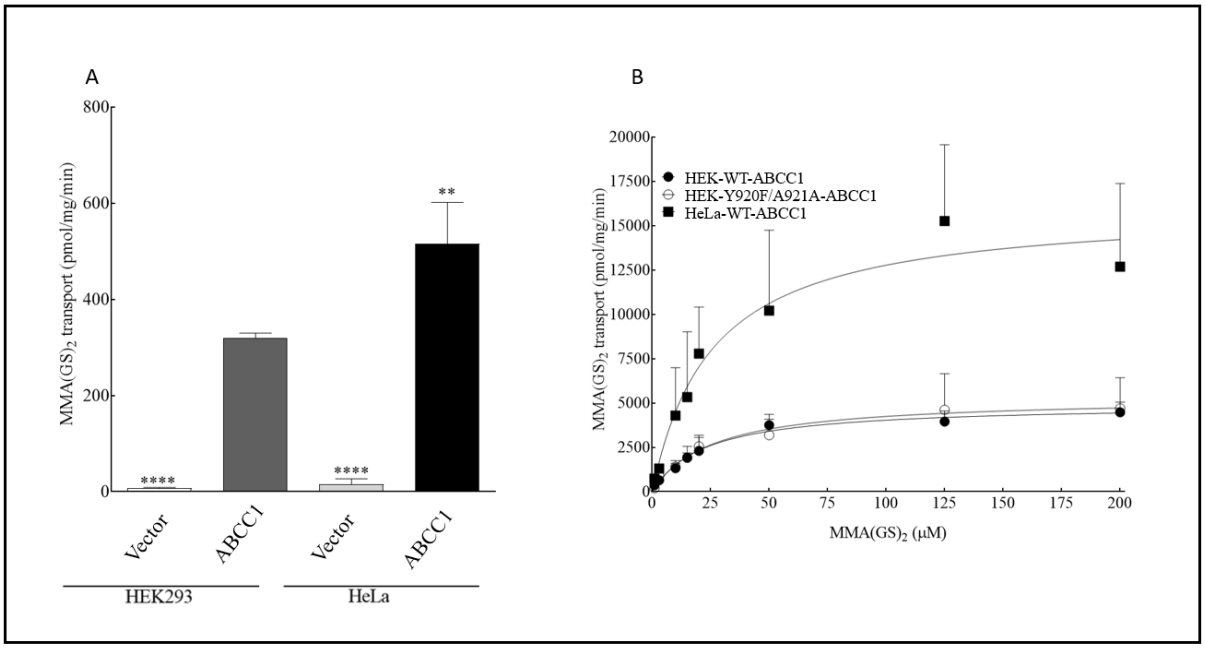

Figure 4.5: ATP-dependent transport of MMA(GS)$_2$ by ABCC1-enriched membrane vesicles. Transport experiments were done with membrane vesicles (20 μg of protein) prepared from HEK293T cells transiently transfected with WT-ABCC1, Y920F/S921A-ABCC1, or empty pcDNA3.1(-) (vector) or from HeLa cells stably transfected with WT-ABCC1 or vector. For individual experiments, transport was done in triplicate, and then reactions were pooled for analysis by ICP-MS. Bars and symbols represent the means (+ S.D.) of at least three independent experiments. (A) Vesicles prepared from HEK293T cells transiently transfected with WT-ABCC1 (dark gray bars) or vector (white bars) or HeLa cells stably transfected with WT-ABCC1 (black bars) or vector (light gray bars) were incubated for 1 min at 37°C in transport buffer with MMA(GS)$_2$ (1 μM). Statistically significant differences in MMA(GS)$_2$ transport were determined using a one way ANOVA followed by a Dunnett's multiple comparisons post hoc test using HEK-WT-ABCC1 as the control group (**$p < 0.01$; ****$p < 0.0001$). (B) Vesicles prepared from HEK293T cells transiently transfected with WT-ABCC1 or Y920F/S921A-ABCC1or from HeLa cells stably transfected with WT-ABCC1 were incubated for 1 min at 37°C with increasing concentrations of MMA(GS)$_2$ (1–200 μM). Data were fitted using a one-site Michaelis-Menten kinetic model with GraphPad Prism®6.

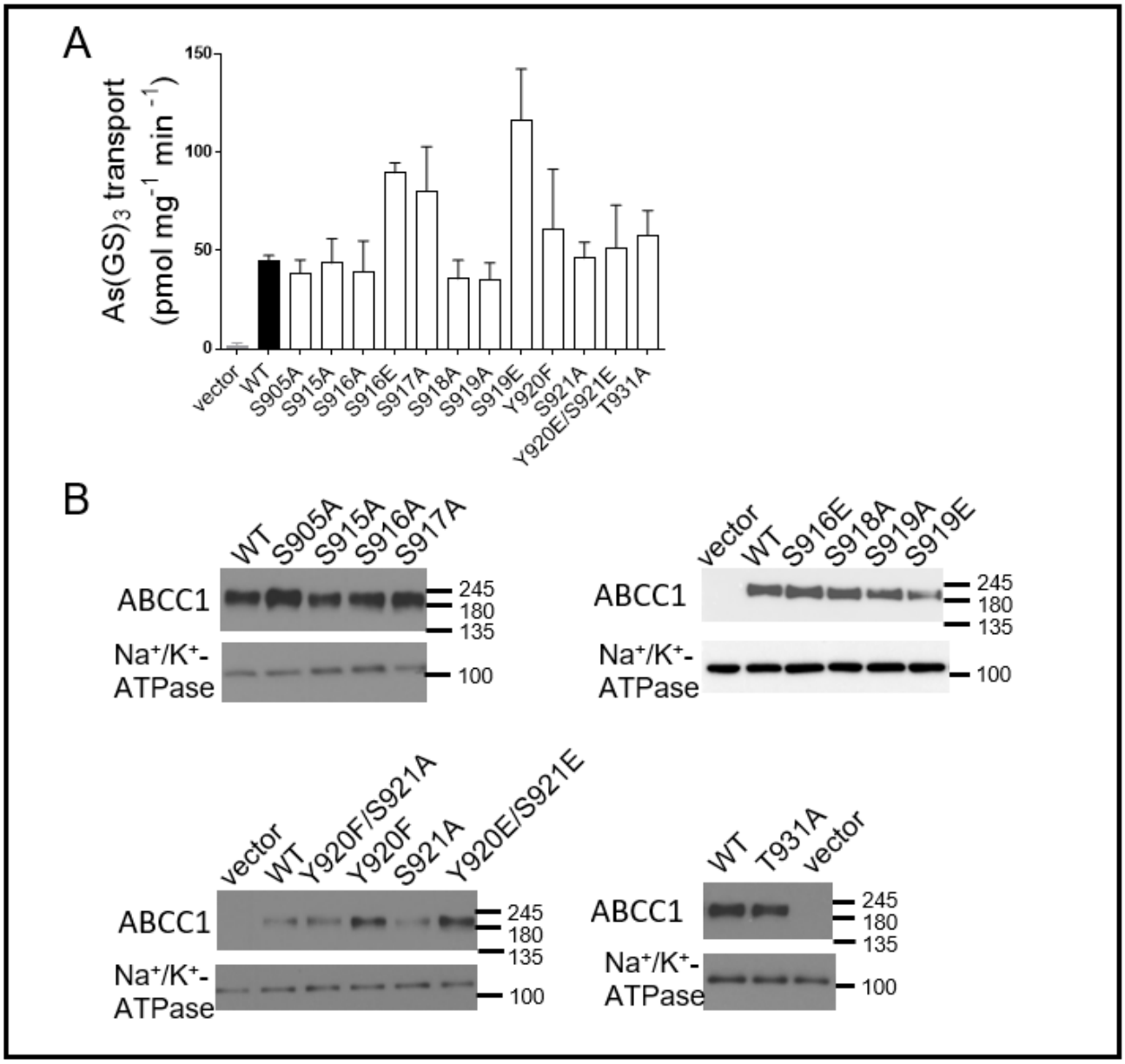

Figure 4.6: Functional evaluation and protein levels of membrane vesicles prepared from HEK293T cells expressing ABCC1-mutants. (A) ATP-dependent uptake of $As(GS)_3$ (1 µM, 40 nCi) by membrane vesicles (20 µg of protein) prepared from HEK293T cells expressing empty pcDNA3.1 vector (vector), wild-type ABCC1 (WT), or potential ABCC1 phosphorylation site mutant. Bars represent the mean (± S.D.) of a triplicate determination in a

single experiment and are corrected for ABCC1 level. Membrane vesicle preparations were identical to those used to characterize DMA^V transport by these mutants. (B) Membrane vesicles (0.5 μg protein per lane) prepared from HEK293T cells (transiently expressing empty pcDNA3.1 vector (vector), WT-, or mutant ABCC1were resolved by 7% SDS-PAGE and immunoblotted with the ABCC1-specifc MAb MRPr1 (1:10,000). Blots were then probed with the Na^+/K^+-ATPase-specific PAb H-300.

1.12.6 Transport of $MMA(GS)_2$ by ABCC1-enriched membrane vesicles.

We have previously shown that MMA^{III} is transported by HEK-ABCC1 in the form $MMA(GS)_2$ and that HeLa-ABCC1 cells confer protection against MMA^{III} relative to HeLa-vector cells (Carew et al., 2011). In the current study, HEK-ABCC1 cells were also found to confer protection against MMA^{III} relative to HEK-vector (Table 4.1). To determine if differences in transport characteristics existed between cell lines, $MMA(GS)_2$ transport by HEK- and HeLa-WT-ABCC1-enriched vesicles was compared. Under the conditions tested, $MMA(GS)_2$ (1 μM) transport by HeLa-WT-ABCC1 vesicles was 1.6-fold higher ($P < 0.01$) than HEK-WT-ABCC1 vesicles (Figure 4.5A).

1.12.7 Kinetic analysis of ABCC1-mediated $MMA(GS)_2$ transport.

To determine if the increased transport of $MMA(GS)_2$ was due to changes in K_m and/or V_{max}, ABCC1-mediated transport of $MMA(GS)_2$ was measured at an initial rate over eight different concentrations of $MMA(GS)_2$ (Figure 4.5B and Table 4.2). HEK- and HeLa-WT-ABCC1 membrane vesicles, were found to have similar apparent affinity for $MMA(GS)_2$ (K_m of 23 ± 2.2 μM and 33 ± 24 μM, respectively), similar to what we have previously reported for HEK-WT-ABCC1 (Carew et al., 2011). In contrast, the V_{max} was 3.4-fold higher for $MMA(GS)_2$ transport by HeLa-WT-ABCC1 (V_{max} of 17 ± 5.3 nmol mg^{-1} min^{-1}) than HEK-WT-ABCC1 (V_{max} of 4.9 ± 0.5 nmol mg^{-1} min^{-1}) membrane vesicles (Figure 4.5B and Table 4.2). In addition, kinetic characterization of $MMA(GS)_2$ transport by the double dephosphorylation-mimicking mutant HEK-Y920F/S921A-ABCC1, previously demonstrated to have substantially

reduced apparent K_m and V_{max} values for $As(GS)_3$ relative to HEK-WT-ABCC1(Shukalek et al., 2016) was completed. Interestingly, HEK-Y920F/S921A-ABCC1 had very similar apparent affinity (K_m of 24 ± 5.5 μM) and capacity (V_{max} of 5.3 ± 2.2 nmol mg^{-1} min^{-1}) to that of HEK-WT-ABCC1 (Figure 4.5B and Table 4.2). Consistent with this, the phosphorylation-mimicking mutant HEK-Y920E/S921E-ABCC1 also had similar apparent affinity and capacity to HEK-WT-ABCC1 (mean K_m of 24 μM, V_{max} of 5.5 nmol mg^{-1} protein min^{-1}, n=2) (Table 4.2). These data suggest that, in contrast with $As(GS)_3$ transport, phosphorylation of Y920/S921 has little influence on the transport of $MMA(GS)_2$ by ABCC1.

1.12.8 Inhibition of $As(GS)_3$ transport by $MMA(GS)_2$.

While the K_m of $As(GS)_3$ for ABCC1 was >10-fold higher for HEK-WT-ABCC1 compared with HeLa-WT-ABCC1 and HEK-Y920F/S921A-ABCC1 (Shukalek et al., 2016), no difference between the apparent K_m value for $MMA(GS)_2$ transport was observed for these membrane vesicles (Figure 4.5 and Table 4.2). This result suggested that $MMA(GS)_2$ and $As(GS)_3$ interact at non-identical binding sites. To begin to characterize the differences in interaction of $As(GS)_3$ and $MMA(GS)_2$ with ABCC1, transport of $As(GS)_3$ (1 μM) by HEK-WT-ABCC1 vesicles was measured in the presence of increasing concentrations of $MMA(GS)_2$ (Figure 4.7A). $MMA(GS)_2$ was found to potently inhibit $As(GS)_3$ transport with an IC_{50} value of 11 ± 1.5 μM.

The inhibition of $As(GS)_3$ transport by $MMA(GS)_2$ was further characterized by measuring the effect of $MMA(GS)_2$ (5, 10, and 15 μM) on $As(GS)_3$ (0.1-20 μM) transport (15 μM shown in Figure 4.7B). Michaelis-Menten analysis showed that $MMA(GS)_2$ at each

concentration tested reduced both the apparent K_m and V_{max} values, suggesting an uncompetitive mode of inhibition with an average K_i of 7.3 ± 5.1 μM (± S.D., n=3). These data are consistent with $MMA(GS)_2$ and $As(GS)_3$ interacting at non-identical binding sites.

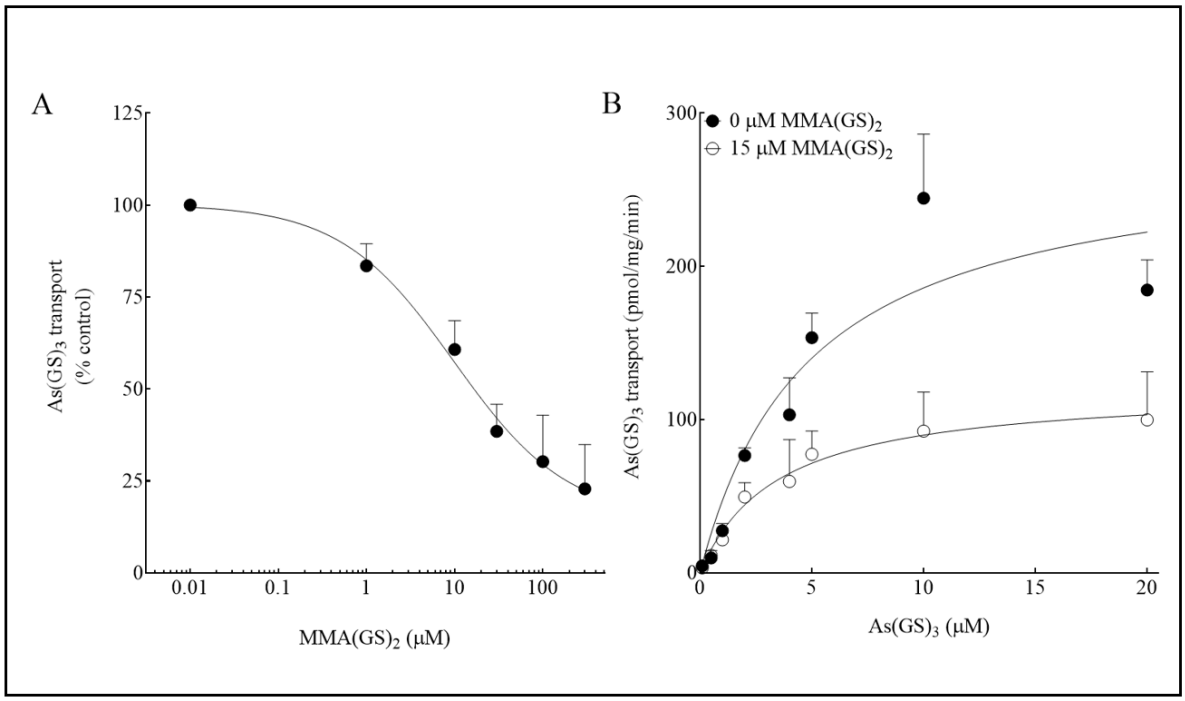

Figure 4.7: $MMA(GS)_2$ inhibits ABCC1 mediated ATP-dependent transport of $As(GS)_3$. Transport experiments were done with membrane vesicles (20 μg of protein) prepared from HEK293T cells transiently transfected with WT-ABCC1. Individual experiments were done in triplicate and ^{73}As quantified using liquid scintillation counting. (A) Vesicles were incubated with $^{73}As(GS)_3$ (1 μM, 40 nCi) for 3 min at 37°C in transport buffer with increasing concentrations of $MMA(GS)_2$ (0.01–300 μM). Symbol represents the mean (+ S.D.) of three independent experiments. (B) Vesicles were incubated with increasing concentrations of $^{73}As(GS)_3$ (0.1–20 μM, 40-100 nCi) for 3 min at 37°C in transport buffer in presence of $MMA(GS)_2$ (15 μM). Data points represent means (+ S.D.) of triplicate determinations in a single experiment. Two independent additional experiments with $MMA(GS)_2$ at 5 and 10 μM were done in order to calculate the K_i (7.3 ± 5.1 μM, ± S.D., n=3).

1.13 Discussion

The proven human carcinogen arsenic naturally contaminates the drinking water of hundreds of millions of people world-wide. One of the most affected countries is Bangladesh, where the arsenic contamination has been referred to as "the largest mass poisoning of a population in history" (Smith et al., 2000). Understanding the cellular handling of arsenic, including efflux pathways, is critical for the prevention and treatment of arsenic-induced disease.

We have investigated the ability of ABCC1 to confer resistance to and/or transport important methylated arsenic metabolites when expressed in HEK293 cells compared to HeLa cells. The cellular resistance conferred by ABCC1 against different arsenic species is useful information, however, resistance levels can be influenced by cellular metabolism and uptake efficiency. To draw conclusions about ABCC1-mediated transport of specific arsenic compounds it was critical to measure their transport directly using ABCC1-enriched membrane vesicles. The population of membrane vesicles that are accumulating ABCC1 substrates are inside-out, allowing the measurement of ATP-dependent transport with minimal influence of metabolism and cellular uptake. This allows the ABCC1 contribution to cellular export of specific arsenic compounds to be evaluated, and allows the accurate determination of kinetic parameters.

The most pronounced difference between cell lines was for DMA^V, which HEK-ABCC1 cells conferred resistance to and HEK-WT-ABCC1 membrane vesicles transported with high apparent affinity and capacity (Table 4.1 and Figure 4.2). This is the first report that ABCC1 is

capable of transporting this important arsenic metabolite. In contrast, HeLa-ABCC1 cells did not confer resistance to DMA^V relative to HeLa-vector cells (Carew et al., 2011), and HeLa-WT-ABCC1 membrane vesicles did not have detectable DMA^V transport activity (Figure 4.2A).

The relative resistance conferred by ABCC1 expressed in HEK293 cells was small, but significant (1.4-fold, $P < 0.05$, Figure 4.1C and Table 4.1). This marginal resistance was in contrast with the high affinity and high capacity transport of DMA^V observed with HEK-WT-ABCC1-enriched membrane vesicles (Figure 4.2C and Table 4.2). A likely explanation for the difference in results between the two assays is that DMA^V is poorly taken up by cells (Delnomdedieu et al., 1995; Dopp et al., 2004; Dopp et al., 2005; Naranmandura et al., 2011; Naranmandura et al., 2007), including HEK293 cells (Banerjee et al., 2014). Thus, it is likely that the data generated with the inside-out ABCC1-enriched membrane vesicles, with no requirement for cell entry, more accurately reflects what is occurring after formation of DMA^V within the cell. Humans are predominantly exposed to As^{III} and As^V in drinking water, which are taken up by cells efficiently (Roggenbeck et al., 2016), and then converted to methylated products (e.g., DMA^V).

As a starting point for determining a mechanism for cell line differences in ABCC1-mediated DMA^V transport, we investigated the potential contribution of differential phosphorylation. Mutation of two phosphorylation sites (Y920/S921-ABCC1), previously reported as responsible for cell line differences in the transport of $As(GS)_3$, to both phospho- or dephospho-mimicking amino acids, surprisingly resulted in a complete loss of DMA^V transport. Individual mutant HEK-Y920F-ABCC1 and HEK-S921A-ABCC1 membrane vesicles, shown

previously to transport $As(GS)_3$ to a similar extent as HEK-WT-ABCC1, also completely lacked DMA^V transport. The inclusion of a PIC during the preparation of HeLa-WT-ABCC1 membrane vesicles did not result in a gain of DMA^V transport activity (although ABCC1-mediated $As(GS)_3$ transport was increased), suggesting that either phosphorylation was not important or a stable phosphorylation site (not influenced by the PIC) was involved. Mutation of multiple other putative phosphorylation sites in the linker region also resulted in a complete loss of HEK-ABCC1 DMA^V transport. Our data suggest that DMA^V transport by HEK-WT-ABCC1 membrane vesicles is extremely sensitive to alterations in the linker region between NBD1 and MSD2. The reasons for this are currently not understood and require further investigation. Differences in post-translational modifications and/or protein:protein interactions that alter the structure of this region could potentially explain the cell line differences in ABCC1-mediated DMA^V transport. Indeed, there is some suggestion in the literature that this linker region is important for protein:protein interactions and that such interactions may be modulated by phosphorylation (Ambadipudi & Georges, 2017; Yang et al., 2012).

ABCC1 transport of DMA^V is the second DMA^V efflux pathway to be identified. Previously, we reported that the related MRP4 transports DMA^V with similar affinity ($K_{0.5}$ 0.22 ± 0.15 μM for MRP4 versus K_m 0.19 ± 0.06 μM for ABCC1), but through a co-operative mechanism (Hill coefficient 2.9 ± 1.2) and assuming equal protein levels, lower capacity (V_{max} 32 ± 3 pmol mg^{-1} protein min^{-1} for MRP4 versus V_{max} 342 ± 37 pmol mg^{-1} protein min^{-1} for ABCC1) [(Banerjee et al., 2014; Roggenbeck et al., 2016) and Table 4.2]. The tissue expression

and cellular localization of MRP4 likely make it critical for urinary elimination of hepatic metabolites (Banerjee et al., 2014). The localization of ABCC1 to the basolateral surface of epithelial cells and expression in specific cell types of most tissues (undetectable protein levels in human hepatocytes), likely makes ABCC1 important for cellular/tissue protection rather than playing a role in arsenic elimination.

DMA^V is an arsenic compound with low toxicity relative to trivalent arsenic species (Moe et al., 2016). The efflux of DMA^V from the cell is critical to prevent the reduction of DMA^V to the highly reactive DMA^{III} (Németi & Gregus, 2013). Furthermore, export of DMA^V would likely prevent product inhibition of arsenic (+3 oxidation state) methyltransferase, allowing the formation and cellular export of more DMA^V. The reducing intracellular environment might suggest that DMA^{III} is the predominant form of dimethylated arsenic within the cell, however, this has been difficult to prove and DMA^V has been detected in human cell lines and mouse liver homogenate (Currier et al., 2011). The highly reactive DMA^{III} is highly protein bound and unlikely to be available for cellular export (Hippler et al., 2011; Shen et al., 2013). An equilibrium between DMA^{III} and DMA^V will exist within the cell, and the high affinity high capacity export of DMA^V by ABCC1 would provide a good mechanism for cellular detoxification.

Out of the five arsenic compounds tested HEK-ABCC1 conferred the highest level of resistance against As^V (9-fold) followed by As^{III} (5-fold). We have previously shown that As^V and As^{III} are converted to $As(GS)_3$ prior to efflux by ABCC1, (Leslie et al., 2004). The reason why HEK-ABCC1 cells confer higher levels of resistance to As^V than As^{III} is not understood.

As^{V} enters cells more slowly (through Na^{+}-dependent phosphate transporters) than As^{III} (through aquaglyceroporins) (Mukhopadhyay et al., 2014; Roggenbeck et al., 2016), and this could influence the methylation and glutathionylation of arsenic and alter the metabolites available for ABCC1 export.

HEK-ABCC1 and HeLa-ABCC1 cell lines both conferred significantly higher levels of resistance to MMA^{III} than their respective vector controls [(Carew et al., 2011) and Table 4.1]. $MMA(GS)_2$ was transported with comparable apparent affinity by HeLa-WT-ABCC1 and HEK-WT-ABCC1 membrane vesicles, however, the V_{max} was 3.4-fold higher for HeLa-ABCC1 membrane vesicles. Kinetic parameters for $MMA(GS)_2$ transport were not significantly different between HEK-WT-ABCC1 and HEK-Y920F/S921A-ABCC1 or HEK-Y920E/S921E-ABCC1, suggesting that differential phosphorylation at these sites is not responsible for the cell line differences in V_{max}. Consistent with these phosphorylation sites being important for the interaction between ABCC1 and $As(GS)_3$, but not ABCC1 and $MMA(GS)_2$, we found that $MMA(GS)_2$ was an uncompetitive inhibitor of $As(GS)_3$ transport. Thus, increasing concentrations of $As(GS)_3$ did not overcome $MMA(GS)_2$ inhibition (Figure 4.7B) providing support for the idea that $As(GS)_3$ and $MMA(GS)_2$ do not share identical binding sites.

Arsenic has previously been reported to activate kinase and inhibit phosphatase pathways (Beauchamp et al., 2015; Rehman et al., 2012), and we had postulated cellular exposure to arsenic would result in a shift to a pro-phosphorylation state of Y920/S921-ABCC1 (Shukalek et al., 2016). This in turn would result in the switch of ABCC1 from a high-affinity,

low capacity transporter of $As(GS)_3$ to a more efficient low affinity, high capacity $As(GS)_3$ transporter (Shukalek et al., 2016). Phosphorylation of these residues appear to be important specifically for $As(GS)_3$, but not for $MMA(GS)_2$ or DMA^V (this study) or as previously reported for methotrexate, LTC_4 or $E_217\beta G$ (Loe, Almquist, Deeley, et al., 1996; Shukalek et al., 2016; Stride et al., 1997). Why phosphorylation of ABCC1 at Y920/S921 has an impact on $As(GS)_3$, but not other arsenic metabolites is unknown. Potentially, ABCC1 exports $As(GS)_3$ over a broad concentration range to reduce As^{III} availability for the formation of more toxic trivalent methylated forms. The K_m values for $As(GS)_3$ (K_m range ~0.3-4 μM) (Leslie et al., 2004; Shukalek et al., 2016) and DMA^V (K_m 0.19 μM) (Table 4.2) are much lower than $MMA(GS)_2$ (K_m range 11-33 μM) [Table 2 and (Carew et al., 2011)]. At low levels of arsenic exposure, ABCC1 is potentially important for the export of $As(GS)_3$ and any DMA^V that is formed (preventing the formation of the highly toxic DMA^{III}). During higher cellular arsenic exposure ABCC1 phosphorylation allows it to still export $As(GS)_3$ efficiently, $MMA(GS)_2$ accumulation might start to occur and ABCC1 would be able to export this as well as DMA^V. It's worth noting that the transport of DMA^V by ABCC1 is remarkably more efficient than reported for any other transporter and arsenical combination (Roggenbeck et al., 2016), providing support for ABCC1 being an important transport pathway for DMA^V under environmentally relevant exposure conditions.

Differences in ABCC1 transport of DMA^V (this study) and $As(GS)_3$ (Shukalek et al., 2016) by membrane vesicles isolated from different cells raises the possibility that ABCC1 could have a distinct role in arsenic efflux, depending upon the tissue and/or cell type expressed

in. ABCC1 has been indirectly implicated in the protection of specific tissues from arsenic toxicity including kidney and brain (Dringen et al., 2016; Kimura et al., 2006; Kimura et al., 2005; Wang et al., 2016). Furthermore, ABCC1 could play a role in resistance to arsenic-based therapies and this could be modified depending upon the tumor type. This study lays the groundwork for further investigation into how the cellular environment influences the function of ABCC1, particularly for the cellular detoxification of important arsenic metabolites.

Acknowledgements

Diane Swanlund is thanked for outstanding technical assistance. Xiufen Lu is gratefully acknowledged for her assistance with ICP-MS. Dr. Susan P.C. Cole (Queen's University) is thanked for providing the HEK/HeLa-ABCC1 and HeLa-vector stable cell lines and the pcDNA3.1(-)ABCC1.

The 73-arsenic used in this research was supplied by the United States Department of Energy Office of Science by the Isotope Program in the Office of Nuclear Physics.

Authorship Contributions

Participated in research design: Banerjee, Kaur, Whitlock, Carew, Le, Leslie

Conducted experiments: Banerjee, Kaur, Whitlock, Carew

Contributed new reagents or analytic tools: Le

Performed data analysis: Banerjee, Kaur, Whitlock, Carew, and Leslie

Wrote or contributed to the writing of the manuscript: Banerjee, Kaur, Whitlock, and Leslie

CHAPTER 5: Characterization of ABCC1 cellular protection against MMA^V

1.14 Introduction

ABCC1 is a long-form ATP-binding cassette (ABC) transporter in subfamily C. ABCC1 structure is organized into five distinct domains: three polytopic MSDs (composed of 17 transmembrane (TM) helices) and two NBDs. ABCC1 has an overall configuration of MSD0 (TM helices 1-5)-MSD1 (TM helices 6-11)-NBD1-MSD2 (TM helices 12-17)-NBD2, with an extracellular NH_2-terminus and an intracellular COOH-terminus. ABCC1 is a 190 kDa, 1531 amino acid phosphoglycoprotein with three utilized *N*-glycosylation sites at Asn19, Asn23 (both at the NH_2-terminus), and Asn1006 (in the first extracellular loop connecting transmembrane helices (TM) 12 to 13 (Hipfner et al., 1997). ABCC1 is the best characterized multidrug resistance transporter (ABCC), and has been implicated in the cellular efflux of chemically diverse endogenous and exogenous compounds through a wide range of experiments, ranging from direct vesicle transport, to cytotoxicity, to expression analyses. The present work is concerned with how ABCC1 handles arsenic. Much progress has been made, including recent work in our lab, in elucidating the roles of ABCC1.

In the 12 years between the isolation of ABCC1 (Cole et al., 1992) due to its high expression in a drug resistant small cell lung cancer cell line, and the first report of the transport of an arsenic GSH conjugate by ABCC1 (Leslie et al., 2004), ABCC1 was well characterized as a transporter of a variety of endogenous compounds: e.g., GSH, GSSG, and organic anions conjugated to sulfate, GSH, or glucuronate (Haimeur et al., 2004). Leslie *et al.* observed that As^{III} in the

presence of GSH, could be transported by ABCC1 as the conjugate $As(GS)_3$ in membrane vesicle experiments similar to those described in the present study. Further, they noted the importance of glutathione transferase P1 (GSTP1) in the conjugate formation to make transport of As^{III} possible. As^{V} was not transported in the presence or absence of GSH (Banerjee et al., 2018; Leslie et al., 2004).

After $As(GS)_3$ was found to be a substrate of ABCC1, the knowledge of mechanisms by which ABCC1 could potentially influence arsenic handling in the body was improved (Table 4.1). Investigations into transport of other chemical species of arsenic showed that ABCC1 also transported methylated forms. Carew et al. (2011) found that ABCC1 conferred cellular protection against MMA^{III} toxicity, but not MMA^{V}, DMA^{III}, or DMA^{V} in HeLa cells. Similar to As^{III}, MMA^{III} resistance was GSH dependent, and membrane vesicle transport showed that the glutathione conjugate, $MMA(GS)_2$ was the transported form (Carew et al., 2011).

After these findings were reported, cell line differences in ABCC1 function were discovered. ABCC1 was found to transport $As(GS)_3$ with a different kinetic profile in HeLa and HEK cells. (Shukalek et al., 2016). This was determined to be dependent on phosphorylation; Y920 and S921 phosphorylation was correlated to changes in affinity and capacity of $As(GS)_3$ transport, and the stability of this phosphorylation was found to be reliant on two glycosylation sites (N19 and N23) (Shukalek et al., 2016).

Given these cell line differences in $As(GS)_3$ transport, further cytotoxicity and transport studies were performed in the two cell lines. $MMA(GS)_2$ transport also had altered kinetics in HEK

cells (3- fold lower capacity), and DMA^V resistance and transport by ABCC1 only occurred when expressed in HEK293 cells as described in Chapter 4 and as published (Banerjee et al., 2018). The cell line differences in the transport of methylated species was not explained by the same phosphorylation differences that accounted for $As(GS)_3$ transport differences. Further in Chapter 4, DMA^V did not inhibit $As(GS)_3$ transport, while $MMA(GS)_2$ did through an uncompetitive mechanism, suggesting that the three arsenic species do not share an identical binding site.

Understanding ABCC1 and how it relates to arsenic handling is important in cancer research. Arsenic is a proven human carcinogen that is transported by ABCC1 (IARC, 2012; Chapter 4). Further, ABCC1 protein levels are associated with poor outcomes in at least three types of cancers, breast cancer, neuroblastoma, and non-small cell lung cancer (Whitlock & Leslie, 2019).

Here, we built on our work in Chapter 4 (Banerjee et al. 2018) to further investigate the role of ABCC1 in arsenic handling. The interaction between ABCC1 and MMA^V was characterized through cytotoxicity experiments, whole cell accumulation, and competitive transport experiments. This work suggests that MMA^V or a metabolite is transported by ABCC1 in HEK but not HeLa cells.

In Table 5.1, the ability of ABCC1 to confer resistance to arsenicals in HEK and HeLa cells is summarized. In these experiments, the concentration of the arsenical necessary to kill 50% of cells is compared in ABCC1-trasnfected cells and vector-transfected cells to obtain a relative resistance (RR). Of the five arsenicals reported before this work, the only arsenical that ABCC1 did not protect HEK cells from was DMA^{III}. In HeLa cells, ABCC1 protects against neither dimethyl species, but does protect against both inorganic forms and MMA^{III}.

In Table 5.2, the reported ability of ABCC1 to transport arsenicals in ABCC1-enriched membrane vesicles is summarized. ABCC1 transport of As^{III}, As^{V}, or MMA^{III} has not been found in HEK or HeLa vesicles. But ABCC1 does transport $As(GS)_3$ and $MMA(GS)_2$. Further, as described in the previous chapter, ABCC1 transports DMA^{V} in HEK but not HeLa vesicles.

Table 5.1. Known arsenic-cytoprotective effects

Arsenic Species	Relative Resistance of ABCC1 compared with empty vector expressing cells[1]	
	HEK	HeLa
As^{III}	5.3 ± 0.9*	2.5 ± 0.3*
As^{V}	9.2 ± 3.6*	2.1 ± 0.5*
MMA^{III}	2.3 ± 0.2*	1.5 ± 0.2*
DMA^{III}	1.2 ± 0.2	1.2 ± 0.4
DMA^{V}	1.4 ± 0.2*	1.0 ± 0.13

* EC_{50} in ABCC1-transfected significantly higher than in vector-transfected
[1] (Banerjee et al., 2018)

Table 5.2. Transport of Arsenic Species by ABCC1-enriched Membrane Vesicles Prepared from HEK293T or HeLa cells.

Arsenic Species	HEK Cells	HeLa Cells
As^{III}	Not tested	None[2]
As^{V}	None[1]	None[2]
$As(GS)_3$	K_m 3.8 μM and V_{max} 307 pmol/mg/min[3]	K_m 0.32 μM and V_{max} 42 pmol/mg/min[3]
MMA^{III}	None[4]	None[4]
$MMA(GS)_2$	K_m 23 μM and V_{max} 4.9 nmol/mg/min[1]	K_m 11[3]-33[1] μM and V_{max} 17 nmol/mg/min[1]
DMA^{III}	Not tested	Not tested
DMA^{V}	K_m 0.19 μM and V_{max} 342 pmol/mg/min[1]	None[1]

[1] (Banerjee et al., 2018)
[2] (Leslie et al., 2004)
[3] (Shukalek et al, 2016)
[4] (Carew et al., 2011)

1.15 Results

1.15.1 Cytotoxicity

During the study of the differences in the ability of ABCC1 expressed in HEK293 and HeLa cells to confer protection against inorganic and methylated arsenic species described in chapter 4 (Banerjee et al., 2018), a substantial increase in the EC_{50} for HEK-ABCC1 cells relative to HEK-vector was also observed for MMA^V. This difference was surprising because it was not previously observed in a HeLa-vector / HeLa-ABCC1 cell pair (Carew et al., 2011). ABCC1 has previously been shown to confer resistance against inorganic arsenicals As^{III} and As^V, when stably expressed in both cell lines, thus they were used as positive controls (Banerjee et al., 2018). HEK293 cells stably expressing ABCC1 had an 8.4-fold higher EC_{50} value for MMA^V compared to their empty vector-expressing counterpart (Fig. 5.1A, Table 5.3). In order to determine if this resistance was GSH-dependent, cells were pretreated with BSO to deplete GSH. GSH depletion resulted in the complete loss of the ABCC1 cytoprotective effect (Fig 5.1B, Table 5.3). MMA^V had been used previously in cytotoxicity tests on ABCC1-transfected HeLa cells, and no resistance was found (Carew et al., 2011). Thus, as a negative control, we repeated that test with HeLa cells, and again found no resistance, despite the cell line showing the expected cytoprotective effect against As^{III} (Fig. 5.1C; Table 5.3).

TABLE 5.3. Resistance of ABCC1- and vector- transfected HEK and HeLa cells to inorganic and methylated arsenic species

[a] RR = average of *n* experiments (ABCC1 EC_{50}/ Vector EC_{50})

Cells	Arsenical	EC_{50} (± S.D.)		Relative Resistance [a]
		Vector	ABCC1	
HEK	As^{V} *(n = 4)*	18.3 ± 3.3 µM	259.3 ± 28.1 µM	14.5*
	MMA^{V} *(n = 6)*	0.50 ± 0.1 mM	4.0 ± 0.7 mM	8.4*
	MMA^{V} + BSO *(n = 4)*	0.20 ± 0.0 mM	0.14 ± 0.0 mM	0.7
HeLa	MMA^{V} *(n = 3)*	2.9 ± 1.3 mM	3.3 ± 0.8 mM	1.2
	As^{III} (*n* = 3)	6.3 ± 1.0 µM	21.5 ± 3.3 µM	3.4*

*ABCC1 Mean EC_{50} significantly higher than Vector EC_{50} ($p < 0.001$; Student's t-test)

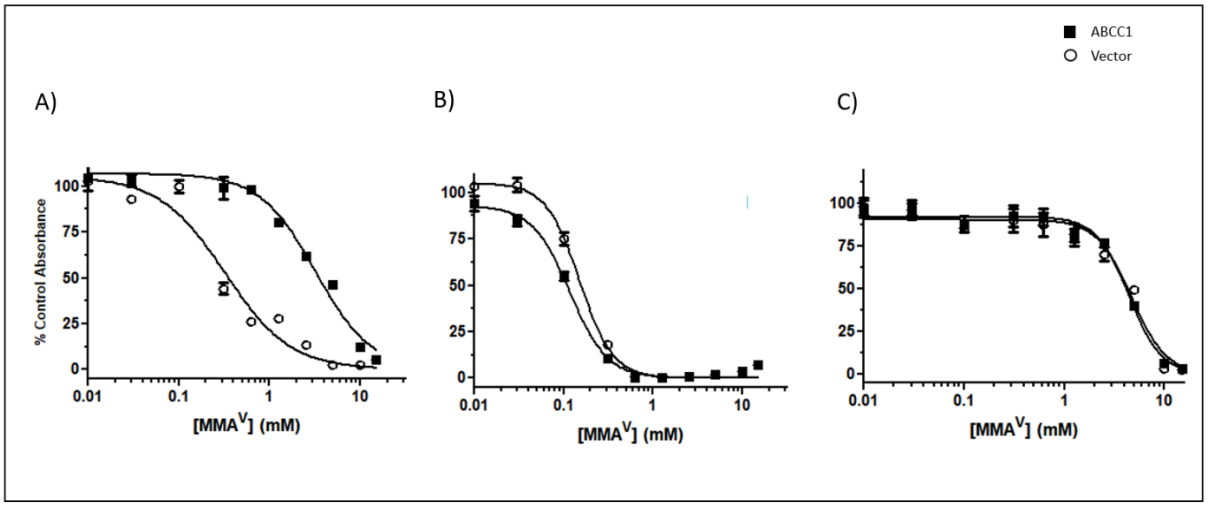

Figure 5.1. Representative cytotoxicity experiments with MMA^V in HEK293 and HeLa cells stably expressing ABCC1 and empty vector. (A, B) HEK 293 cells stably expressing ABCC1 were compared with vector-transfected cells in their ability to survive a range of concentrations of MMA^V in the (A) absence and (B) presence of the GSH-depletion reagent BSO. (C) HeLa cells stably expressing human ABCC1 were compared with vector-transfected cells in their ability to survive a range of concentrations of MMA^V. Each data point represents an average of four determinations ±SD, in a single experiment. Mean EC_{50} values of at least three independent experiments are summarized in Table 5.3.

1.15.2 Speciation

Due to potential intracellular metabolism of MMA^V the ability of ABCC1 to confer cellular protection against MMA^V, does not necessarily mean that MMA^V is the transported chemical form. To investigate the chemical form transported by ABCC1, the arsenic species present extracellularly after treatment of cells with MMA^V, were analyzed using an established HPLC-ICP-MS method (Chen et al., 2013). HEK-V, and HEK-ABCC1 cells were grown in the presence or absence of 100 μM MMA^V for 24 hours. After the 24-hour exposure, the growth media was collected. In parallel, additional cells treated under the same conditions, were washed and then incubated in arsenic-free media under regular growth conditions for two hours and the efflux media was collected. The samples were then analyzed by the HPLC-ICP-MS method, along with the following standards: MMA^V, DMA^V, monomethylmonothiol arsonic acid (MMMTA), Dimethylmonothioarsinic acid (DMMTA), and Dimethyldithioarsinic acid (DMDTA). The data are included as Appendix 3. Arsenic standards are shown in Figure A.3.1. Controls, including MMA^V- containing media without cells, and media used to grow cells without arsenic are shown in Figure A.3.2. The growth and efflux media from cells grown with MMA^V are shown in Figure A.3.3.

Thioarsenicals were included as standards because they have been found in urine in humans after arsenic exposure, making them another potential metabolite to consider when searching for the ABCC1-related mechanism of arsenic resistance in HEK cells (Raml et al., 2005; Raml et al., 2007) . No thioarsenicals were found in any conditions except the thioarsenic standards. MMA^V was found in all cases where MMA^V was added. A relatively minor peak that potentially correlates with the DMA^V retention time was detected in the post-wash efflux media of both HEK-V and HEK-ABCC1 cells (A.3.3 C, D). This peak was not seen in the non-washed media (A.3.3 A, B) or the media from the arsenic-free conditions (A.3.2). Where the potential DMA^V peak was observed, it indicated higher concentration in the efflux media of HEK-V cells than HEK-ABCC1 cells.

1.15.3 Accumulation

To determine if ABCC1 was reducing the toxicity of MMA^V through cellular export of arsenic, whole cell arsenic accumulation assays were done. HeLa-ABCC1/HeLa-vector and HEK-ABCC1/HEK-vector cells were exposed to MMA^V in cell culture media for 24 hours and then total arsenic was quantified by ICP-MS. For both cell line pairs, ABCC1-transfected cells accumulated less arsenic than vector-transfected cells did. In all, HeLa cells accumulated 2-fold more arsenic per cell than their corresponding HEK counterpart (Figure 5.2A). The presence of ABCC1 was associated with an average reduction in arsenic accumulation of 46 ± 9% in HEK cells, and 31 ± 11% in HeLa cells (Fig 5.2B). Thus, consistent with the cytotoxicity data, the accumulation of total arsenic, after exposure to MMA^V, is reduced by ABCC1 to a greater extent in HEK cells than in HeLa cells.

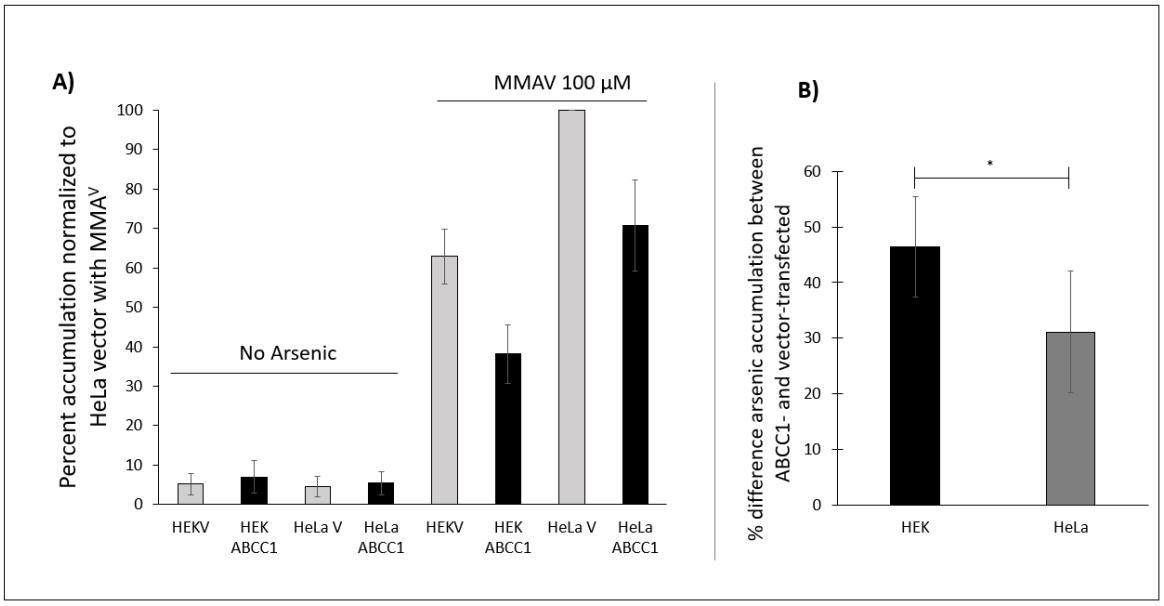

Figure 5.2. (A) Whole cell accumulation of arsenic in HEK293 and HeLa cells after MMA^V exposure. Cells were incubated either with arsenic-free or MMA^V (100 µM)-containing media. After 24 hr incubation, cells were, harvested, counted, washed and lysed, and the arsenic in the lysate was quantified with ICP-MS. Bars represent means of triplicate determinations (±S.D.) in a single experiment and similar results were obtained in two additional experiments. (B) Average percent difference between ABCC1-transfected and vector-transfected cell lines in accumulation of total arsenic after 24 hour exposure to 100 µM MMA^V. Error bars represent SD (n=3). *Significantly different ($p < 0.05$; paired t-test).

1.15.4 Inhibition

To further study the interaction of ABCC1 with MMA^V, the ability of MMA^V to inhibit ABCC1 transport of two well characterized ABCC1 substrates, $^{73}As(GS)_3$ and ^3H-LTC_4 was investigated (Conseil et al., 2019; Leslie et al., 2004; Shukalek et al., 2016). Previous studies have shown that inhibition of ABCC1 can be dependent upon the presence of physiological concentrations of GSH (Loe, Almquist, Deeley, et al., 1996). Thus, for ^3H-LTC_4 transport assays were conducted in the presence and absence of GSH (3 mM). The stability of $As(GS)_3$, requires the presence of excess GSH being present in the transport buffer, therefore all conditions were +GSH. For $^{73}As(GS)_3$, 10 μM and 100 μM MMA^V had no effect on transport (Figure 5.3). For ^3H-LTC4, 100 μM, and 1000 μM MMA^V did not inhibit LTC_4 transport (Fig. 5.4). However, there was a small but significant stimulatory effect of MMA^V at 100 μM of MMA^V with or without GSH (Fig 5.4). In the presence of GSH, 100 μM MMA^V resulted in a 10% higher transport level of LTC_4 than in the MMA^V-free condition. In the absence of GSH, 100 μM MMA^V stimulated LTC_4 transport by 18% compared with the MMA^V-free condition. Further, in the absence of GSH, all conditions showed approximately 60% increased transport as compared to its counterpart in the +GSH condition (Figure 5.4). This was unexpected because reduced GSH usually has no effect on LTC_4 transport, and this observation is likely due to GSH oxidation (Leslie, Mao, et al., 2001; Loe, Almquist, Deeley, et al., 1996).

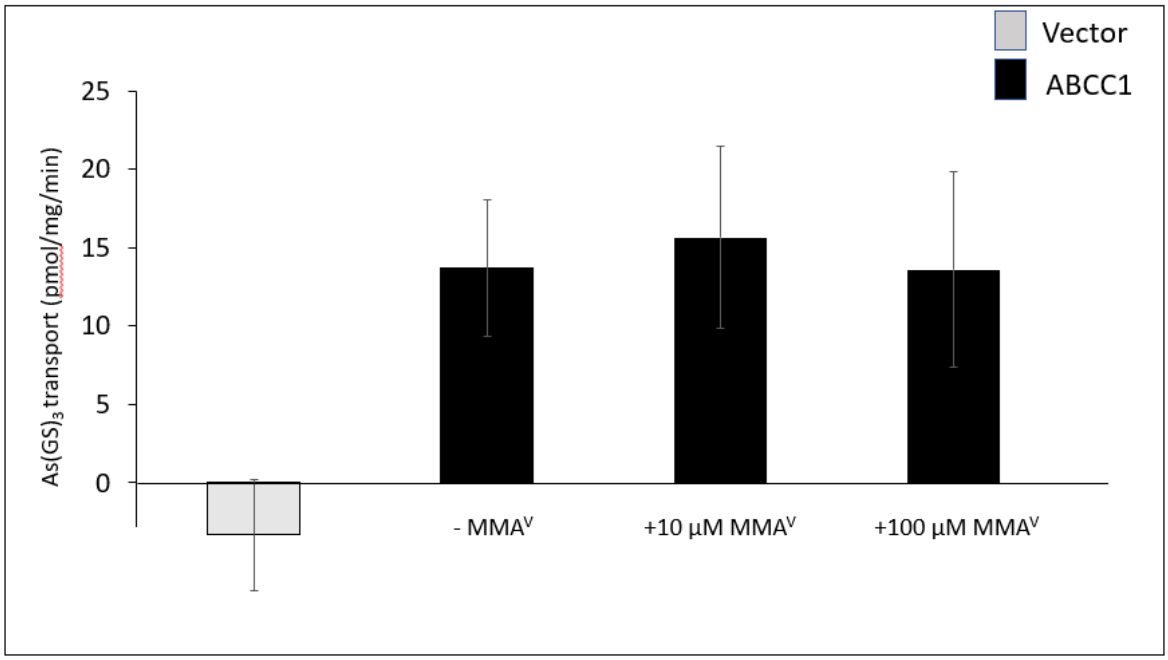

Figure 5.3. $As(GS)_3$ transport by ABCC1-transfected or vector-transfected plasma membrane vesicles in the presence and absence of MMA^V. Plasma membrane-enriched vesicles made from HEK293 cells transfected with ABCC1 or an empty vector were incubated with a transport reaction mix containing $As(GS)_3$. All transport reactions contained 3 mM of GSH. The data points represent the difference in the mean $As(GS)_3$ vesicle accumulation detected in the presence and absence of ATP at a 3 minute time point. Error bars represent the SD of 3 replicate determinations in a single experiment.

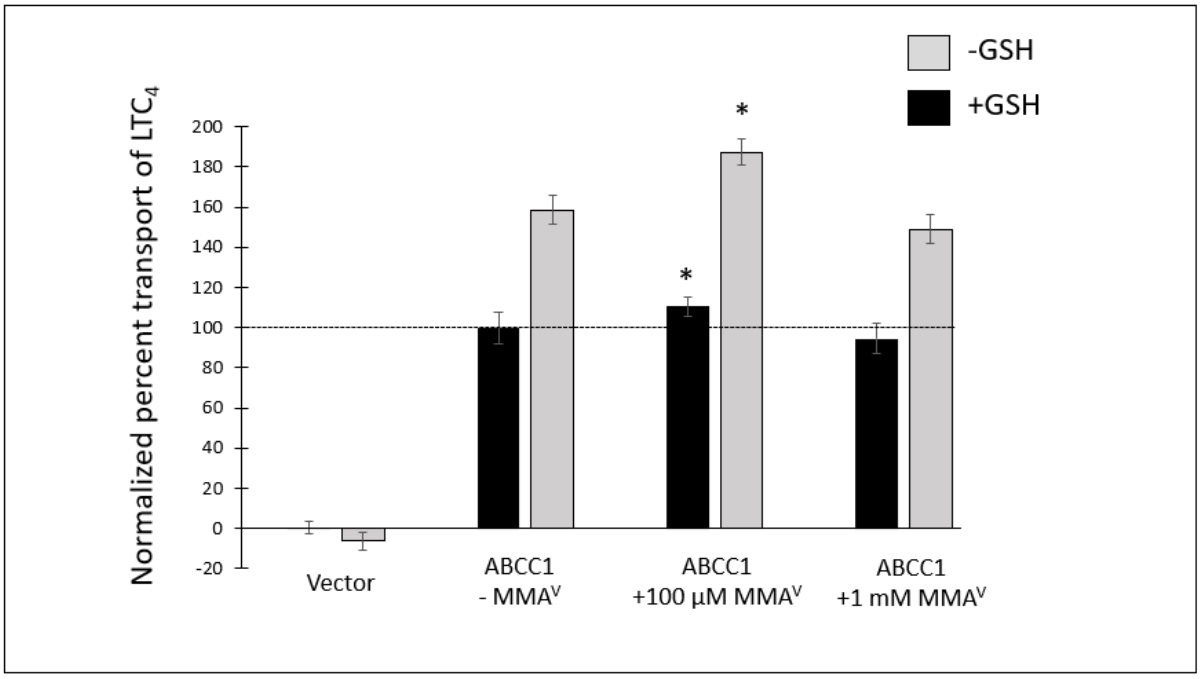

Figure 5.4. LTC_4 transport by vector-expressing or by ABCC1-expressing plasma membrane vesicles in the presence and absence of MMA^V with and without GSH. Plasma membrane-enriched vesicles made from HEK293 cells transfected with vector or ABCC1 were incubated with transport reaction mix containing LTC_4. The bars represent the difference in the mean LTC_4 detected in the presence and absence of ATP after allowing transport for 20 seconds at 23°C. Dark bars represent experiments done in the presence of GSH, and light bars in the absence of GSH. The dashed line shows the data are normalized such that the GSH+ condition without MMA^V is set equal to 100%. Each bar represents three independent experiments, each with three replicate determinations. Error bars represent the SD of the three means of replicate determinations.

*Significantly increased compared to the MMA^V-free condition (paired t-test; $p<0.05$).

1.16 Discussion

In this chapter, we found that HEK cells, but not HeLa cells, were protected by ABCC1 from MMA^V in a glutathione-dependent manner. This was partially explained by whole cell accumulation data, which followed the same cell line differences. The results of competition studies suggests that if MMA^V is being transported by ABCC1, the binding site is non-identical to that of $As(GS)_3$ and LTC_4.

It is worth noting that this report is not in conflict with Carew et al. (2011b), which previously did not find a protective effect of ABCC1 against MMA^V in HeLa cells; indeed, that finding was replicated, but new results were found in HEK293 cells. This finding was not the first cell line difference observed. Work done previously on $As(GS)_3$, $MMA(GS)_2$, and DMA^V transport, including in Chapter 4, also found differences between HEK293 and HeLa cells (Banerjee et al., 2018; Shukalek et al., 2016). The most mechanistic and clear explanation for these cell differences comes from work done by Shukalek et al. (2016) on $As(GS)_3$, which described differences between the cell lines, related to differences in dual phosphorylation at Y920/S921, and N-glycosylation at N19/N23. However, while this was true for $As(GS)_3$, those phosphorylation sites have been ruled out as an explanation for cell line differences in DMA^V and $MMA(GS)_2$ transport (Banerjee et al., 2018). Thus, it is not immediately clear why ABCC1 in different cell lines behaves differently with respect to MMA^V.

While ABCC1 resistance against MMA^V was robust and reproducible, conclusions could not be drawn regarding MMA^V transport by ABCC1 using data from these experiments. Ideally, transport assays with membrane vesicles prepared from HEK 293 and HeLa cells expressing empty vector and ABCC1 should have been completed to determine directly if MMA^V was the transported species. In fact, much effort was put into trying to achieve this, however, after 8 transport experiments using the ICP-MS method for quantification, I was unable to achieve a conclusive result due to high sample variability. Positive arsenic control $MMA(GS)_2$ failed during these experiments while positive controls for transport reagents and vesicle preparations worked. These data suggested instrumentation issues, and indeed the ICP-MS used was reaching the end of its service life. To clarify the role of ABCC1 in the cytotoxicity protection reported in this chapter, future work should repeat these experiments using either ^{14}C-MMA^V (to avoid ICP-MS) or a different ICP-MS should be used.

Due to the lack of transport data, potential ABCC1 transport of MMA^V was studied using less-direct approaches. Instead of measuring transport of MMA^V into vesicles, accumulation in whole cells was evaluated. The cell line differences were at least partially explained by ABCC1 by looking at whole cell accumulation, as the cell line which was protected by ABCC1 against MMA^V was the same cell line that had the larger accumulation reduction due to ABCC1. This strongly suggests that ABCC1 is effluxing arsenic after treatment with MMA^V, but we cannot draw conclusions regarding the chemical form of arsenic being transported. The fact that an MMA^V peak was found in the efflux media means that it is possible MMA^V is the species being

effluxed. However, there is what appears to be a small DMA^V peak and some unknown other small peaks in the efflux media, so another explanation is also possible. It is interesting that in both HEK and HeLa cells, the ABCC1-expressing cell line accumulated less arsenic. It's not clear why ABCC1-expression correlates with a decrease in accumulation in both cell lines, but confers cytotoxicity protection only in the HEK line. The fact that the reduction in accumulation of arsenic (ABCC1 vs vector) in HEK cells is greater than the reduction in HeLa cells suggests there may be a threshold for arsenic above which the protective effect cannot be achieved. In this interpretation, the HEK-ABCC1 reduction in accumulation would have dropped the cellular levels below the threshold required to see a protective effect, while HeLa-ABCC1 did not reach such a reduction.

Differences in cellular uptake of MMA^V are also a potential explanation for differences in cytoprotective effect of ABCC1 between the cell lines. This explanation would rely on some difference in uptake being enough to overshadow or compensate for any ABBC1-dependent effects. There could also be an uptake threshold, slightly different from the aforementioned threshold. There could be high enough uptake in HEK293 cells to meet the toxicity threshold, but not enough uptake in HeLa cells. If uptake were a relevant factor, it would be expected that the cell line which took up arsenic more rapidly would be more affected by the presence or absence of ABCC1. That is, ABCC1 should be a more important factor in cells which are taking up arsenic more quickly, all else equal. The accumulation studies reported in Figure 5.2A show that accumulation of arsenic in cells exposed to MMA^V is not higher in HEK293 cells than in

HeLa cells. This is true even in the empty vector conditions and thus an uptake difference is not a likely explanation for the apparent cytoprotective effect. The effect attributable to ABCC1 shown in Figure 5.2B suggests that ABCC1 activity is more impactful in HEK293 cells than in HeLa.

It is worth considering the possibility that MMA^V resistance occurs through the previously described DMA^V route, due to the fact that MMA^V can be converted to other metabolites, including DMA^V in cells. While small amounts of what appears to be DMA^V were detected in the speciation experiments, there was more in the HEK-vector efflux media than in the HEK-ABCC1 efflux media, which does not support the interpretation of DMA^V efflux being responsible for the observed resistance. Further, MMA^V is more toxic to cells than DMA^V is as measured by EC_{50}, and the relative resistance conferred by ABCC1 against MMA^V is much higher than that conferred against DMA^V. This may come as a surprise if MMA^V were being rapidly converted to DMA^V in cells and the DMA^V -transport ability of ABCC1 was causing the protection against MMA^V. That is, if rapid conversion to DMA^V explained this effect, the resistance against cytotoxicity of MMA^V would be expected to be more similar to that of DMA^V. Further, DMA^V transport is insensitive to GSH (Banerjee et al., 2018), while MMA^v resistance requires GSH. Thus conversion to DMA^V followed by ABCC1 export, does not explain the resistance.

The GSH depletion in cytotoxicity experiments supports the notion that GSH is required by ABCC1 to transport MMA^V. This could be via a coupled mechanism, via stimulation without GSH transport, or via a conjugation-dependent mechanism. It is possible that MMA^V is reduced and conjugated to GSH, or that a cotransporter or allosteric modulator function of GSH exists. Given that HeLa-ABCC1 is a better transporter of $MMA(GS)_2$ than HEK-ABCC1 is (Chapter 4, Figure 4.5), $MMA(GS)_2$ is unlikely to be the transported species that explains cell line differences in resistance to MMA^V. This may follow the model of transport of the anticancer drug vincristine (GSH is required for vincristine transport and vincristine stimulates GSH transport) (Cole, 2014; Loe et al., 1998), or of estrone sulfate (stimulated by GSH but no corresponding stimulation of GSH export) (Qian, Song, et al., 2001; Rothnie et al., 2008). Our inhibition attempts suggest that it is unlikely that MMA^V has an identical binding site to that of LTC_4 or $AS(GS)_3$, if it is indeed transported. However, it may be worth conducting further inhibition experiments with higher concentrations of MMA^V to be more certain.

Taken together, this work raises new questions. It remains to be confirmed with direct transport assays whether MMA^V is being transported and how GSH is involved, given that GSH is necessary for MMA^V cellular protection by ABCC1. Characterizing transport with membrane vesicles would allow transport mechanism to be thoroughly explored. Experiments could include MMA^V transport in the presence and absence of GSH as well as non-reducing analogs. This could help to rule out the possibility that GSH is necessary because ABCC1 transports

MMA^V as a GSH conjugate. Further, transport experiments could be pursued from another angle by using radioactive MMA^V, rendering mass spectrometry unnecessary.

Also, future work could create more value by continuing binding site investigations through competition experiments in an attempt to better understand how this arsenical is interacting with ABCC1 from a structural aspect. Continuing this investigation and building this knowledge base expands the tools at our disposal in controlling the two variables of ABCC1 function most relevant to medicine: how effectively it protects cells from carcinogens, and how it can get in the way of chemotherapy.

Chapter 6. General Discussion

1.17 Overall Summary

In Chapter 3 species differences in hABCC4 and mAbcc4 were characterized. In contrast with hABCC4, mAbcc4 did not confer resistance to arsenic in HEK cells. However, MEF-Abcc4$^{+/+}$ cells conferred higher levels of resistance to arsenate (but not arsenite, MMA^{III}, MMA^{V}, DMA^{III}, or DMA^{V}) than MEF-Abcc4$^{-/-}$ cells. Mouse Abcc4 did not transport arsenic as $MMA(GS)_2$ or DMA^{V}, but hABCC4 did. The epitope for the M_4I-10 ABCC4 antibody was mapped and found to be conserved between species. This led to the initiation of two projects presented in Appendices 1 and 2, Appendix 1 to create mAbcc4/hABCC4 chimeras for narrowing down the binding site of hABCC4 for DMA^{V} and $MMA(GS)_2$ and Appendix 2 the investigation of rAbcc4 and its role in protecting cells from and transporting arsenicals.

In Chapter 4, it was discovered that ABCC1 protects HEK cells from DMA^{V}, DMA^{V} was shown to be transported by ABCC1, but only in HEK293 cells and not in HeLa cells. This cell line difference was not explainable by phosphorylation as was the case with the cell line difference in $As(GS)_3$ characterized by Shukalek et al. (2016).

ABCC1 resistance against MMA^{V} was explored in Chapter 5. We discovered that ABCC1 confers resistance in HEK cells against MMA^{V}, and that protection is GSH dependent. This resistance was not observed when ABCC1 was expressed in HeLa cells. Through accumulation and speciation experiments, we produced evidence that suggests MMA^{V} is

the arsenic species that is being transported by ABCC1. This includes accumulation experiments that show a link between ABCC1 and decreased arsenic accumulation after MMA^V exposure, and the detection of MMA^V as the predominant arsenical in the efflux media after cells are exposed to MMA^V. It is not conclusive, however, whether ABCC1 is transporting MMA^V because this has not been demonstrated with vesicle transport studies.

1.18 Summary and context: Chapter 3

Chapter 3 is about species differences in arsenic handling at the protein level. We can draw some caution in our use of mouse models from the stark differences observed between mAbcc4 and hABCC4, and we can also use these differences to investigate binding sites. In Appendix 1, this knowledge of species differences was leveraged. Constructing chimera proteins that are part mouse and part human can help us narrow down important regions by asking of any chimera, does it act more like mouse or more like human for a given substrate. The chimera strategy and proof of concept in Appendix 1 helps expand the scope of this species difference work.

This work also reinforces the notion that a protein's environment can influence its function. In Chapter 3 we saw a mouse protein that was totally non-protective against arsenic in human cells exert an apparent protective effect in mouse cells. This was, however, observed in two different experimental systems, one using over-expressing transfected cells (HEK293) and the other using mAbcc4 knockdown (MEF).

Further work in Appendix 2 shows that rAbcc4 has an intermediate function between human and mouse, in that it confers resistance against some of the arsenicals hABCC4 confers resistance to in HEK cells, and transports DMA^V at an intermediate level.

More knowledge about the differences in arsenic-handling at the protein, cell, tissue, and whole-body level is urgently needed. Active research in chemotherapeutics uses mouse models to make predictions about efficacy and safety of using arsenic compounds at high doses in humans to battle cancers (Hao et al., 2016). Much of the work done to understand the physiological function of mAbcc4/hABCC4 has used $Abcc4^{(-/-)}$ mice (Berthier et al., 2019; Kruh et al., 2007). Thus, all we can do to understand species differences in this area will better equip us to interpret the valuable results from work with mouse models.

One way to minimize species differences while still using animal models, particularly relevant to drug research, is by studying how mice with humanized livers metabolize compounds. These mice have most of their hepatocytes replaced by human hepatocytes via transplantation in combination with immunosuppression (Naritomi et al., 2018). Even in these studies, predictions gleaned from mouse models often do not match actual human metabolism parameters. Understanding species differences in the function of key proteins is likely relevant in understanding and resolving these discrepancies.

1.19 Summary and context: Chapters 4 and 5

In Chapter 4, we find that ABCC1 confers resistance against and transports DMA^V, and that it confers resistance against and may transport MMA^V. This widens the already major role that ABCC1 has in arsenic handling. Here, we see that the cellular environment in which ABCC1 is in can influence its function. For multiple arsenic metabolites, ABCC1 acts very differently in HeLa and HEK cells. ABCC1 only influences the toxicity of MMA^V and DMA^V in HEK cells and only ABCC1-enriched membrane vesicles prepared from HEK cells transport DMA^V. ABCC1 decreases accumulation of MMA^V to different extents depending on which cell line it is expressed in.

Direct transport of MMA^V by ABCC1, with membrane vesicles has yet to be reliably measured. Further, it remains unclear why the cytoprotective effect of ABCC1 is GSH-dependent. Future work in this area is required to explore the role of GSH in the relationship between MMA^V and ABCC1. Further investigation of the binding site should also be pursued, perhaps extending the competitive binding experiments shown in this chapter to other substrates.

1.20 Overall significance

In one sentence, this thesis offers insights into how arsenic is handled by ABCCs, and how that handling differs depending on species orthologue and cellular environment.

Why do we want to know about the relationship between ABCCs and arsenic? Arsenic presents health challenges in at least two interesting ways: First, it is a proven carcinogen to which hundreds of millions of people are exposed at dangerous levels. Second, it is currently used as an anti-cancer therapy with plans and research underway to use it against a growing number of types of cancer.

The usefulness of this research can be divided into two types: predictive and interventionist. As outlined in Chapter 3, knowledge about levels and SNPs of ABCCs can be used to predict the effects of exposure. An example of how this type of knowledge could be used is in allocating resources to purify groundwater. Some individuals and some populations need access to ground water with less arsenic more urgently than others.

When using arsenic as an anticancer agent, we want to know how it will be handled in the body. The expression of ABCCs in cancerous tissue can help us predict how our interventions will work. Further, control over the function of ABCCs, perhaps pharmacologically, may assist us in using arsenic in cancer therapy. Ultimately, we want ABCCs to provide cellular protection when the effects of arsenic are unwanted (e.g., exposure in drinking water) but we don't want ABCCs to provide this protection when the effects of arsenic are necessary (cancer therapy).

Investigating the relationship between arsenic and ABCCs, including the use of animal models, brings us closer to being able to predict what effect these proteins will have, and intervene in their effects when necessary. Because of this work, we are better positioned to safely and accurately conduct crucial research into arsenic-handling using animal models.

References

Abla, N., Chinn, L. W., Nakamura, T., Liu, L., Huang, C. C., Johns, S. J., . . . Kroetz, D. L. (2008). The human multidrug resistance protein 4 (MRP4, ABCC4): functional analysis of a highly polymorphic gene. *J Pharmacol Exp Ther*, *325*(3), 859-868. https://doi.org/10.1124/jpet.108.136523

Ally, M. S., Ransohoff, K., Sarin, K., Atwood, S. X., Rezaee, M., Bailey-Healy, I., . . . Colevas, A. D. (2016). Effects of Combined Treatment With Arsenic Trioxide and Itraconazole in Patients With Refractory Metastatic Basal Cell Carcinoma. *JAMA Dermatol*, *152*(4), 452-456. https://doi.org/10.1001/jamadermatol.2015.5473

Ambadipudi, R., & Georges, E. (2017). Sequences in Linker-1 domain of the multidrug resistance associated protein (MRP1 or ABCC1) bind to tubulin and their binding is modulated by phosphorylation. *Biochem Biophys Res Commun*, *482*(4), 1001-1006. https://doi.org/10.1016/j.bbrc.2016.11.147

Assem, M., Schuetz, E. G., Leggas, M., Sun, D., Yasuda, K., Reid, G., . . . Schuetz, J. D. (2004). Interactions between hepatic Mrp4 and Sult2a as revealed by the constitutive androstane receptor and Mrp4 knockout mice. *J Biol Chem*, *279*(21), 22250-22257. https://doi.org/10.1074/jbc.M314111200

Bakos, E., Evers, R., Szakács, G., Tusnády, G. E., Welker, E., Szabó, K., . . . Sarkadi, B. (1998). Functional multidrug resistance protein (MRP1) lacking the N-terminal transmembrane domain. *The Journal of Biological Chemistry*, *273*(48), 32167-32175.

Ballatori, N., Krance, S. M., Marchan, R., & Hammond, C. L. (2009). Plasma membrane glutathione transporters and their roles in cell physiology and pathophysiology. *Mol Aspects Med*, *30*(1-2), 13-28. https://doi.org/10.1016/j.mam.2008.08.004

Ballatori, N., Krance, S. M., Notenboom, S., Shi, S., Tieu, K., & Hammond, C. L. (2009). Glutathione dysregulation and the etiology and progression of human diseases. *Biol Chem*, *390*(3), 191-214. https://doi.org/10.1515/BC.2009.033

Banerjee, M., Carew, M. W., Roggenbeck, B. A., Whitlock, B. D., Naranmandura, H., Le, X. C., & Leslie, E. M. (2014). A Novel Pathway for Arsenic Elimination: Human Multidrug Resistance Protein 4 (MRP4/ABCC4) Mediates Cellular Export of Dimethylarsinic Acid (DMAV) and the Diglutathione Conjugate of Monomethylarsonous Acid (MMAIII). *Mol Pharmacol*, *86*(2), 168-179. https://doi.org/mol.113.091314 [pii]
10.1124/mol.113.091314

Banerjee, M., Carew, M. W., Roggenbeck, B. A., Whitlock, B. D., Naranmandura, H., Le, X. C., & Leslie, E. M. (2014). A novel pathway for arsenic elimination: human multidrug resistance protein 4 (MRP4/ABCC4) mediates cellular export of dimethylarsinic acid (DMAV) and the diglutathione conjugate of monomethylarsonous acid (MMAIII). *Molecular Pharmacology*, *86*(2), 168-179. https://doi.org/10.1124/mol.113.091314

Banerjee, M., Kaur, G., Whitlock, B. D., Carew, M. W., Le, X. C., & Leslie, E. M. (2018). Multidrug Resistance Protein 1 (MRP1/ABCC1)-Mediated Cellular Protection and Transport of Methylated Arsenic Metabolites Differs between Human Cell Lines. *Drug Metab Dispos*, *46*(8), 1096-1105. https://doi.org/10.1124/dmd.117.079640

Banerjee, M., Marensi, V., Conseil, G., Le, X. C., Cole, S. P., & Leslie, E. M. (2016). Polymorphic variants of MRP4/ABCC4 differentially modulate the transport of methylated arsenic metabolites and physiological organic anions. *Biochem Pharmacol*, *120*, 72-82. https://doi.org/10.1016/j.bcp.2016.09.016

Beauchamp, E. M., Kosciuczuk, E. M., Serrano, R., Nanavati, D., Swindell, E. P., Viollet, B., . . . Platanias, L. C. (2015). Direct binding of arsenic trioxide to AMPK and generation of inhibitory effects on acute myeloid leukemia precursors. *Mol Cancer Ther*, *14*(1), 202-212. https://doi.org/10.1158/1535-7163.MCT-14-0665-T

Beedholm-Ebsen, R., van de Wetering, K., Hardlei, T., Nexo, E., Borst, P., & Moestrup, S. K. (2010). Identification of multidrug resistance protein 1 (MRP1/ABCC1) as a molecular gate for cellular export of cobalamin. *Blood*, *115*(8), 1632-1639. https://doi.org/10.1182/blood-2009-07-232587

Berthier, J., Arnion, H., Saint-Marcoux, F., & Picard, N. (2019). Multidrug resistance-associated protein 4 in pharmacology: Overview of its contribution to pharmacokinetics, pharmacodynamics and pharmacogenetics. *Life Sci*, *231*, 116540. https://doi.org/10.1016/j.lfs.2019.06.015

Bu, N., Wang, H. Y., Hao, W. H., Liu, X., Xu, S., Wu, B., . . . Naranmandura, H. (2011). Generation of thioarsenicals is dependent on the enterohepatic circulation in rats. *Metallomics*, *3*(10), 1064-1073. https://doi.org/10.1039/c1mt00036e

Bureta, C., Saitoh, Y., Tokumoto, H., Sasaki, H., Maeda, S., Nagano, S., . . . Setoguchi, T. (2019). Synergistic effect of arsenic trioxide, vismodegib and temozolomide on glioblastoma. *Oncol Rep*, *41*(6), 3404-3412. https://doi.org/10.3892/or.2019.7100

Bustaffa, E., Stoccoro, A., Bianchi, F., & Migliore, L. (2014). Genotoxic and epigenetic mechanisms in arsenic carcinogenicity. *Arch Toxicol*, *88*(5), 1043-1067. https://doi.org/10.1007/s00204-014-1233-7

Carew, M. W., & Leslie, E. M. (2010). Selenium-dependent and -independent transport of arsenic by the human multidrug resistance protein 2 (MRP2/ABCC2): implications for the mutual detoxification of arsenic and selenium. *Carcinogenesis*, *31*(8), 1450-1455. https://doi.org/10.1093/carcin/bgq125

Carew, M. W., Naranmandura, H., Shukalek, C. B., Le, X. C., & Leslie, E. M. (2011). Monomethylarsenic diglutathione transport by the human multidrug resistance protein 1 (MRP1/ABCC1). *Drug Metabolism and Disposition: The Biological Fate of Chemicals*, *39*(12), 2298-2304. https://doi.org/10.1124/dmd.111.041673

Chantemargue, B., Di Meo, F., Berka, K., Picard, N., Arnion, H., Essig, M., . . . Trouillas, P. (2018). Structural patterns of the human ABCC4/MRP4 exporter in lipid bilayers rationalize clinically observed polymorphisms. *Pharmacol Res*, *133*, 318-327. https://doi.org/10.1016/j.phrs.2018.02.029

Cheepala, S. B., Pitre, A., Fukuda, Y., Takenaka, K., Zhang, Y., Wang, Y., . . . Schuetz, J. D. (2015). The ABCC4 membrane transporter modulates platelet aggregation. *Blood*, *126*(20), 2307-2319. https://doi.org/10.1182/blood-2014-08-595942

Chen, B., Lu, X., Shen, S., Arnold, L. L., Cohen, S. M., & Le, X. C. (2013). Arsenic speciation in the blood of arsenite-treated F344 rats. *Chem Res Toxicol*, *26*(6), 952-962. https://doi.org/10.1021/tx400123q

Chen, Z.-S., Lee, K., Walther, S., Raftogianis, R. B., Kuwano, M., Zeng, H., & Kruh, G. D. (2002). Analysis of methotrexate and folate transport by multidrug resistance protein 4 (ABCC4): MRP4 is a component of the methotrexate efflux system. *Cancer Research*, *62*(11), 3144-3150.

Chen, Z. S., Lee, K., & Kruh, G. D. (2001). Transport of cyclic nucleotides and estradiol 17-beta-D-glucuronide by multidrug resistance protein 4. Resistance to 6-mercaptopurine and 6-thioguanine. *J Biol Chem*, *276*(36), 33747-33754. https://doi.org/10.1074/jbc.M104833200

Ci, L., Kusuhara, H., Adachi, M., Schuetz, J. D., Takeuchi, K., & Sugiyama, Y. (2007). Involvement of MRP4 (ABCC4) in the luminal efflux of ceftizoxime and cefazolin in the kidney. *Mol Pharmacol*, *71*(6), 1591-1597. https://doi.org/10.1124/mol.106.031823

Cicconi, L., & Lo-Coco, F. (2016). Current management of newly diagnosed acute promyelocytic leukemia. *Ann Oncol*, *27*(8), 1474-1481. https://doi.org/10.1093/annonc/mdw171

Cohen, S. M., Arnold, L. L., Eldan, M., Lewis, A. S., & Beck, B. D. (2006). Methylated arsenicals: the implications of metabolism and carcinogenicity studies in rodents to human risk assessment. *Crit Rev Toxicol*, *36*(2), 99-133.

Cole, S. P. (2014). Targeting Multidrug Resistance Protein 1 (MRP1, ABCC1): Past, Present, and Future. *Annu Rev Pharmacol Toxicol*, *54*, 95-117. https://doi.org/10.1146/annurev-pharmtox-011613-135959

Cole, S. P., Bhardwaj, G., Gerlach, J. H., Mackie, J. E., Grant, C. E., Almquist, K. C., . . . Deeley, R. G. (1992). Overexpression of a transporter gene in a multidrug-resistant human lung cancer cell line. *Science (New York, N.Y.)*, *258*(5088), 1650-1654.

Cole, S. P., & Deeley, R. G. (2006). Transport of glutathione and glutathione conjugates by MRP1. *Trends Pharmacol Sci*, *27*(8), 438-446.

Cole, S. P. C. (2014). Multidrug resistance protein 1 (MRP1, ABCC1), a "multitasking" ATP-binding cassette (ABC) transporter. *The Journal of Biological Chemistry*, *289*(45), 30880-30888. https://doi.org/10.1074/jbc.R114.609248

Conseil, G., Arama-Chayoth, M., Tsfadia, Y., & Cole, S. P. C. (2019). Structure-guided probing of the leukotriene C. *FASEB J*, *33*(10), 10692-10704. https://doi.org/10.1096/fj.201900140R

Conseil, G., & Cole, S. P. (2013). Two polymorphic variants of ABCC1 selectively alter drug resistance and inhibitor sensitivity of the multidrug and organic anion transporter multidrug resistance protein 1. *Drug Metab Dispos*, *41*(12), 2187-2196. https://doi.org/10.1124/dmd.113.054213

Cui, J., & Jing, C. (2019). A review of arsenic interfacial geochemistry in groundwater and the role of organic matter. *Ecotoxicol Environ Saf*, *183*, 109550. https://doi.org/10.1016/j.ecoenv.2019.109550

Cui, X., Kobayashi, Y., Hayakawa, T., & Hirano, S. (2004). Arsenic speciation in bile and urine following oral and intravenous exposure to inorganic and organic arsenics in rats. *Toxicol Sci*, *82*(2), 478-487. https://doi.org/10.1093/toxsci/kfh265

Cullen, W. R. (2014). Chemical mechanism of arsenic biomethylation. *Chem Res Toxicol*, *27*(4), 457-461. https://doi.org/10.1021/tx400441h

Currier, J. M., Svoboda, M., de Moraes, D. P., Matousek, T., Dědina, J., & Stýblo, M. (2011). Direct analysis of methylated trivalent arsenicals in mouse liver by hydride generation-cryotrapping-atomic absorption spectrometry. *Chem Res Toxicol*, *24*(4), 478-480. https://doi.org/10.1021/tx200060c

Dankers, A. C., Mutsaers, H. A., Dijkman, H. B., van den Heuvel, L. P., Hoenderop, J. G., Sweep, F. C., . . . Masereeuw, R. (2013). Hyperuricemia influences tryptophan metabolism via inhibition of multidrug resistance protein 4 (MRP4) and breast cancer resistance protein (BCRP). *Biochim Biophys Acta*, *1832*(10), 1715-1722. https://doi.org/10.1016/j.bbadis.2013.05.002

Dawson, R. J., & Locher, K. P. (2006). Structure of a bacterial multidrug ABC transporter. *Nature*, *443*(7108), 180-185. https://doi.org/nature05155 [pii]
10.1038/nature05155

De Chaudhuri, S., Ghosh, P., Sarma, N., Majumdar, P., Sau, T. J., Basu, S., . . . Giri, A. K. (2008). Genetic variants associated with arsenic susceptibility: study of purine nucleoside phosphorylase, arsenic (+3) methyltransferase, and glutathione S-transferase omega genes. *Environ Health Perspect*, *116*(4), 501-505. https://doi.org/10.1289/ehp.10581

de Waart, D. R., Paulusma, C. C., Kunne, C., & Oude Elferink, R. P. (2006). Multidrug resistance associated protein 2 mediates transport of prostaglandin E2. *Liver Int*, *26*(3), 362-368. https://doi.org/10.1111/j.1478-3231.2005.01234.x

de Waart, D. R., van de Wetering, K., Kunne, C., Duijst, S., Paulusma, C. C., & Oude Elferink, R. P. (2012). Oral availability of cefadroxil depends on ABCC3 and ABCC4. *Drug Metab Dispos*, *40*(3), 515-521. https://doi.org/10.1124/dmd.111.041731

de Wolf, C. J., Yamaguchi, H., van der Heijden, I., Wielinga, P. R., Hundscheid, S. L., Ono, N., . . . Borst, P. (2007). cGMP transport by vesicles from human and mouse erythrocytes. *FEBS J*, *274*(2), 439-450. https://doi.org/10.1111/j.1742-4658.2006.05591.x

Decouture, B., Dreano, E., Belleville-Rolland, T., Kuci, O., Dizier, B., Bazaa, A., . . . Gaussem, P. (2015). Impaired platelet activation and cAMP homeostasis in MRP4-deficient mice. *Blood*, *126*(15), 1823-1830. https://doi.org/10.1182/blood-2015-02-631044

Deeley, R. G., & Cole, S. P. (2006). Substrate recognition and transport by multidrug resistance protein 1 (ABCC1). *FEBS Lett*, *580*(4), 1103-1111. https://doi.org/10.1016/j.febslet.2005.12.036

Delnomdedieu, M., Styblo, M., & Thomas, D. J. (1995). Time dependence of accumulation and binding of inorganic and organic arsenic species in rabbit erythrocytes. *Chem Biol Interact*, *98*(1), 69-83. https://doi.org/10.1016/0009-2797(95)03636-z

Deng, J., Coy, D., Zhang, W., Sunkara, M., Morris, A. J., Wang, C., . . . Jungsuwadee, P. (2015). Elevated glutathione is not sufficient to protect against doxorubicin-induced nuclear damage in heart in multidrug resistance-associated protein 1 (Mrp1/Abcc1) null mice. *J Pharmacol Exp Ther*, *355*(2), 272-279. https://doi.org/10.1124/jpet.115.225490

Ding, X., Zhang, A., Li, C., Ma, L., Tang, S., Wang, Q., . . . Li, J. (2021). The role of H3K9me2-regulated base excision repair genes in the repair of DNA damage induced by arsenic in HaCaT cells and the effects of Ginkgo biloba extract intervention. *Environ Toxicol*, *36*(5), 850-860. https://doi.org/10.1002/tox.23088

Dopp, E., Hartmann, L. M., Florea, A. M., von Recklinghausen, U., Pieper, R., Shokouhi, B., . . . Obe, G. (2004). Uptake of inorganic and organic derivatives of arsenic associated with induced cytotoxic and genotoxic effects in Chinese hamster ovary (CHO) cells. *Toxicol Appl Pharmacol*, *201*(2), 156-165. https://doi.org/10.1016/j.taap.2004.05.017

Dopp, E., Hartmann, L. M., von Recklinghausen, U., Florea, A. M., Rabieh, S., Zimmermann, U., . . . Rettenmeier, A. W. (2005). Forced uptake of trivalent and pentavalent methylated and inorganic arsenic and its cyto-/genotoxicity in fibroblasts and hepatoma cells. *Toxicol Sci*, *87*(1), 46-56. https://doi.org/10.1093/toxsci/kfi218

Dringen, R., Spiller, S., Neumann, S., & Koehler, Y. (2016). Uptake, Metabolic Effects and Toxicity of Arsenate and Arsenite in Astrocytes. *Neurochem Res*, *41*(3), 465-475. https://doi.org/10.1007/s11064-015-1570-9

Drobna, Z., Naranmandura, H., Kubachka, K. M., Edwards, B. C., Herbin-Davis, K., Styblo, M., . . . Thomas, D. J. (2009). Disruption of the arsenic (+3 oxidation state) methyltransferase gene in the mouse alters the phenotype for methylation of arsenic and affects distribution and retention of orally administered arsenate. *Chem Res Toxicol*, *22*(10), 1713-1720. https://doi.org/10.1021/tx900179r

Drobná, Z., Walton, F. S., Harmon, A. W., Thomas, D. J., & Stýblo, M. (2010). Interspecies differences in metabolism of arsenic by cultured primary hepatocytes. *Toxicol Appl Pharmacol*, *245*(1), 47-56. https://doi.org/10.1016/j.taap.2010.01.015

Drobná, Z., Walton, F. S., Paul, D. S., Xing, W., Thomas, D. J., & Stýblo, M. (2010). Metabolism of arsenic in human liver: the role of membrane transporters. *Arch Toxicol*, *84*(1), 3-16. https://doi.org/10.1007/s00204-009-0499-7

Duan, X., Zhao, G., Han, X., Ren, J., Li, H., Chen, P., . . . Ju, S. (2021). Arsenic trioxide-loaded CalliSpheres: . *Oncol Rep*, *46*(1). https://doi.org/10.3892/or.2021.8075

El-Sheikh, A. A., van den Heuvel, J. J., Koenderink, J. B., & Russel, F. G. (2007). Interaction of nonsteroidal anti-inflammatory drugs with multidrug resistance protein (MRP) 2/ABCC2- and MRP4/ABCC4-mediated methotrexate transport. *J Pharmacol Exp Ther*, *320*(1), 229-235. https://doi.org/10.1124/jpet.106.110379

El-Sheikh, A. A., van den Heuvel, J. J., Krieger, E., Russel, F. G., & Koenderink, J. B. (2008). Functional role of arginine 375 in transmembrane helix 6 of multidrug resistance protein 4 (MRP4/ABCC4). *Mol Pharmacol*, *74*(4), 964-971. https://doi.org/10.1124/mol.107.043661

Evers, R., Cnubben, N. H. P., Wijnholds, J., van Deemter, L., van Bladeren, P. J., & Borst, P. (1997). Transport of glutathione prostaglandin A conjugates by the multidrug resistance protein 1. *FEBS Letters*, *419*, 112-116.

Falchi, L., Verstovsek, S., Ravandi-Kashani, F., & Kantarjian, H. M. (2016). The evolution of arsenic in the treatment of acute promyelocytic leukemia and other myeloid neoplasms: Moving toward an effective oral, outpatient therapy. *Cancer*, *122*(8), 1160-1168. https://doi.org/10.1002/cncr.29852

Ferslew, B. C., Köck, K., Bridges, A. S., & Brouwer, K. L. (2014). Role of multidrug resistance-associated protein 4 in the basolateral efflux of hepatically derived enalaprilat. *Drug Metab Dispos*, *42*(9), 1567-1574. https://doi.org/10.1124/dmd.114.057554

Furmanski, B. D., Hu, S., Fujita, K.-I., Li, L., Gibson, A. A., Janke, L. J., . . . Baker, S. D. (2013). Contribution of ABCC4-mediated gastric transport to the absorption and efficacy of dasatinib. *Clinical Cancer Research: An Official Journal of the American Association for Cancer Research*, *19*(16), 4359-4370. https://doi.org/10.1158/1078-0432.CCR-13-0980

Gailer, J., George, G. N., Pickering, I. J., Prince, R. C., Younis, H. S., & Winzerling, J. J. (2002). Biliary excretion of [(GS)(2)AsSe](-) after intravenous injection of rabbits with arsenite and selenate. *Chem Res Toxicol*, *15*(11), 1466-1471. https://doi.org/10.1021/tx025538s

Garelick, H., Jones, H., Dybowska, A., & Valsami-Jones, E. (2008). Arsenic pollution sources. *Rev Environ Contam Toxicol*, *197*, 17-60.

Garnier, N., Redstone, G. G., Dahabieh, M. S., Nichol, J. N., del Rincon, S. V., Gu, Y., . . . Miller, W. H. (2014). The novel arsenical darinaparsin is transported by cystine

importing systems. *Mol Pharmacol*, *85*(4), 576-585. https://doi.org/10.1124/mol.113.089433
Grant, C. E., Gao, M., DeGorter, M. K., Cole, S. P., & Deeley, R. G. (2008). Structural determinants of substrate specificity differences between human multidrug resistance protein (MRP) 1 (ABCC1) and MRP3 (ABCC3). *Drug Metab Dispos*, *36*(12), 2571-2581. https://doi.org/10.1124/dmd.108.022491
Gregus, Z., Roos, G., Geerlings, P., & Németi, B. (2009). Mechanism of thiol-supported arsenate reduction mediated by phosphorolytic-arsenolytic enzymes: II. Enzymatic formation of arsenylated products susceptible for reduction to arsenite by thiols. *Toxicol Sci*, *110*(2), 282-292. https://doi.org/10.1093/toxsci/kfp113
Haimeur, A., Conseil, G., Deeley, R. G., & Cole, S. P. (2004). The MRP-related and BCRP/ABCG2 multidrug resistance proteins: biology, substrate specificity and regulation. *Curr Drug Metab*, *5*(1), 21-53.
Haimeur, A., Deeley, R. G., & Cole, S. P. (2002). Charged amino acids in the sixth transmembrane helix of multidrug resistance protein 1 (MRP1/ABCC1) are critical determinants of transport activity. *J Biol Chem*, *277*(44), 41326-41333.
Hao, L., Ran, W., Xiang-Xin, L., Lu-Qun, W., & Xiao-Ning, Y. (2016). Carnosic Acid-combined Arsenic Trioxide Antileukaemia Cells in the Establishment of NB4/SCID Mouse Model. *Basic Clin Pharmacol Toxicol*, *119*(3), 259-266. https://doi.org/10.1111/bcpt.12580
Hara, Y., Sassi, Y., Guibert, C., Gambaryan, N., Dorfmüller, P., Eddahibi, S., . . . Hulot, J. S. (2011). Inhibition of MRP4 prevents and reverses pulmonary hypertension in mice. *J Clin Invest*, *121*(7), 2888-2897. https://doi.org/10.1172/JCI45023
Hasegawa, M., Kusuhara, H., Adachi, M., Schuetz, J. D., Takeuchi, K., & Sugiyama, Y. (2007). Multidrug resistance-associated protein 4 is involved in the urinary excretion of hydrochlorothiazide and furosemide. *J Am Soc Nephrol*, *18*(1), 37-45. https://doi.org/10.1681/asn.2005090966
Healy, S. M., Wildfang, E., Zakharyan, R. A., & Aposhian, H. V. (1999). Diversity of inorganic arsenite biotransformation. *Biol Trace Elem Res*, *68*(3), 249-266. https://doi.org/10.1007/BF02783907
Hipfner, D. R., Almquist, K. C., Leslie, E. M., Gerlach, J. H., Grant, C. E., Deeley, R. G., & Cole, S. P. (1997). Membrane topology of the multidrug resistance protein (MRP). A study of glycosylation-site mutants reveals an extracytosolic NH2 terminus. *J Biol Chem*, *272*(38), 23623-23630.
Hippler, J., Zdrenka, R., Reichel, R. A. D., Weber, D. G., P, R., Johnen, G., . . . Hirner, A. V. (2011). Intracellular, time-resolved speciation and quantification of arsenic compounds in human urothelial and hepatoma cells. *Journal of Analytical Atomic Spectrometry*(12).
Hoque, M. T., Conseil, G., & Cole, S. P. (2009). Involvement of NHERF1 in apical membrane localization of MRP4 in polarized kidney cells. *Biochem Biophys Res Commun*, *379*(1), 60-64. https://doi.org/10.1016/j.bbrc.2008.12.014

Hu, J., Hu, B., Deng, L., Cheng, L., Fan, Q., & Lu, C. (2021). Arsenic sulfide inhibits the progression of gastric cancer through regulating the circRNA_ASAP2/Wnt/β-catenin pathway. *Anticancer Drugs*. https://doi.org/10.1097/CAD.0000000000001246

Hubaux, R., Becker-Santos, D. D., Enfield, K. S., Rowbotham, D., Lam, S., Lam, W. L., & Martinez, V. D. (2013). Molecular features in arsenic-induced lung tumors. *Molecular Cancer*, *12*, 20. https://doi.org/10.1186/1476-4598-12-20

Hughes, M. F., Edwards, B. C., Herbin-Davis, K. M., Saunders, J., Styblo, M., & Thomas, D. J. (2010). Arsenic (+3 oxidation state) methyltransferase genotype affects steady-state distribution and clearance of arsenic in arsenate-treated mice. *Toxicol Appl Pharmacol*, *249*(3), 217-223. https://doi.org/10.1016/j.taap.2010.09.017

Hunt, K. M., Srivastava, R. K., Elmets, C. A., & Athar, M. (2014). The mechanistic basis of arsenicosis: pathogenesis of skin cancer. *Cancer Lett*, *354*(2), 211-219. https://doi.org/10.1016/j.canlet.2014.08.016

IARC. (2012). (International Agency for Research on Cancer): A Review of Human Carcinogens: C. Arsenic, Metals, Fibres and Dusts. In. Lyon, France: World Health Organization Press.

Imaoka, T., Kusuhara, H., Adachi, M., Schuetz, J. D., Takeuchi, K., & Sugiyama, Y. (2007). Functional involvement of multidrug resistance-associated protein 4 (MRP4/ABCC4) in the renal elimination of the antiviral drugs adefovir and tenofovir. *Mol Pharmacol*, *71*(2), 619-627. https://doi.org/10.1124/mol.106.028233

Ito, K., Olsen, S. L., Qiu, W., Deeley, R. G., & Cole, S. P. (2001). Mutation of a single conserved tryptophan in multidrug resistance protein 1 (MRP1/ABCC1) results in loss of drug resistance and selective loss of organic anion transport. *J Biol Chem*, *276*(19), 15616-15624.

Janke, D., Mehralivand, S., Strand, D., Gödtel-Armbrust, U., Habermeier, A., Gradhand, U., . . . Lang, T. (2008). 6-mercaptopurine and 9-(2-phosphonyl-methoxyethyl) adenine (PMEA) transport altered by two missense mutations in the drug transporter gene ABCC4. *Hum Mutat*, *29*(5), 659-669. https://doi.org/10.1002/humu.20694

Jedlitschky, G., Leier, I., Buchholz, U., Barnouin, K., Kurz, G., & Keppler, D. (1996). Transport of glutathione, glucuronate, and sulfate conjugates by the MRP gene-encoded conjugate export pump. *Cancer Res*, *56*(5), 988-994.

Jedlitschky, G., Tirschmann, K., Lubenow, L. E., Nieuwenhuis, H. K., Akkerman, J. W., Greinacher, A., & Kroemer, H. K. (2004). The nucleotide transporter MRP4 (ABCC4) is highly expressed in human platelets and present in dense granules, indicating a role in mediator storage. *Blood*, *104*(12), 3603-3610. https://doi.org/10.1182/blood-2003-12-4330

Johnson, Z. L., & Chen, J. (2017). Structural Basis of Substrate Recognition by the Multidrug Resistance Protein MRP1. *Cell*, *168*(6), 1085.e1089. https://doi.org/10.1016/j.cell.2017.01.041

Johnson, Z. L., & Chen, J. (2018). ATP Binding Enables Substrate Release from Multidrug Resistance Protein 1. *Cell*, *172*(1-2), 81-89.e10. https://doi.org/10.1016/j.cell.2017.12.005

Kala, S. V., Kala, G., Prater, C. I., Sartorelli, A. C., & Lieberman, M. W. (2004). Formation and urinary excretion of arsenic triglutathione and methylarsenic diglutathione. *Chem Res Toxicol*, *17*(2), 243-249. https://doi.org/10.1021/tx0342060

Kala, S. V., Neely, M. W., Kala, G., Prater, C. I., Atwood, D. W., Rice, J. S., & Lieberman, M. W. (2000). The MRP2/cMOAT transporter and arsenic-glutathione complex formation are required for biliary excretion of arsenic. *J Biol Chem*, *275*(43), 33404-33408. https://doi.org/10.1074/jbc.M007030200

Kanamitsu, K., Kusuhara, H., Schuetz, J. D., Takeuchi, K., & Sugiyama, Y. (2017). Investigation of the Importance of Multidrug Resistance-Associated Protein 4 (Mrp4/Abcc4) in the Active Efflux of Anionic Drugs Across the Blood-Brain Barrier. *J Pharm Sci*, *106*(9), 2566-2575. https://doi.org/10.1016/j.xphs.2017.04.040

Kaur, G., Javed, W., Ponomarenko, O., Shekh, K., Swanlund, D. P., Zhou, J. R., . . . Leslie, E. M. (2020). Human red blood cell uptake and sequestration of arsenite and selenite: Evidence of seleno-bis(S-glutathionyl) arsinium ion formation in human cells. *Biochem Pharmacol*, *180*, 114141. https://doi.org/10.1016/j.bcp.2020.114141

Kaushansky, K., Shoemaker, S. G., Broudy, V. C., Lin, N. L., Matous, J. V., Alderman, E. M., . . . Pearce, M. K. (1992). Structure-function relationships of interleukin-3. An analysis based on the function and binding characteristics of a series of interspecies chimera of gibbon and murine interleukin-3. *J Clin Invest*, *90*(5), 1879-1888. https://doi.org/10.1172/JCI116065

Kenyon, E. M., Hughes, M. F., Adair, B. M., Highfill, J. H., Crecelius, E. A., Clewell, H. J., & Yager, J. W. (2008). Tissue distribution and urinary excretion of inorganic arsenic and its methylated metabolites in C57BL6 mice following subchronic exposure to arsenate in drinking water. *Toxicol Appl Pharmacol*, *232*(3), 448-455. https://doi.org/10.1016/j.taap.2008.07.018

Khairul, I., Wang, Q. Q., Jiang, Y. H., Wang, C., & Naranmandura, H. (2017). Metabolism, toxicity and anticancer activities of arsenic compounds. *Oncotarget*, *8*(14), 23905-23926. https://doi.org/10.18632/oncotarget.14733

Kimura, A., Ishida, Y., Hayashi, T., Wada, T., Yokoyama, H., Sugaya, T., . . . Kondo, T. (2006). Interferon-gamma plays protective roles in sodium arsenite-induced renal injury by up-regulating intrarenal multidrug resistance-associated protein 1 expression. *Am J Pathol*, *169*(4), 1118-1128. https://doi.org/10.2353/ajpath.2006.060024

Kimura, A., Ishida, Y., Wada, T., Yokoyama, H., Mukaida, N., & Kondo, T. (2005). MRP-1 expression levels determine strain-specific susceptibility to sodium arsenic-induced renal injury between C57BL/6 and BALB/c mice. *Toxicol Appl Pharmacol*, *203*(1), 53-61. https://doi.org/10.1016/j.taap.2004.07.013

Kligerman, A. D., Doerr, C. L., Tennant, A. H., Harrington-Brock, K., Allen, J. W., Winkfield, E., . . . DeMarini, D. M. (2003). Methylated trivalent arsenicals as candidate ultimate genotoxic forms of arsenic: induction of chromosomal mutations but not gene mutations. *Environ Mol Mutagen*, *42*(3), 192-205. https://doi.org/10.1002/em.10192

Klokouzas, A., Wu, C. P., van Veen, H. W., Barrand, M. A., & Hladky, S. B. (2003). cGMP and glutathione-conjugate transport in human erythrocytes. *Eur J Biochem*, *270*(18), 3696-3708. https://doi.org/10.1046/j.1432-1033.2003.03753.x

Koichi Kuroda, Kaoru Yoshida, Akira Yasukawa, Hideki Wanibuchi, Shoji Fukushima, & Endo, G. (2001). *Enteric bacteria may play a role in mammalian arsenic metabolism*. A. O. Chemistry.

Konig, J., Hartel, M., Nies, A. T., Martignoni, M. E., Guo, J., Buchler, M. W., . . . Keppler, D. (2005). Expression and localization of human multidrug resistance protein (ABCC) family members in pancreatic carcinoma. *Int J Cancer*, *115*(3), 359-367. https://doi.org/10.1002/ijc.20831

Kovacevic, Z., Sahni, S., Lok, H., Davies, M. J., Wink, D. A., & Richardson, D. R. (2017). Regulation and control of nitric oxide (NO) in macrophages: Protecting the "professional killer cell" from its own cytotoxic arsenal via MRP1 and GSTP1. *Biochimica Et Biophysica Acta*, *1861*(5 Pt A), 995-999. https://doi.org/10.1016/j.bbagen.2017.02.021

Kritharis, A., Bradley, T. P., & Budman, D. R. (2013). The evolving use of arsenic in pharmacotherapy of malignant disease. *Ann Hematol*, *92*(6), 719-730. https://doi.org/10.1007/s00277-013-1707-3

Kruh, G. D., Belinsky, M. G., Gallo, J. M., & Lee, K. (2007). Physiological and pharmacological functions of Mrp2, Mrp3 and Mrp4 as determined from recent studies on gene-disrupted mice. *Cancer Metastasis Rev*, *26*(1), 5-14. https://doi.org/10.1007/s10555-007-9039-1

Lee, K., Klein-Szanto, A. J., & Kruh, G. D. (2000). Analysis of the MRP4 drug resistance profile in transfected NIH3T3 cells. *J Natl Cancer Inst*, *92*(23), 1934-1940. https://doi.org/10.1093/jnci/92.23.1934

Leggas, M., Adachi, M., Scheffer, G. L., Sun, D., Wielinga, P., Du, G., . . . Schuetz, J. D. (2004). Mrp4 Confers Resistance to Topotecan and Protects the Brain from Chemotherapy. In *Mol Cell Biol* (Vol. 24, pp. 7612-7621). https://doi.org/10.1128/mcb.24.17.7612-7621.2004

Leier, I., Jedlitschky, G., Buchholz, U., Cole, S. P., Deeley, R. G., & Keppler, D. (1994). The MRP gene encodes an ATP-dependent export pump for leukotriene C4 and structurally related conjugates. *The Journal of Biological Chemistry*, *269*(45), 27807-27810.

Leslie, E. M. (2012). Arsenic-glutathione conjugate transport by the human multidrug resistance proteins (MRPs/ABCCs). *Journal of Inorganic Biochemistry*, *108*, 141-149. https://doi.org/10.1016/j.jinorgbio.2011.11.009

Leslie, E. M., Deeley, R. G., & Cole, S. P. (2001). Toxicological relevance of the multidrug resistance protein 1, MRP1 (ABCC1) and related transporters. *Toxicology*, *167*(1), 3-23.

Leslie, E. M., Deeley, R. G., & Cole, S. P. C. (2005). Multidrug resistance proteins: role of P-glycoprotein, MRP1, MRP2, and BCRP (ABCG2) in tissue defense. *Toxicology and Applied Pharmacology*, *204*(3), 216-237. https://doi.org/10.1016/j.taap.2004.10.012

Leslie, E. M., Haimeur, A., & Waalkes, M. P. (2004). Arsenic transport by the human multidrug resistance protein 1 (MRP1/ABCC1). Evidence that a tri-glutathione conjugate is required. *J Biol Chem*, *279*(31), 32700-32708. https://doi.org/10.1074/jbc.M404912200

Leslie, E. M., Ito, K., Upadhyaya, P., Hecht, S. S., Deeley, R. G., & Cole, S. P. (2001). Transport of the beta -O-glucuronide conjugate of the tobacco-specific carcinogen 4-(methylnitrosamino)-1-(3-pyridyl)-1-butanol (NNAL) by the multidrug resistance protein 1 (MRP1). Requirement for glutathione or a non-sulfur-containing analog. *J Biol Chem*, *276*(30), 27846-27854.

Leslie, E. M., Létourneau, I. J., Deeley, R. G., & Cole, S. P. (2003). Functional and structural consequences of cysteine substitutions in the NH2 proximal region of the human multidrug resistance protein 1 (MRP1/ABCC1). *Biochemistry*, *42*(18), 5214-5224. https://doi.org/10.1021/bi027076n

Leslie, E. M., Mao, Q., Oleschuk, C. J., Deeley, R. G., & Cole, S. P. (2001). Modulation of multidrug resistance protein 1 (MRP1/ABCC1) transport and atpase activities by interaction with dietary flavonoids. *Mol Pharmacol*, *59*(5), 1171-1180. https://doi.org/10.1124/mol.59.5.1171

Leslie, E. M., Watkins, P. B., Kim, R. B., & Brouwer, K. L. (2007). Differential inhibition of rat and human Na+-dependent taurocholate cotransporting polypeptide (NTCP/SLC10A1)by bosentan: a mechanism for species differences in hepatotoxicity. *J Pharmacol Exp Ther*, *321*(3), 1170-1178. https://doi.org/10.1124/jpet.106.119073

Lev, S., Blechman, J., Nishikawa, S., Givol, D., & Yarden, Y. (1993). Interspecies molecular chimeras of kit help define the binding site of the stem cell factor. *Mol Cell Biol*, *13*(4), 2224-2234.

Li, J., Sun, Y., Zhang, X., Hu, Y., Li, T., Wang, Z., . . . Chen, B. (2018). A methyltransferase gene from arbuscular mycorrhizal fungi involved in arsenic methylation and volatilization. *Chemosphere*, *209*, 392-400. https://doi.org/10.1016/j.chemosphere.2018.06.092

Lin, F., Marchetti, S., Pluim, D., Iusuf, D., Mazzanti, R., Schellens, J. H., . . . van Tellingen, O. (2013). Abcc4 together with abcb1 and abcg2 form a robust cooperative drug efflux system that restricts the brain entry of camptothecin

analogues. *Clin Cancer Res*, *19*(8), 2084-2095. https://doi.org/10.1158/1078-0432.CCR-12-3105
Lin, Z. P., Zhu, Y. L., Johnson, D. R., Rice, K. P., Nottoli, T., Hains, B. C., . . . Sartorelli, A. C. (2008). Disruption of cAMP and prostaglandin E2 transport by multidrug resistance protein 4 deficiency alters cAMP-mediated signaling and nociceptive response. *Mol Pharmacol*, *73*(1), 243-251. https://doi.org/10.1124/mol.107.039594
Liu, C., Janke, L. J., Yang, J. J., Evans, W. E., Schuetz, J. D., & Relling, M. V. (2017). Differential effects of thiopurine methyltransferase (TPMT) and multidrug resistance-associated protein gene 4 (MRP4) on mercaptopurine toxicity. *Cancer Chemother Pharmacol*, *80*(2), 287-293. https://doi.org/10.1007/s00280-017-3361-2
Liu, J. X., Zhou, G. B., Chen, S. J., & Chen, Z. (2012). Arsenic compounds: revived ancient remedies in the fight against human malignancies. *Curr Opin Chem Biol*, *16*(1-2), 92-98. https://doi.org/10.1016/j.cbpa.2012.01.015
Liu, W., & Liu, Y. (2021). Roles of Multidrug Resistance Protein 4 in Microbial Infections and Inflammatory Diseases. *Microb Drug Resist*. https://doi.org/10.1089/mdr.2020.0020
Liu, Y. J., Fan, X. Y., Zhang, D. D., Xia, Y. Z., Hu, Y. J., Jiang, F. L., . . . Liu, Y. (2020). Dual Inhibition of Pyruvate Dehydrogenase Complex and Respiratory Chain Complex Induces Apoptosis by a Mitochondria-Targeted Fluorescent Organic Arsenical in vitro and in vivo. *ChemMedChem*, *15*(6), 552-558. https://doi.org/10.1002/cmdc.201900686
Liu, Z. (2010). Roles of vertebrate aquaglyceroporins in arsenic transport and detoxification. *Adv Exp Med Biol*, *679*, 71-81. https://doi.org/10.1007/978-1-4419-6315-4_6
Liu, Z., Boles, E., & Rosen, B. P. (2004). Arsenic trioxide uptake by hexose permeases in Saccharomyces cerevisiae. *J Biol Chem*, *279*(17), 17312-17318. https://doi.org/10.1074/jbc.M314006200
Liu, Z., Carbrey, J. M., Agre, P., & Rosen, B. P. (2004). Arsenic trioxide uptake by human and rat aquaglyceroporins. *Biochem Biophys Res Commun*, *316*(4), 1178-1185. https://doi.org/10.1016/j.bbrc.2004.03.003
Liu, Z., Sanchez, M. A., Jiang, X., Boles, E., Landfear, S. M., & Rosen, B. P. (2006). Mammalian glucose permease GLUT1 facilitates transport of arsenic trioxide and methylarsonous acid. *Biochem Biophys Res Commun*, *351*(2), 424-430. https://doi.org/10.1016/j.bbrc.2006.10.054
Loe, D. W., Almquist, K. C., Cole, S. P., & Deeley, R. G. (1996). ATP-dependent 17 beta-estradiol 17-(beta-D-glucuronide) transport by multidrug resistance protein (MRP). Inhibition by cholestatic steroids. *J Biol Chem*, *271*(16), 9683-9689.
Loe, D. W., Almquist, K. C., Deeley, R. G., & Cole, S. P. (1996). Multidrug resistance protein (MRP)-mediated transport of leukotriene C4 and chemotherapeutic agents

in membrane vesicles. Demonstration of glutathione-dependent vincristine transport. *The Journal of Biological Chemistry*, *271*(16), 9675-9682.
Loe, D. W., Deeley, R. G., & Cole, S. P. (1998). Characterization of vincristine transport by the M(r) 190,000 multidrug resistance protein (MRP): evidence for cotransport with reduced glutathione. *Cancer Research*, *58*(22), 5130-5136.
Lorico, A., Rappa, G., Finch, R. A., Yang, D., Flavell, R. A., & Sartorelli, A. C. (1997). Disruption of the murine MRP (multidrug resistance protein) gene leads to increased sensitivity to etoposide (VP-16) and increased levels of glutathione. *Cancer Research*, *57*, 5238-5242.
Lu, M., Wang, H., Li, X. F., Lu, X., Cullen, W. R., Arnold, L. L., . . . Le, X. C. (2004). Evidence of hemoglobin binding to arsenic as a basis for the accumulation of arsenic in rat blood. *Chem Res Toxicol*, *17*(12), 1733-1742. https://doi.org/10.1021/tx049756s
Mandal, P. (2017). Molecular insight of arsenic-induced carcinogenesis and its prevention. *Naunyn Schmiedebergs Arch Pharmacol*, *390*(5), 443-455. https://doi.org/10.1007/s00210-017-1351-x
Marafante, E., Vahter, M., & Envall, J. (1985). The role of the methylation in the detoxication of arsenate in the rabbit. *Chem Biol Interact*, *56*(2-3), 225-238. https://doi.org/10.1016/0009-2797(85)90008-0
Mass, M. J., Tennant, A., Roop, B. C., Cullen, W. R., Styblo, M., Thomas, D. J., & Kligerman, A. D. (2001). Methylated trivalent arsenic species are genotoxic. *Chem Res Toxicol*, *14*(4), 355-361.
Matous, J. V., Langley, K., & Kaushansky, K. (1996). Structure-function relationships of stem cell factor: an analysis based on a series of human-murine stem cell factor chimera and the mapping of a neutralizing monoclonal antibody. *Blood*, *88*(2), 437-444.
Matsumiya, W., Kusuhara, S., Hayashibe, K., Maruyama, K., Kusuhara, H., Tagami, M., . . . Negi, A. (2012). Forskolin modifies retinal vascular development in Mrp4-knockout mice. *Invest Ophthalmol Vis Sci*, *53*(13), 8029-8035. https://doi.org/10.1167/iovs.12-10781
McDermott, J. R., Jiang, X., Beene, L. C., Rosen, B. P., & Liu, Z. (2010). Pentavalent methylated arsenicals are substrates of human AQP9. *Biometals*, *23*(1), 119-127. https://doi.org/10.1007/s10534-009-9273-9
Meister, A. (1988). Glutathione metabolism and its selective modification. *J Biol Chem*, *263*(33), 17205-17208.
Meng, Y., Feng, R., Yang, Z., Liu, T., Huo, T., & Jiang, H. (2021). Oxidative stress induced by realgar in neurons: p38 MAPK and ERK1/2 perturb autophagy and induce the p62-Keap1-Nrf2 feedback loop to activate the Nrf2 signalling pathway. *J Ethnopharmacol*, 114582. https://doi.org/10.1016/j.jep.2021.114582
Miah, M. F., Conseil, G., & Cole, S. P. (2016). N-linked glycans do not affect plasma membrane localization of multidrug resistance protein 4 (MRP4) but selectively

alter its prostaglandin E2 transport activity. *Biochem Biophys Res Commun*, *469*(4), 954-959. https://doi.org/10.1016/j.bbrc.2015.12.095

Miao, Z., Wu, L., Lu, M., Meng, X., Gao, B., Qiao, X., . . . Xue, D. (2015). Analysis of the transcriptional regulation of cancer-related genes by aberrant DNA methylation of the cis-regulation sites in the promoter region during hepatocyte carcinogenesis caused by arsenic. *Oncotarget*, *6*(25), 21493-21506. https://doi.org/10.18632/oncotarget.4085

Mizuno, N., Takahashi, T., Kusuhara, H., Schuetz, J. D., Niwa, T., & Sugiyama, Y. (2007). Evaluation of the role of breast cancer resistance protein (BCRP/ABCG2) and multidrug resistance-associated protein 4 (MRP4/ABCC4) in the urinary excretion of sulfate and glucuronide metabolites of edaravone (MCI-186; 3-methyl-1-phenyl-2-pyrazolin-5-one). *Drug Metab Dispos*, *35*(11), 2045-2052. https://doi.org/10.1124/dmd.107.016352

Moe, B., Peng, H., Lu, X., Chen, B., Chen, L. W. L., Gabos, S., . . . Le, X. C. (2016). Comparative cytotoxicity of fourteen trivalent and pentavalent arsenic species determined using real-time cell sensing. *J Environ Sci (China)*, *49*, 113-124. https://doi.org/10.1016/j.jes.2016.10.004

Morgan, J. A., Cheepala, S. B., Wang, Y., Neale, G., Adachi, M., Nachagari, D., . . . Schuetz, J. D. (2012). Deregulated hepatic metabolism exacerbates impaired testosterone production in Mrp4-deficient mice. *J Biol Chem*, *287*(18), 14456-14466. https://doi.org/10.1074/jbc.M111.319681

Mueller, C. F., Widder, J. D., McNally, J. S., McCann, L., Jones, D. P., & Harrison, D. G. (2005). The role of the multidrug resistance protein-1 in modulation of endothelial cell oxidative stress. *Circ Res*, *97*(7), 637-644. https://doi.org/10.1161/01.RES.0000183734.21112.b7

Mukhopadhyay, R., Bhattacharjee, H., & Rosen, B. P. (2014). Aquaglyceroporins: generalized metalloid channels. *Biochim Biophys Acta*, *1840*(5), 1583-1591. https://doi.org/10.1016/j.bbagen.2013.11.021

Murray, J., Valli, E., Yu, D. M. T., Truong, A. M., Gifford, A. J., Eden, G. L., . . . Fletcher, J. I. (2017). Suppression of the ATP-binding cassette transporter ABCC4 impairs neuroblastoma tumour growth and sensitises to irinotecan in vivo. *Eur J Cancer*, *83*, 132-141. https://doi.org/10.1016/j.ejca.2017.06.024

Naranmandura, H., Carew, M. W., Xu, S., Lee, J., Leslie, E. M., Weinfeld, M., & Le, X. C. (2011). Comparative toxicity of arsenic metabolites in human bladder cancer EJ-1 cells. *Chem Res Toxicol*, *24*(9), 1586-1596. https://doi.org/10.1021/tx200291p

Naranmandura, H., Ibata, K., & Suzuki, K. T. (2007). Toxicity of dimethylmonothioarsinic acid toward human epidermoid carcinoma A431 cells. *Chem Res Toxicol*, *20*(8), 1120-1125. https://doi.org/10.1021/tx700103y

Naranmandura, H., Ogra, Y., Iwata, K., Lee, J., Suzuki, K. T., Weinfeld, M., & Le, X. C. (2009). Evidence for toxicity differences between inorganic arsenite and

thioarsenicals in human bladder cancer cells. *Toxicol Appl Pharmacol*, *238*(2), 133-140. https://doi.org/10.1016/j.taap.2009.05.006
Naritomi, Y., Sanoh, S., & Ohta, S. (2018). Chimeric mice with humanized liver: Application in drug metabolism and pharmacokinetics studies for drug discovery. *Drug Metab Pharmacokinet*, *33*(1), 31-39. https://doi.org/10.1016/j.dmpk.2017.11.001
Naujokas, M. F., Anderson, B., Ahsan, H., Aposhian, H. V., Graziano, J. H., Thompson, C., & Suk, W. A. (2013). The broad scope of health effects from chronic arsenic exposure: update on a worldwide public health problem. *Environ Health Perspect*, *121*(3), 295-302. https://doi.org/10.1289/ehp.1205875
Nies, A. T., Jedlitschky, G., Konig, J., Herold-Mende, C., Steiner, H. H., Schmitt, H. P., & Keppler, D. (2004). Expression and immunolocalization of the multidrug resistance proteins, MRP1-MRP6 (ABCC1-ABCC6), in human brain. *Neuroscience*, *129*(2), 349-360. https://doi.org/10.1016/j.neuroscience.2004.07.051
Németi, B., & Gregus, Z. (2009a). Glutathione-supported arsenate reduction coupled to arsenolysis catalyzed by ornithine carbamoyl transferase. *Toxicol Appl Pharmacol*, *239*(2), 154-161. https://doi.org/10.1016/j.taap.2009.02.011
Németi, B., & Gregus, Z. (2009b). Mechanism of thiol-supported arsenate reduction mediated by phosphorolytic-arsenolytic enzymes: I. The role of arsenolysis. *Toxicol Sci*, *110*(2), 270-281. https://doi.org/10.1093/toxsci/kfp112
Németi, B., & Gregus, Z. (2013). Reduction of dimethylarsinic acid to the highly toxic dimethylarsinous acid by rats and rat liver cytosol. *Chem Res Toxicol*, *26*(3), 432-443. https://doi.org/10.1021/tx300505v
Omasits, P. (2013). In: Bioinformatics.
Ono, N., Van der Heijden, I., Scheffer, G. L., Van de Wetering, K., Van Deemter, E., De Haas, M., . . . Borst, P. (2007). Multidrug resistance-associated protein 9 (ABCC12) is present in mouse and boar sperm. *Biochem J*, *406*(1), 31-40. https://doi.org/10.1042/bj20070292
Ose, A., Ito, M., Kusuhara, H., Yamatsugu, K., Kanai, M., Shibasaki, M., . . . Sugiyama, Y. (2009). Limited brain distribution of [3R,4R,5S]-4-acetamido-5-amino-3-(1-ethylpropoxy)-1-cyclohexene-1-carboxylate phosphate (Ro 64-0802), a pharmacologically active form of oseltamivir, by active efflux across the blood-brain barrier mediated by organic anion transporter 3 (Oat3/Slc22a8) and multidrug resistance-associated protein 4 (Mrp4/Abcc4). *Drug Metab Dispos*, *37*(2), 315-321. https://doi.org/10.1124/dmd.108.024018
Paumi, C. M., Wright, M., Townsend, A. J., & Morrow, C. S. (2003). Multidrug resistance protein (MRP) 1 and MRP3 attenuate cytotoxic and transactivating effects of the cyclopentenone prostaglandin, 15-deoxy-Delta(12,14)prostaglandin J2 in MCF7 breast cancer cells. *Biochemistry*, *42*(18), 5429-5437. https://doi.org/10.1021/bi027347u

Peklak-Scott, C., Townsend, A. J., & Morrow, C. S. (2005). Dynamics of glutathione conjugation and conjugate efflux in detoxification of the carcinogen, 4-nitroquinoline 1-oxide: contributions of glutathione, glutathione S-transferase, and MRP1. *Biochemistry*, *44*(11), 4426-4433.

Petrick, J. S., Ayala-Fierro, F., Cullen, W. R., Carter, D. E., & Vasken Aposhian, H. (2000). Monomethylarsonous acid (MMA(III)) is more toxic than arsenite in Chang human hepatocytes. *Toxicol Appl Pharmacol*, *163*(2), 203-207. https://doi.org/10.1006/taap.1999.8872

Pham, D. H., Kudira, R., Xu, L., Valencia, C. A., Ellis, J. L., Shi, T., . . . Miethke, A. (2021). Deleterious Variants in ABCC12 are Detected in Idiopathic Chronic Cholestasis and Cause Intrahepatic Bile Duct Loss in Model Organisms. *Gastroenterology*. https://doi.org/10.1053/j.gastro.2021.03.026

Pineiro, R., Maffucci, T., & Falasca, M. (2011). The putative cannabinoid receptor GPR55 defines a novel autocrine loop in cancer cell proliferation. *Oncogene*, *30*(2), 142-152. https://doi.org/10.1038/onc.2010.417

Platanias, L. C. (2009). Biological responses to arsenic compounds. *J Biol Chem*, *284*(28), 18583-18587. https://doi.org/10.1074/jbc.R900003200

Podgorski, J., & Berg, M. (2020). Global threat of arsenic in groundwater. *Science*, *368*(6493), 845-850. https://doi.org/10.1126/science.aba1510

Prakash, C., Soni, M., & Kumar, V. (2016). Mitochondrial oxidative stress and dysfunction in arsenic neurotoxicity: A review. *J Appl Toxicol*, *36*(2), 179-188. https://doi.org/10.1002/jat.3256

Qian, Y. M., Qiu, W., Gao, M., Westlake, C. J., Cole, S. P., & Deeley, R. G. (2001). Characterization of binding of leukotriene C4 by human multidrug resistance protein 1: evidence of differential interactions with NH2- and COOH-proximal halves of the protein. *J Biol Chem*, *276*(42), 38636-38644. https://doi.org/10.1074/jbc.M107025200

M107025200 [pii]

Qian, Y. M., Song, W. C., Cui, H., Cole, S. P., & Deeley, R. G. (2001). Glutathione stimulates sulfated estrogen transport by multidrug resistance protein 1. *J Biol Chem*, *276*(9), 6404-6411.

Rahman, M. M., Ng, J. C., & Naidu, R. (2009). Chronic exposure of arsenic via drinking water and its adverse health impacts on humans. *Environ Geochem Health*, *31 Suppl 1*, 189-200. https://doi.org/10.1007/s10653-008-9235-0

Ramaen, O., Leulliot, N., Sizun, C., Ulryck, N., Pamlard, O., Lallemand, J. Y., . . . Jacquet, E. (2006). Structure of the human multidrug resistance protein 1 nucleotide binding domain 1 bound to Mg2+/ATP reveals a non-productive catalytic site. *J Mol Biol*, *359*(4), 940-949. https://doi.org/10.1016/j.jmb.2006.04.005

Raml, R., Goessler, W., Traar, P., Ochi, T., & Francesconi, K. A. (2005). Novel thioarsenic metabolites in human urine after ingestion of an arsenosugar, 2',3'-

dihydroxypropyl 5-deoxy-5-dimethylarsinoyl-beta-D-riboside. *Chem Res Toxicol*, *18*(9), 1444-1450. https://doi.org/10.1021/tx050111h

Raml, R., Rumpler, A., Goessler, W., Vahter, M., Li, L., Ochi, T., & Francesconi, K. A. (2007). Thio-dimethylarsinate is a common metabolite in urine samples from arsenic-exposed women in Bangladesh. *Toxicol Appl Pharmacol*, *222*(3), 374-380. https://doi.org/10.1016/j.taap.2006.12.014

Ray, A. S., Cihlar, T., Robinson, K. L., Tong, L., Vela, J. E., Fuller, M. D., . . . Rhodes, G. R. (2006). Mechanism of active renal tubular efflux of tenofovir. *Antimicrob Agents Chemother*, *50*(10), 3297-3304. https://doi.org/10.1128/AAC.00251-06

Reay, P. F., & Asher, C. J. (1977). Preparation and purification of 74As-labeled arsenate and arsenite for use in biological experiments. *Anal Biochem*, *78*(2), 557-560.

Rehman, K., Chen, Z., Wang, W. W., Wang, Y. W., Sakamoto, A., Zhang, Y. F., . . . Suzuki, N. (2012). Mechanisms underlying the inhibitory effects of arsenic compounds on protein tyrosine phosphatase (PTP). *Toxicol Appl Pharmacol*, *263*(3), 273-280. https://doi.org/10.1016/j.taap.2012.06.019

Reid, G., Wielinga, P., Zelcer, N., van der Heijden, I., Kuil, A., de Haas, M., . . . Borst, P. (2003). The human multidrug resistance protein MRP4 functions as a prostaglandin efflux transporter and is inhibited by nonsteroidal antiinflammatory drugs. *Proc Natl Acad Sci U S A*, *100*(16), 9244-9249. https://doi.org/10.1073/pnas.1033060100

Ren, X., McHale, C. M., Skibola, C. F., Smith, A. H., Smith, M. T., & Zhang, L. (2011). An emerging role for epigenetic dysregulation in arsenic toxicity and carcinogenesis. *Environ Health Perspect*, *119*(1), 11-19. https://doi.org/10.1289/ehp.1002114

Rius, M., Hummel-Eisenbeiss, J., Hofmann, A. F., & Keppler, D. (2006). Substrate specificity of human ABCC4 (MRP4)-mediated cotransport of bile acids and reduced glutathione. *Am J Physiol Gastrointest Liver Physiol*, *290*(4), G640-649. https://doi.org/10.1152/ajpgi.00354.2005

Rius, M., Hummel-Eisenbeiss, J., & Keppler, D. (2008). ATP-dependent transport of leukotrienes B4 and C4 by the multidrug resistance protein ABCC4 (MRP4). *J Pharmacol Exp Ther*, *324*(1), 86-94. https://doi.org/10.1124/jpet.107.131342

Rius, M., Nies, A. T., Hummel-Eisenbeiss, J., Jedlitschky, G., & Keppler, D. (2003). Cotransport of reduced glutathione with bile salts by MRP4 (ABCC4) localized to the basolateral hepatocyte membrane. *Hepatology*, *38*(2), 374-384. https://doi.org/10.1053/jhep.2003.50331

Rius, M., Thon, W. F., Keppler, D., & Nies, A. T. (2005). Prostanoid transport by multidrug resistance protein 4 (MRP4/ABCC4) localized in tissues of the human urogenital tract. *J Urol*, *174*(6), 2409-2414. https://doi.org/10.1097/01.ju.0000180411.03808.cb

Robbiani, D. F., Finch, R. A., Jager, D., Muller, W. A., Sartorelli, A. C., & Randolph, G. W. (2000). The leukotriene C4 transporter MRP1 regulates CCL19 (MIP-3B, ELC)-dependent mobilization of dendritic cells to lymph nodes. *103*, 757-768.

Roggenbeck, B. A., Banerjee, M., & Leslie, E. M. (2016). Cellular arsenic transport pathways in mammals. *J Environ Sci (China)*, *49*, 38-58. https://doi.org/10.1016/j.jes.2016.10.001

Roggenbeck, B. A., Carew, M. W., Charrois, G. J., Douglas, D. N., Kneteman, N. M., Lu, X., . . . Leslie, E. M. (2015). Characterization of arsenic hepatobiliary transport using sandwich-cultured human hepatocytes. *Toxicol Sci*, *145*(2), 307-320. https://doi.org/10.1093/toxsci/kfv051

Rothnie, A., Conseil, G., Lau, A. Y., Deeley, R. G., & Cole, S. P. (2008). Mechanistic differences between GSH transport by multidrug resistance protein 1 (MRP1/ABCC1) and GSH modulation of MRP1-mediated transport. *Mol Pharmacol*, *74*(6), 1630-1640. https://doi.org/10.1124/mol.108.049080

Russel, F. G., Koenderink, J. B., & Masereeuw, R. (2008). Multidrug resistance protein 4 (MRP4/ABCC4): a versatile efflux transporter for drugs and signalling molecules. *Trends Pharmacol Sci*, *29*(4), 200-207. https://doi.org/10.1016/j.tips.2008.01.006

Sage, A. P., Minatel, B. C., Ng, K. W., Stewart, G. L., Dummer, T. J. B., Lam, W. L., & Martinez, V. D. (2017). Oncogenomic disruptions in arsenic-induced carcinogenesis. *Oncotarget*, *8*(15), 25736-25755. https://doi.org/10.18632/oncotarget.15106

Sakamoto, H., Hara, H., Hirano, K., & Adachi, T. (1999). Enhancement of glucuronosyl etoposide transport by glutathione in multidrug resistance-associated protein-overexpressing cells. *Cancer Letters*, *135*(1), 113-119.

Sane, R., Wu, S. P., Zhang, R., & Gallo, J. M. (2014). The effect of ABCG2 and ABCC4 on the pharmacokinetics of methotrexate in the brain. *Drug Metab Dispos*, *42*(4), 537-540. https://doi.org/10.1124/dmd.113.055228

Sassi, Y., Abi-Gerges, A., Fauconnier, J., Mougenot, N., Reiken, S., Haghighi, K., . . . Hulot, J. S. (2012). Regulation of cAMP homeostasis by the efflux protein MRP4 in cardiac myocytes. *FASEB J*, *26*(3), 1009-1017. https://doi.org/10.1096/fj.11-194027

Sassi, Y., Lipskaia, L., Vandecasteele, G., Nikolaev, V. O., Hatem, S. N., Cohen Aubart, F., . . . Hulot, J. S. (2008). Multidrug resistance-associated protein 4 regulates cAMP-dependent signaling pathways and controls human and rat SMC proliferation. *J Clin Invest*, *118*(8), 2747-2757. https://doi.org/10.1172/jci35067

Sassi, Y. A.-G. A., Fauconnier J, Mougenot N, Reiken S, Haghighi K, Kranias EG, Marks AR, Lacampagne A, Engelhardt S, Hatem SN, Lompre AM, Hulot JS. (2019). Regulation of cAMP homeostasis by the efflux protein MRP4 in cardiac myocytes. - PubMed - NCBI. *Federation of American Societies for Experimental Biology*, *23*(3), 1009-1017.

Schläwicke Engström, K., Broberg, K., Concha, G., Nermell, B., Warholm, M., & Vahter, M. (2007). Genetic polymorphisms influencing arsenic metabolism: evidence from Argentina. *Environ Health Perspect*, *115*(4), 599-605. https://doi.org/10.1289/ehp.9734

Schuetz, J. D., Connelly, M. C., Sun, D., Paibir, S. G., Flynn, P. M., Srinivas, R. V., . . . Fridland, A. (1999). MRP4: A previously unidentified factor in resistance to nucleoside-based antiviral drugs. *Nat Med*, *5*(9), 1048-1051. https://doi.org/10.1038/12487

Shankar, S., Shanker, U., & Shikha. (2014). Arsenic contamination of groundwater: a review of sources, prevalence, health risks, and strategies for mitigation. *ScientificWorldJournal*, *2014*, 304524. https://doi.org/10.1155/2014/304524

Shen, S., Li, X. F., Cullen, W. R., Weinfeld, M., & Le, X. C. (2013). Arsenic binding to proteins. *Chem Rev*, *113*(10), 7769-7792. https://doi.org/10.1021/cr300015c

Shi, H., Shi, X., & Liu, K. J. (2004). Oxidative mechanism of arsenic toxicity and carcinogenesis. *Mol Cell Biochem*, *255*(1-2), 67-78.

Shukalek, C. B., Swanlund, D. P., Rousseau, R. K., Weigl, K. E., Marensi, V., Cole, S. P., & Leslie, E. M. (2016). Arsenic Triglutathione [As(GS)3] Transport by Multidrug Resistance Protein 1 (MRP1/ABCC1) is Selectively Modified by Phosphorylation of Tyr920/Ser921 and Glycosylation of Asn19/Asn23. *Mol Pharmacol*, *90*(2), 127-139. https://doi.org/10.1124/mol.116.103648

Sinha, C., Ren, A., Arora, K., Moon, C. S., Yarlagadda, S., Zhang, W., . . . Naren, A. P. (2013). Multi-drug resistance protein 4 (MRP4)-mediated regulation of fibroblast cell migration reflects a dichotomous role of intracellular cyclic nucleotides. *J Biol Chem*, *288*(6), 3786-3794. https://doi.org/10.1074/jbc.M112.435925

Slot, A. J., Molinski, S. V., & Cole, S. P. C. (2011). Mammalian multidrug-resistance proteins (MRPs). *Essays in Biochemistry*, *50*(1), 179-207. https://doi.org/10.1042/bse0500179

Smeets, P. H., van Aubel, R. A., Wouterse, A. C., van den Heuvel, J. J., & Russel, F. G. (2004). Contribution of multidrug resistance protein 2 (MRP2/ABCC2) to the renal excretion of p-aminohippurate (PAH) and identification of MRP4 (ABCC4) as a novel PAH transporter. *J Am Soc Nephrol*, *15*(11), 2828-2835. https://doi.org/10.1097/01.ASN.0000143473.64430.AC

Smith, A. H., Lingas, E. O., & Rahman, M. (2000). Contamination of drinking-water by arsenic in Bangladesh: a public health emergency. *Bull World Health Organ*, *78*(9), 1093-1103.

Stride, B. D., Cole, S. P. C., & Deeley, R. G. (1999). Localization of a substrate specificity domain in the multidrug resistance protein. *Journal of Biological Chemistry*, *274*, 22877-22883.

Stride, B. D., Grant, C. E., Loe, D. W., Hipfner, D. R., Cole, S. P. C., & Deeley, R. G. (1997). Pharmacological characterization of the murine and human orthologs of multidrug resistance protein in transfected human embryonic kidney cells. *Molecular Pharmacology*, *52*, 344-353.

Struck, A. W., Thompson, M. L., Wong, L. S., & Micklefield, J. (2012). S-adenosyl-methionine-dependent methyltransferases: highly versatile enzymes in biocatalysis, biosynthesis and other biotechnological applications. *Chembiochem*, *13*(18), 2642-2655. https://doi.org/10.1002/cbic.201200556

Styblo, M., Del Razo, L. M., Vega, L., Germolec, D. R., LeCluyse, E. L., Hamilton, G. A., . . . Thomas, D. J. (2000). Comparative toxicity of trivalent and pentavalent inorganic and methylated arsenicals in rat and human cells. *Arch Toxicol*, *74*(6), 289-299.

Sundaram, M., Yao, S. Y., Ng, A. M., Griffiths, M., Cass, C. E., Baldwin, S. A., & Young, J. D. (1998). Chimeric constructs between human and rat equilibrative nucleoside transporters (hENT1 and rENT1) reveal hENT1 structural domains interacting with coronary vasoactive drugs. *J Biol Chem*, *273*(34), 21519-21525. https://doi.org/10.1074/jbc.273.34.21519

Suzuki, K. T., Tomita, T., Ogra, Y., & Ohmichi, M. (2001). Glutathione-conjugated arsenics in the potential hepato-enteric circulation in rats. *Chem Res Toxicol*, *14*(12), 1604-1611. https://doi.org/10.1021/tx0155496

Taguchi, Y., Saeki, K., & Komano, T. (2002). Functional analysis of MRP1 cloned from bovine. *FEBS letters*, *521*(1-3), 211-213.

Takabe, K., Kim, R. H., Allegood, J. C., Mitra, P., Ramachandran, S., Nagahashi, M., . . . Spiegel, S. (2010). Estradiol induces export of sphingosine 1-phosphate from breast cancer cells via ABCC1 and ABCG2. *J Biol Chem*, *285*(14), 10477-10486. https://doi.org/10.1074/jbc.M109.064162

Takenaka, K., Morgan, J. A., Scheffer, G. L., Adachi, M., Stewart, C. F., Sun, D., . . . Schuetz, J. D. (2007). Substrate overlap between Mrp4 and Abcg2/Bcrp affects purine analogue drug cytotoxicity and tissue distribution. *Cancer Res*, *67*(14), 6965-6972. https://doi.org/10.1158/0008-5472.CAN-06-4720

Teva. (2018). Product Monograph for Trisenox (Arsenic Tiroxide). In: Teva Canada Innovation.

Thomas, D. J., Li, J., Waters, S. B., Xing, W., Adair, B. M., Drobna, Z., . . . Styblo, M. (2007). Arsenic (+3 oxidation state) methyltransferase and the methylation of arsenicals. *Exp Biol Med (Maywood)*, *232*(1), 3-13.

Thomas, D. J., Waters, S. B., & Styblo, M. (2004). Elucidating the pathway for arsenic methylation. *Toxicol Appl Pharmacol*, *198*(3), 319-326. https://doi.org/10.1016/j.taap.2003.10.020

Tirona, R. G., Leake, B. F., Podust, L. M., & Kim, R. B. (2004). Identification of amino acids in rat pregnane X receptor that determine species-specific activation. *Mol Pharmacol*, *65*(1), 36-44. https://doi.org/10.1124/mol.65.1.36

Tiscornia, G., Singer, O., & Verma, I. M. (2006). Production and purification of lentiviral vectors. *Nat Protoc*, *1*(1), 241-245. https://doi.org/10.1038/nprot.2006.37

Tokar, E. J., Benbrahim-Tallaa, L., Ward, J. M., Lunn, R., Sams, R. L., & Waalkes, M. P. (2010). Cancer in experimental animals exposed to arsenic and arsenic compounds. *Crit Rev Toxicol*, *40*(10), 912-927. https://doi.org/10.3109/10408444.2010.506641

Tribull, T. E., Bruner, R. H., & Bain, L. J. (2003). The multidrug resistance-associated protein 1 transports methoxychlor and protects the seminiferous epithelium from injury. *Toxicol Lett*, *142*(1-2), 61-70.

Trofimova, D. N., & Deeley, R. G. (2018). Structural Studies of Multidrug Resistance Protein 1 Using "Almost" Cysless Template. *Drug Metabolism and Disposition: The Biological Fate of Chemicals*, *46*(6), 794-804. https://doi.org/10.1124/dmd.117.078709

Upadhyay, M. K., Shukla, A., Yadav, P., & Srivastava, S. (2019). A review of arsenic in crops, vegetables, animals and food products. *Food Chem*, *276*, 608-618. https://doi.org/10.1016/j.foodchem.2018.10.069

V, S. K., Raman, R. K., Talukder, A., Mahanty, A., Sarkar, D. J., Das, B. K., . . . Mohanty, B. P. (2021). Arsenic Bioaccumulation and Identification of Low-Arsenic-Accumulating Food Fishes for Aquaculture in Arsenic-Contaminated Ponds and Associated Aquatic Ecosystems. *Biol Trace Elem Res*. https://doi.org/10.1007/s12011-021-02858-0

Vahter, M. (1999). Methylation of inorganic arsenic in different mammalian species and population groups. *Sci Prog*, *82 (Pt 1)*, 69-88. https://doi.org/10.1177/003685049908200104

Vahter, M. (2002). Mechanisms of arsenic biotransformation. *Toxicology*, *181-182*, 211-217.

Vahter, M., Couch, R., Nermell, B., & Nilsson, R. (1995). Lack of methylation of inorganic arsenic in the chimpanzee. *Toxicol Appl Pharmacol*, *133*(2), 262-268. https://doi.org/10.1006/taap.1995.1150

Vahter, M., Marafante, E., & Dencker, L. (1984). Tissue distribution and retention of 74As-dimethylarsinic acid in mice and rats. *Arch Environ Contam Toxicol*, *13*(3), 259-264.

van Aubel, R. A., Smeets, P. H., Peters, J. G., Bindels, R. J., & Russel, F. G. (2002). The MRP4/ABCC4 gene encodes a novel apical organic anion transporter in human kidney proximal tubules: putative efflux pump for urinary cAMP and cGMP. *J Am Soc Nephrol*, *13*(3), 595-603.

Van Aubel, R. A., Smeets, P. H., van den Heuvel, J. J., & Russel, F. G. (2005). Human organic anion transporter MRP4 (ABCC4) is an efflux pump for the purine end metabolite urate with multiple allosteric substrate binding sites. *Am J Physiol Renal Physiol*, *288*(2), F327-333. https://doi.org/10.1152/ajprenal.00133.2004

van de Ven, R., de Groot, J., Reurs, A. W., Wijnands, P. G., van de Wetering, K., Schuetz, J. D., . . . Scheffer, G. L. (2009). Unimpaired immune functions in the absence of Mrp4 (Abcc4). *Immunol Lett*, *124*(2), 81-87. https://doi.org/10.1016/j.imlet.2009.04.007

van de Ven, R., Scheffer, G. L., Reurs, A. W., Lindenberg, J. J., Oerlemans, R., Jansen, G., . . . de Gruijl, T. D. (2008). A role for multidrug resistance protein 4 (MRP4; ABCC4) in human dendritic cell migration. *Blood*, *112*(6), 2353-2359. https://doi.org/10.1182/blood-2008-03-147850

Villa-Bellosta, R., & Sorribas, V. (2010). Arsenate transport by sodium/phosphate cotransporter type IIb. *Toxicol Appl Pharmacol*, *247*(1), 36-40. https://doi.org/10.1016/j.taap.2010.05.012

Vogt, K., Mahajan-Thakur, S., Wolf, R., Bröderdorf, S., Vogel, C., Böhm, A., . . . Rauch, B. H. (2018). Release of Platelet-Derived Sphingosine-1-Phosphate Involves Multidrug Resistance Protein 4 (MRP4/ABCC4) and Is Inhibited by Statins. *Thromb Haemost*, *118*(1), 132-142. https://doi.org/10.1160/TH17-04-0291

Wang, Q. Q., Thomas, D. J., & Naranmandura, H. (2015). Importance of being thiomethylated: formation, fate, and effects of methylated thioarsenicals. *Chem Res Toxicol*, *28*(3), 281-289. https://doi.org/10.1021/tx500464t

Wang, Y., Chen, M., Zhang, Y., Huo, T., Fang, Y., Jiao, X., . . . Jiang, H. (2016). Effects of realgar on GSH synthesis in the mouse hippocampus: Involvement of system XAG(-), system XC(-), MRP-1 and Nrf2. *Toxicol Appl Pharmacol*, *308*, 91-101. https://doi.org/10.1016/j.taap.2016.07.006

Weigl, K. E. (2005). *Biochemical Investigations of the Human Multidrug Resistance Protein 1 (MRP1/ABCC1): Analysis of N-Glycosylation and Topology* Queen's University]. Kingston, Ontario.

Wen, J., Luo, J., Huang, W., Tang, J., Zhou, H., & Zhang, W. (2015). The Pharmacological and Physiological Role of Multidrug-Resistant Protein 4. *J Pharmacol Exp Ther*, *354*(3), 358-375. https://doi.org/10.1124/jpet.115.225656

Whitlock, B. (2021). Telomere Length and Arsenic: Improving Animal Models of Toxicity by Choosing Mice With Shorter Telomeres. *Int J Toxicol*, *40*(3), 211-217. https://doi.org/10.1177/10915818211009844

Whitlock, B. D., & Leslie, E. M. (2019). Chapter 2 - Efflux transporters in anti-cancer drug
resistance: Molecular and functional identification and characterization of multidrug resistance proteins (MRPs/ABCCs). In *Drug Efflux Pumps in Cancer Resistance Pathways: From Molecular Recognition and Characterization to Possible Inhibition Strategies in Chemotherapy* (Vol. 8, pp. 31-65). Elsevier.

WHO. (2012). Arsenic fact sheet. In. Geneva: World Health Organization.

Wielinga, P. R., Reid, G., Challa, E. E., van der Heijden, I., van Deemter, L., de Haas, M., . . . Borst, P. (2002). Thiopurine metabolism and identification of the thiopurine metabolites transported by MRP4 and MRP5 overexpressed in human embryonic kidney cells. *Mol Pharmacol*, *62*(6), 1321-1331. https://doi.org/10.1124/mol.62.6.1321

Wijnholds, J., Evers, R., van Leusden, M. R., Mol, C. A., Zaman, G. J., Mayer, U., . . . Borst, P. (1997). Increased sensitivity to anticancer drugs and decreased inflammatory response in mice lacking the multidrug resistance-associated protein. *Nature Medicine*, *3*(11), 1275-1279.

Wittgen, H. G., van den Heuvel, J. J., Krieger, E., Schaftenaar, G., Russel, F. G., & Koenderink, J. B. (2012). Phenylalanine 368 of multidrug resistance-associated protein 4 (MRP4/ABCC4) plays a crucial role in substrate-specific transport activity. *Biochem Pharmacol*, *84*(3), 366-373. https://doi.org/10.1016/j.bcp.2012.04.012

Xin, J., Zhang, K., Huang, J., Luo, X., Gong, X., Yang, Z., . . . Gao, J. (2018). Facile synthesis of aquo-cisplatin arsenite multidrug nanocomposites for overcoming drug resistance and efficient combination therapy. *Biomater Sci*, *7*(1), 262-271. https://doi.org/10.1039/c8bm01039k

Yamada, A., Maeda, K., Kamiyama, E., Sugiyama, D., Kondo, T., Shiroyanagi, Y., . . . Sugiyama, Y. (2007). Multiple human isoforms of drug transporters contribute to the hepatic and renal transport of olmesartan, a selective antagonist of the angiotensin II AT1-receptor. *Drug Metab Dispos*, *35*(12), 2166-2176. https://doi.org/10.1124/dmd.107.017459

Yang, Y., Li, Z., Mo, W., Ambadipudi, R., Arnold, R. J., Hrncirova, P., . . . Zhang, J. T. (2012). Human ABCC1 interacts and colocalizes with ATP synthase α, revealed by interactive proteomics analysis. *J Proteome Res*, *11*(2), 1364-1372. https://doi.org/10.1021/pr201003g

Yao, S. Y., Ng, A. M., Vickers, M. F., Sundaram, M., Cass, C. E., Baldwin, S. A., & Young, J. D. (2002). Functional and molecular characterization of nucleobase transport by recombinant human and rat equilibrative nucleoside transporters 1 and 2. Chimeric constructs reveal a role for the ENT2 helix 5-6 region in nucleobase translocation. *J Biol Chem*, *277*(28), 24938-24948. https://doi.org/10.1074/jbc.M200966200

Yokohira, M., Arnold, L. L., Pennington, K. L., Suzuki, S., Kakiuchi-Kiyota, S., Herbin-Davis, K., . . . Cohen, S. M. (2010). Severe systemic toxicity and urinary bladder cytotoxicity and regenerative hyperplasia induced by arsenite in arsenic (+3 oxidation state) methyltransferase knockout mice. A preliminary report. *Toxicol Appl Pharmacol*, *246*(1-2), 1-7. https://doi.org/10.1016/j.taap.2010.04.013

Yokohira, M., Arnold, L. L., Pennington, K. L., Suzuki, S., Kakiuchi-Kiyota, S., Herbin-Davis, K., . . . Cohen, S. M. (2011). Effect of sodium arsenite dose administered in the drinking water on the urinary bladder epithelium of female arsenic (+3 oxidation state) methyltransferase knockout mice. *Toxicol Sci*, *121*(2), 257-266. https://doi.org/10.1093/toxsci/kfr051

Zakharyan, R. A., Wildfang, E., & Aposhian, H. V. (1996). Enzymatic methylation of arsenic compounds. III. The marmoset and tamarin, but not the rhesus, monkeys are deficient in methyltransferases that methylate inorganic arsenic. *Toxicol Appl Pharmacol*, *140*(1), 77-84. https://doi.org/10.1006/taap.1996.0199

Zamek-Gliszczynski, M. J., Nezasa, K., Tian, X., Bridges, A. S., Lee, K., Belinsky, M. G., . . . Brouwer, K. L. (2006). Evaluation of the role of multidrug resistance-associated protein (Mrp) 3 and Mrp4 in hepatic basolateral excretion of sulfate and glucuronide metabolites of acetaminophen, 4-methylumbelliferone, and harmol in Abcc3-/- and Abcc4-/- mice. *J Pharmacol Exp Ther*, *319*(3), 1485-1491. https://doi.org/10.1124/jpet.106.110106

Zelcer, N., Reid, G., Wielinga, P., Kuil, A., van der Heijden, I., Schuetz, J. D., & Borst, P. (2003). Steroid and bile acid conjugates are substrates of human multidrug-

resistance protein (MRP) 4 (ATP-binding cassette C4). *Biochem J*, *371*(Pt 2), 361-367.

Zeng, H., Chen, Z.-s., Belinsky, M. G., Rea, P. A., & Kruh, G. D. (2001). Transport of methotrexate (MTX) and folates by multidrug resistance protein (MRP) 3 and MRP1: Effect of polyglutamylation on MTX transport. *Cancer Research*, *61*, 7225-7232.

Zhang, D.-w., Cole, S. P. C., & Deeley, R. G. (2002). Determinants of the substrate binding specificity of multidrug resistance protein (MRP1): role of amino acid residues with hydrogen bonding potential in predicted transmembrane helix 17. *Journal of Biological Chemistry*, *277*, 20934-20941.

Zhang, D. W., Nunoya, K., Vasa, M., Gu, H. M., Cole, S. P., & Deeley, R. G. (2006). Mutational analysis of polar amino acid residues within predicted transmembrane helices 10 and 16 of multidrug resistance protein 1 (ABCC1): effect on substrate specificity. *Drug Metab Dispos*, *34*(4), 539-546. https://doi.org/10.1124/dmd.105.007740

Zhang, W., Deng, J., Sunkara, M., Morris, A. J., Wang, C., St Clair, D., & Vore, M. (2015). Loss of multidrug resistance-associated protein 1 potentiates chronic doxorubicin-induced cardiac dysfunction in mice. *J Pharmacol Exp Ther*, *355*(2), 280-287. https://doi.org/10.1124/jpet.115.225581

Zhang, Z., & Chen, J. (2016). Atomic Structure of the Cystic Fibrosis Transmembrane Conductance Regulator. *Cell*, *167*(6), 1597.e1599. https://doi.org/10.1016/j.cell.2016.11.014

Zhou, Q., & Xi, S. (2018). A review on arsenic carcinogenesis: Epidemiology, metabolism, genotoxicity and epigenetic changes. *Regul Toxicol Pharmacol*, *99*, 78-88. https://doi.org/10.1016/j.yrtph.2018.09.010

APPENDIX 1: Investigating binding sites through interspecies chimeras of mAbcc4 and hABCC4

A.1.1: Introduction

Species differences between hABCC4 and mAbcc4 were investigated in Chapter 3 partially to lay a foundation for precisely determining the binding site(s) in hABCC4 for arsenicals.

This work is inspired by two relevant trends, the convergence of which may offer a new tool that can be used to investigate and better understand how arsenic is handled from the biochemical to the whole-organism level. First, different species, even when genetically similar, can handle arsenic very differently. Second, as differences about arsenic handling outcomes are learned, we are often able to trace the differences back to a correlation with a SNP or group of amino acids. Thus, species differences that we can readily observe might be leveraged into a database of genetic and protein sequence-variation that can be used to draw helpful correlations between sequence, structure, and function.

One way I propose to make use of this concept is to use inter-species chimera proteins to investigate and narrow down regions of interest. In the context of this work, it would be most helpful to be able to splice proteins of species with different arsenic-handling abilities, and then test the chimera protein against either of the two source species.

Interspecies chimeric proteins, also known as interspecies recombinant proteins, have often been used to localize binding and functional domains when the proteins of different species are observed to behave differently (Kaushansky et al., 1992; Leslie et al., 2007; Lev et al., 1993; Matous et al., 1996; Stride et al., 1999; Sundaram et al., 1998; Tirona et al., 2004; Yao et al., 2002).

This work is exploratory at this point, not only in the species and chemicals chosen, but in that we must first ask whether creating inter-species chimera proteins can even yield a product functional enough to test with our current abilities and assays. If the chimera protein were to be nonfunctional or function as a midpoint between the two starting proteins, it would not be very useful. This has happened in the past, where a mouse-human chimera displayed neither mouse nor human binding character (Lev et al., 1993). In such a case, correlations between function and sequence cannot readily be made, and this does not yield useful information about binding sites. But if the chimera displayed decidedly human or mouse characteristics detectable in our experiments, then early inferences could be drawn about the important regions for the binding/transport of the substrate in question. This would be done by linking the knowledge of outcome, in this case transport activity, with knowledge of sequence.

Results and Discussion

Here I describe a successful pilot project and initial discoveries and lay out some straightforward steps toward using this approach to uncover important information about binding sites.

A.

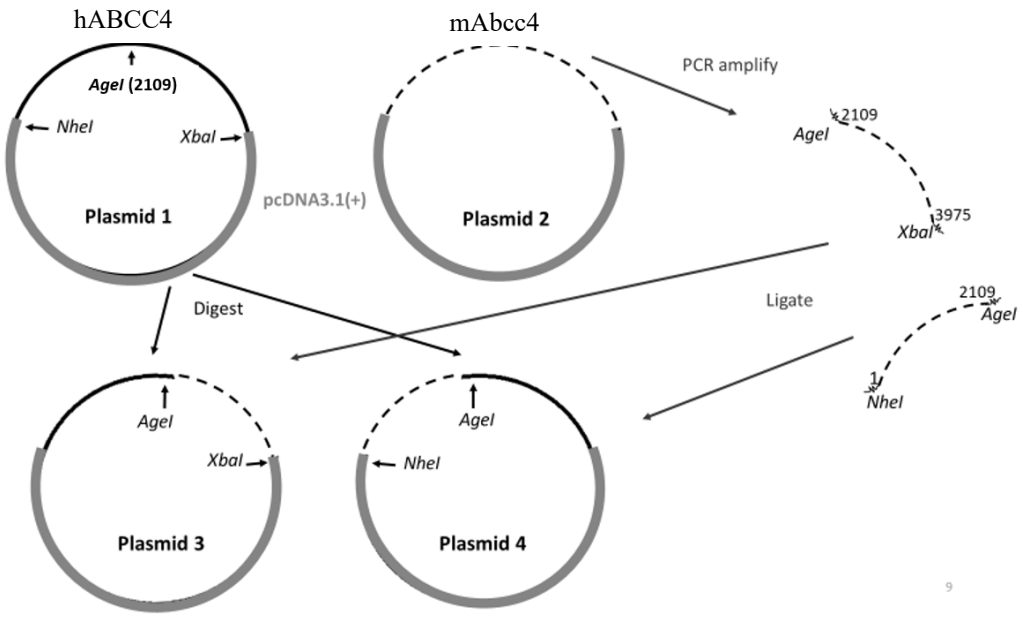

B.

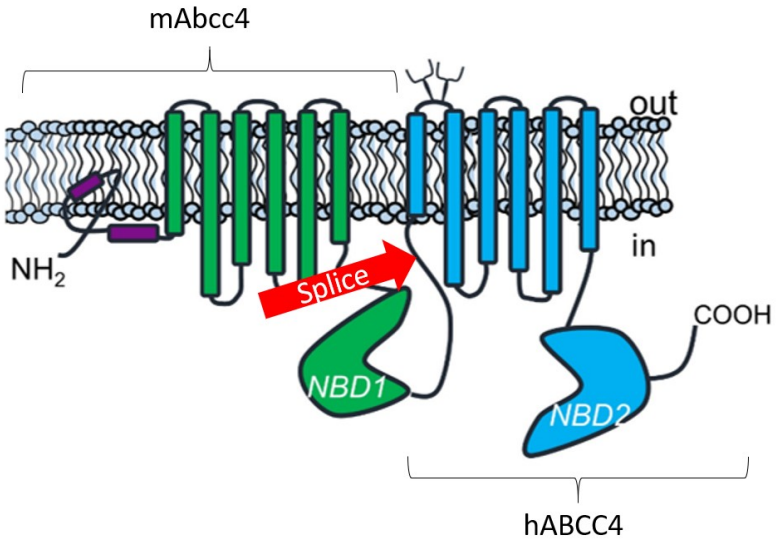

Figure A.1.1. A) Chimera construction scheme. Restriction site digests were used to create an opening in the hABCC4 construct into which the PCR amplified mAbcc4 product could be ligated to form a complete mouse-human chimera mAbcc4/hABCC4 construct. Plasmid 4 encodes the single chimera protein tested and described in this appendix, $mAbcc4_{1-703}$/$hABCC4_{704-1325}$. B) Topology model showing predicted location of splice cite with

mAbcc4 half and hABCC4 half of protein labeled. Panel B modified from Whitlock and Leslie 2019, used with permission from publisher Elsevier.

A.1.2. Chimera transport

One chimera protein was obtained and tested in this work, mAbcc4$_{1-703}$/hABCC4$_{704-1325.}$ The plasmid encoding it and the splice site predicted topology is diagrammed in Figure A.1.1. The m-H chimera was sequenced in its entirety to verify that it consisted of the mouse orthologue from nucleotide 1-2109, and the human orthologue from residues 2110-3975. The plasmid was successfully transfected into HEK293 cells and membrane vesicles were prepared as described in Section 2.2.15.

Two separate membrane vesicle preparations were tested for $E_2$17βG transport activity. Each vesicle preparation was tested in three independent experiments, each of which used triplicate determinations. All preparations were functional, except for the empty vector-transfected cell-derived vesicles used as a negative control. The chimera protein exhibited mAbcc4-like transport activity, with roughly three- and four-fold higher transport than hABCC4 in the first and second membrane vesicle preparation, respectively (Fig. A.1.2). This increase from hABCC4 was significant for both mAbcc4 and chimera, in both preparations ($p < 0.01$). hABCC4-enriched vesicles transported $E_2$17βG at 9.0 ± 5.0 pmol/mg total protein/min, mAbcc4 at 26.3 ± 6.0 pmol/mg/min, and the chimera at 31.9 ± 9.8 pmol/mg/min (prep 1); and hABCC4 vesicles transported $E_2$17βG at 10.1 ± 2.6 pmol/mg/min, mAbcc4 at 50.7 ± 12.2 pmol/mg/min, and chimera at 38.7 ±

11.4pmol/mg/min (prep 2). When corrected for relative protein levels detected by western blot, the activity of the chimera was 12-fold and 16-fold higher than hABCC4 in prep 1 and 2, respectively (Fig. A.1.3)

Thus, the region in mAbcc4 important for higher $E_2$17βG transport appears to reside in the N-terminal half of the protein. This method narrows the search for key binding site residues to a few dozen, in only a few regions, and means that the number cycles of gene engineering→transfection→culture→vesicle prep→transport to determine the binding site precisely is around 5 if the chimeras construction strategy is done carefully, whereas without this guidance, site-directed mutagenesis at each of the residues in potentially influential areas with the corresponding vesicle preparations and transport would be cost- and time-prohibitive.

The next steps in this work are to create other chimeras and use the present and future chimeras to test different hABCC4 substrates. To continue investigating $E_2$17βG transport, the next two proteins could be made (1) with the first quarter mouse sequence and the last three quarters human; and, (2) with the first, third and fourth quarters human and only the second quarter mouse. At this point, a strategic decision will have to be made when to transition from making chimera proteins and choosing one orthologue and conducting site-directed mutagenesis to narrow down on specific amino acids. To make this strategic

decision, the discussion in Appendix 2 and the information in Table 1.3 offer examples of how to select amino acids which are expected to be important.

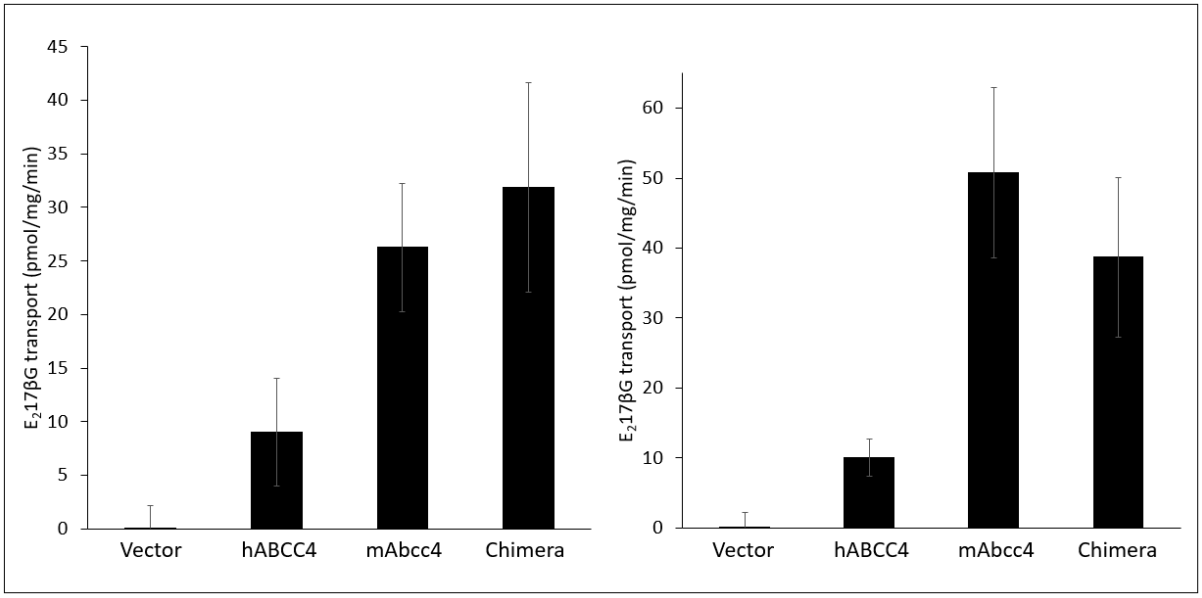

Figure A.1.2. Human, mouse, and mAbcc4$_{1\text{-}703}$/hABCC4$_{704\text{-}1325}$ (Chimera) transport of $E_2$17βG in membrane vesicles. Membrane preparation 1 (left) and preparation 2(right) Error bars are standard deviations from 3 independent experimental replicates. Each of the replicates (three for each preparation) had 3 independent determinations. Vesicles (5 µg protein per experiment) were incubated with $E_2$17βG (400 nM, 40 nCi) for 1.5 minutes. The transport was stopped by dilution in ice-cold tris-sucrose buffer (TSB), the vesicles were filtered and washed, and the $E_2$17βG was quantified in a liquid scintillation counter.

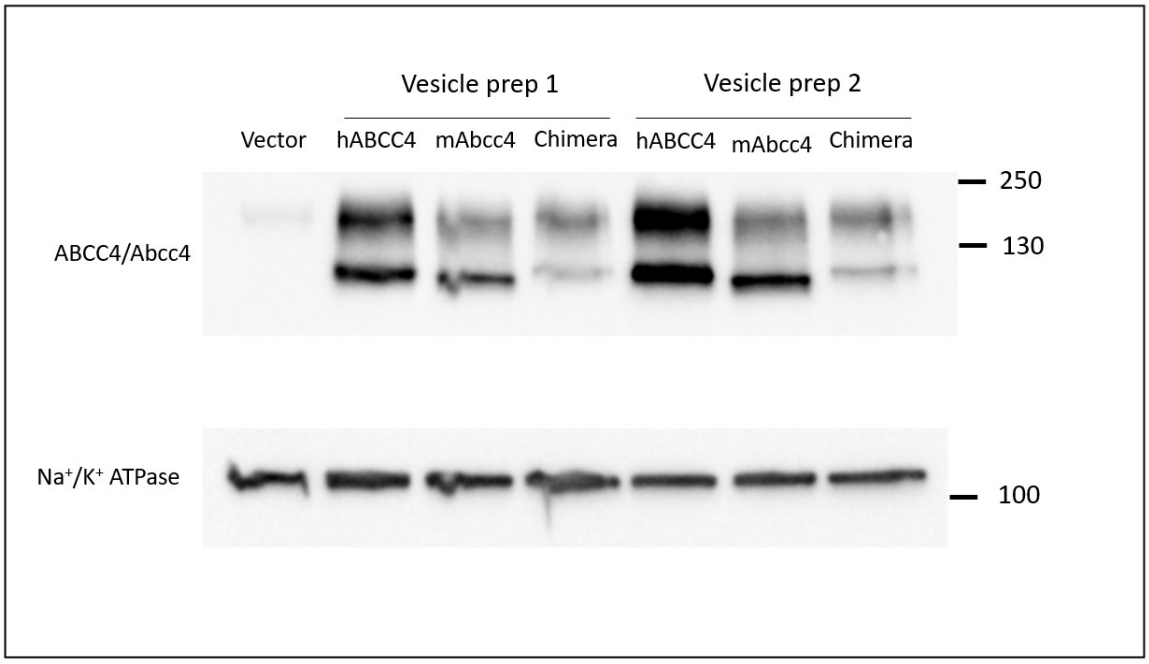

Figure A.1.3. Western blot monitoring protein levels of hABCC4, mAbcc4, and mAbcc4$_{1\text{-}703}$/hABCC4$_{704\text{-}1325}$ (chimera)-enriched membrane vesicles prepared from transiently transfected HEK293 cells. The same preparations were used in Figure A.1.2. Na^+/K^+ ATPase shown as a loading control. ABCC4/Abcc4 protein levels were determined by resolving 1 µg of total protein from membrane vesicles prepared from HEK293 cells expressing pcDNA3.1(+)-neomycin (vector), pcDNA3.1(+)-hABCC4, or pcDNA3.1(+)-mAbcc4, pcDNA3.1(+)-m/hChimera using a 5% acrylamide gel. Samples were transferred to a PVDF membrane and probed with M$_4$I-10 antibody. Blots were then stripped and reprobed for Na^+/K^+-ATPase as a loading control. Both antibodies used at 1:10,000 dilution in skim milk.

Appendix 2. Rat Abcc4: cytotoxicity protection, transport, and binding site implications.

Introduction

Further to the work in Chapter 3 on differences between mAbcc4 and hABCC4, we explored how rAbcc4 might also differ from the other species. rAbcc4 and mAbcc4 are 95% identical, giving a narrower range of differing amino acids as a starting point investigating important regions for substrate binding. Rats also provide an alternative animal model.

As noted in s 1.4.2, mice and rats handle arsenic differently on a whole-body level, and so we must be careful when trying to attribute certain outcomes *in vivo* to a particular protein or pathway. However, if more specific protein-level differences between the species are discovered, this can be used with our knowledge of sequence differences to advance our quest to find binding sites. Similar methods used in Chapter 3 to investigate the species differences between hABCC4 and mAbcc4 were used to investigate rAbcc4.

Two HEK clones stably expressing rAbcc4 were developed and used in tetrazolium base (MTS) cytotoxicity experiments described in section 2.2.6 to test the influence of rAbcc4 on arsenic toxicity. Membrane vesicles expressing rAbcc4 were also tested for the ability to transport $MMA(GS)_2$ and DMA^V, previously shown to be transported by hABCC4

(Banerjee et al., 2014). Further, as striking differences were observed between mAbcc4 and hABCC4 for $E_2$17βG transport and 6-MP resistance, with mAbcc4 displaying much greater transport activity and protection, respectively than hABCC4, these were also tested for rAbcc4.

Results

Cytotoxicity

Two cell line clones stably expressing rAbcc4 were successfully established, clones 1D4 and 2D2. Although Abcc4 levels changed slightly over time, clone 1D4 clearly had more rAbcc4 than clone 2D2 (Figure A.2.1). On average, after correcting for protein loading, clone 1D4 had a 1.8-fold higher level of rAbcc4 than clone 2D2.

In both clones, resistance for 6-MP, the positive control, was strong and consistently conferred by rAbcc4, with a relative resistance of 4.0 for clone 1D4, and 4.2 for the lower-rAbcc4 level clone 2D2. Resistance to 6-MP was not changed by lower protein levels. For the higher level rAbcc4 cell clone 1D4, significant resistance was found for, As^V (RR of 1.5) and MMA^V (RR of 1.9). For the lower level rAbcc4 cell clone 2D2, no significant resistance was observed for any of the arsenicals tested Tables A.2.1 and A.2.2)

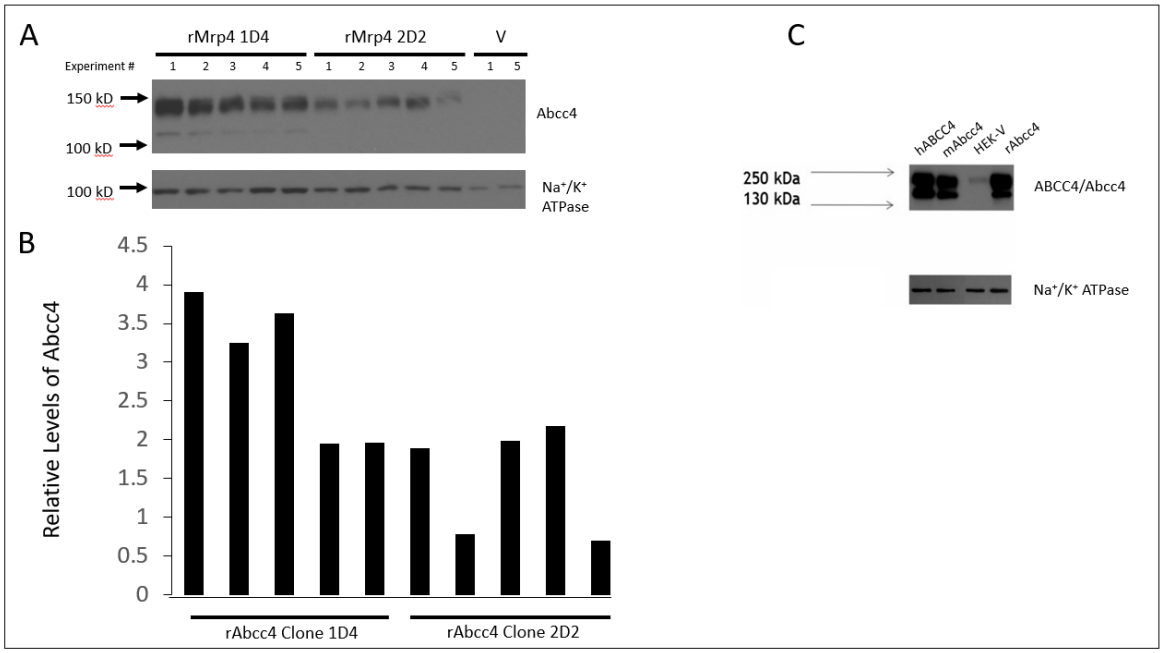

Figure A.2.1. Expression of rAbcc4 in stable cell lines and membrane vesicles used for cytotoxicity and transport experiments, respectively. (A) Rat Abcc4 level (top) and sodium-potassium ATPase expression (bottom) as a loading control. A 1-2 million cell pellet was saved from every cytotoxicity experiment, lysed, blotted, and probed for both proteins. (B) Relative expression, corrected for loading, or rAbcc4 from five cytotoxicity experiments with both rAbcc4 clones, with the lowest expressing sample arbitrarily set to 1. (C) Levels of rAbcc4 expression (top) and Na^+/K^+-ATPase expression (bottom) as a loading control for plasma membrane-enriched vesicles from preparations arising from transient transfections.

Table A.2.1. Higher level rAbcc4 clone 1D4 confers resistance to As^{V} and MMA^{V} in stable HEK293 cells

	EC_{50} (± S.D.) (μM)		Relative Resistance[a]
	Vector	rAbcc4-1D4	
As^{III} (*n = 3)*	5.2 ± 1.8	5.5 ± 3.6	1.1
As^{V} *(n =4)*	25.7 ± 9.3	39.1 ± 8.3*	1.5
MMA^{III} *(n = 3)*	1.6 ± 0.5	1.5 ± 0.9	0.9
MMA^{V} *(n = 3)*	722 ± 184	1357 ± 149*	1.9
DMA^{III} (n = 3)	1.6 ± 0.6	1.7 ± 0.5	1.1
DMA^{V} *(n = 3)*	938 ± 161	563 ± 107	0.6
6-MP *(n = 6)*	4.8 ± 2.2	19.1 ± 6.9*	4.0

*EC_{50} for HEK-rAbcc4-1D410 is significantly different from HEK-Vector, $P < 0.05$ (Student's *t* test). [a]Ratio of EC_{50}HEK-rAbcc4/ EC_{50} HEK-Vector

Table A.2.2. Lower level rAbcc4 stable HEK293 clone 2D2 does not confer resistance to arsenicals.

	EC_{50} (± S.D.) (μM)		Relative Resistance[a]
	Vector	rAbcc4-2D2	
As^{III} (*n = 3)*	5.3 ± 2.4	5.5 ± 3.6	1.0
As^{V} *(n = 3)*	27.8 ± 9.3	34.8± 13.1	1.3
MMA^{III} *(n = 3)*	1.5 ± 0.2	2.0 ± 0.6	1.3
MMA^{V} *(n = 3)*	696 ± 234	945 ± 54	1.4
DMA^{III} (n = 3)	1.8 ± 0.5	1.9 ± 1.1	1.1
DMA^{V} *(n = 3)*	1010 ± 233	1201 ± 268	1.2
6-MP *(n = 6)*	4.4 ± 1.5	18.4 ± 5.7*	4.2

*EC_{50} for HEK-rAbcc4-2D2 is significantly different from HEK-Vector, $P < 0.05$ (Student's *t* test). [a]Ratio of EC_{50}HEK-rAbcc4/ EC_{50} HEK-Vector

Transport

Building on knowledge of the ability of hABCC4, but not mAbcc4, to transport DMA^V and $MMA(GS)_2$, and the difference between hABCC4 and mAbcc4 in $E_2$17βG trasnport, rAbcc4 was investigated (Banerjee et al. 2014 and Section 3.2.3). In vesicles prepared from transiently transfected HEK293 cells, rAbcc4 transported the DMA^V, but not $E_2$17βG or $MMA(GS)_2$. For DMA^V, rAbcc4 vesicles had an activity of 8.3 pmol/mg total protein/min, only 16% of the transport activity of hABCC4 (53.3 pmol/mg/min). Rat Abcc4 did not transport $MMA(GS)_2$, while as expected, hABCC4 did (24.7 pmol/mg/min) (Fig. A.2.2) (Banerjee, 2014) For both DMA^V and $MMA(GS)_2$, vector and mAbcc4-expressing vesicles were run in parallel and transport was not detected (Figure A.2.2). rAbcc4 transport of $E_2$17βG was compared to mAbcc4, and rAbcc4 activity was only 15% that of mAbcc4, and not significantly different from vector (54 (mouse versus 8 (rat) pmol/mg total protein/min) (Figure A.2.2). Human ABCC4 vesicles were included in experiments and consistently achieved transport above vector, as seen previously in Figure 3.4B. ABCC4/Abcc4 levels were similar and consistent between human, mouse and rat conditions throughout all transport experiments (Figure A.2.1C).

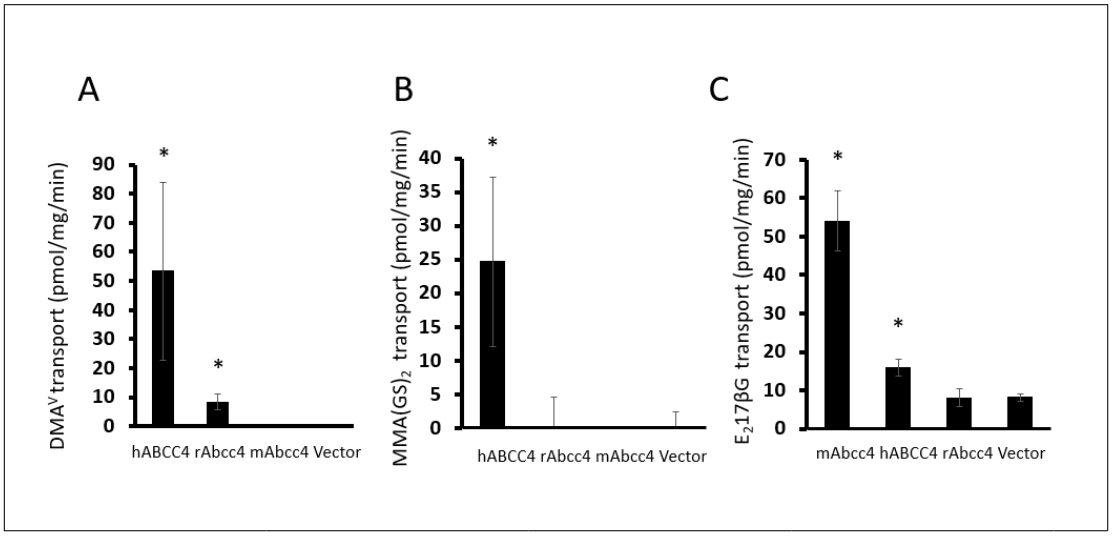

Figure A.2.2. The transport of DMA^V, $MMA(GS)_2$, and $E_2$17βG by hABCC4-, mAbcc4-, and rAbcc4- enriched membrane vesicles prepared from transiently transfected HEK293 cells. Arsenic transport was measured in membrane vesicles (20 µg protein per experiment) by incubating them with (A) DMA^V for 5 minutes or (B) $MMA(GS)_2$ for 3 minutes (both at 1 µM). Transport was stopped by diluting in ice-cold TSB and the vesicles were pelleted and processed for arsenic quantification by inductively coupled plasma mass spectrometry. (C) Vesicles (5 µg protein per experiment) were incubated with $E_2$17βG (400 nM, 40 nCi) for 1.5 minutes. The transport was stopped by dilution in ice-cold tris-sucrose buffer (TSB), the vesicles were filtered and washed, and the $E_2$17βG was quantified in a liquid scintillation counter. All incubations were at 37ºC. Bars represent mean determinations of three independent experiments with standard deviation (SD). *Significantly greater than vector (A, B, C) and different from each other (A, C) (one way ANOVA with Bonferroni post hoc correction).

Discussion

Rat Abcc4 confers resistance, in the higher Abcc4-level cell line (1D4), to As^{V} and MMA^{V}. This is a new arsenic resistance pattern not seen in either the human orthologue (protects against all tested arsenicals except As^{III}) or the mouse (protected against no arsenicals tested to date) (Banerjee et al., 2014 and section 3.2.2 above). The rat orthologue can be thought of as somewhat intermediate between the human and mouse orthologues in its ability to confer protection against arsenic in cytotoxicity experiments. rAbcc4 acts very similarly to hABCC4 with respect to its conferral of resistance against the positive control 6-MP.

It is noteworthy that, while levels of rAbcc4 in HEK-rAbcc4 cell lines correlated with a cytoprotective effect against arsenicals, both the low-level (2D2) and high-level (1D4) rAbcc4 cell lines led to the same protection against 6-MP. This may be explained by the fact that 6-MP is thought to be transported as its nucleotide metabolite, which is the toxic species (Chen et al., 2001; Wielinga et al., 2002). There may be a threshold for efflux of this metabolite which is sufficient to saturate the protective effect, given the rate of metabolism of 6-MP. The similar protection from both the high- and low-expressing cell lines suggests that both amounts of protein are sufficient to reach this threshold and saturate the protective mechanism. In this model, one would expect to see reductions in protein levels lead to a reduction in cytoprotective effect at some lower expression level below the threshold.

Arsenate is rapidly reduced to arsenite in cells, so a protein conferring resistance against arsenate but not arsenite seems counterintuitive but is consistent with hABCC4 characteristics shown in Table 3.1 and mAbcc4 characteristics shown in MEF cells in Table 3.2. Since arsenite is taken up more rapidly into cells than arsenate is, it could be that the efflux process is overwhelmed by massive uptake in the case of arsenite, hiding any apparent cytoprotective effect. Also, given that rAbcc4 transports DMA^V, a mechanism is possible by which slower uptake of arsenate allows for the reductive methylation steps to proceed fast enough to avoid toxicity before the DMA^V form is reached and can be effluxed. There could also be other transported species yet to be discovered. There is no reason why DMA^V transport capabilities alone cannot fully explain the arsenate resistance, as long as there is a pathway in the cellular metabolism capabilities to get from arsenate to DMA^V.

Reconciling the transport results with the cytoxicity results are not as easy as with hABCC4 or mAbcc4 in HEK cells. In hABCC4, DMA^V and $MMA(GS)_2$ transport explain the cytotoxitcy results. In mAbcc4, the lack of transport of anything explains the lack of protection in cytotoxicity experiments. But with rAbcc4, we see only DMA^V being transported. So it remains to be explained exactly how arsenic can enter the cell as arsenate, and be transported out as DMA^V in order to reconcile the cytotoxicity and transport data. In the metabolic pathway from arsenate to DMA^V, we expect to see the monomethylated

species, and dimethylated trivalent species present to some extent. But the protein does not protect against these in cytotoxicity experiments.

I propose two answers to this. First, we may be running into the detection limits of the MTS cytotoxicity assay. It is possible that we are only seeing the starkest effects, and in reality, there are more subtle but significant protective effects for other arsenicals. This possibility is supported by the fact that in both cell line clones, the 6-MP resistance was strong, but only in the cell line clone with higher protein levels is there any arsenic resistance. Perhaps by making the assay more robust (i.e. using the higher expressing clone), we allowed for enough sensitivity to see the more subtle protective effect against arsenic. If we could make the assay even more robust, by having even higher protein levels, or even more carefully eliminating background signal and colorimetric saturation, or another way, we may start to see the even more subtle protective effect against other arsenicals. If in this more robust hypothetical assay, the cytotoxicity results looked more like the hABCC4 cytotoxicity results in Banerjee 2014, the transport data could be fully reconciled to the cytotoxicity data.

Secondly, it may be explained by gradients and relative toxicities and stabilities. If the transport data are correct, and DMA^V really is the only arsenical being transported, then this efflux should create a lower concentration on one side of the metabolic reaction chain (Fig. 1.1) and shift the equilibrium to encourage more reductive methylation. As^{III} would

become MMA^{V} and MMA^{III} would become DMA^{V}, all at a higher rate. Given that the pentavalent methylated species are the least toxic, and that the trivalent methylated species are the least stable, we may be able to explain the lack of cytotoxicity protection as a low baseline toxicity due to instability (insufficient time to act), or low toxicity. That is, if the toxicity was low to begin with, the protein has a lot more work to do to show a shift in the EC_{50} curve, and we may simply not detect it.

Implications for binding site investigation

How can we use rAbcc4 in our species differences studies? With the data collected from the hABCC4, mAbcc4, and rAbcc4 transport of $E_2$17βG, we can run an example of how to prioritize residues for investigation with mutagenesis and chimera studies.

To summarize what we know, mAbcc4 transports $E_2$17βG with approximately 3-fold higher activity than hABCC4 does. rAbcc4 does not transport $E_2$17βG under the conditions tested. The mouse-human chimera described in Appendix 1 transports $E_2$17βG with high activity most similar to that of mAbcc4.

Given that the first half of mAbcc4 contains residues that increase $E_2$17βG transport relative to hABCC4 (A.1.2), and that rAbcc4 does not transport $E_2$17βG, the residues of interest can be narrowed down significantly. There are 55 residues that are non-identical between rAbcc4 and mAbcc4, and of these we can eliminate from our list 23 from the

COOH-terminal half. We can also lower the priority from the NH_2-terminal half, 17 in NBD1 (as relevant mutations are rarer here according to Table 1.3) and 3 in extracellular loops to leave the priority residues of interest for further work: 5 in TMs, and 7 in CLs (Fig A.2.3). Given that we are looking for sites that can make contact with the substrate before or during transport, we need to look intracellularly and in the pore, which draws our focus to the CL and TM regions. We are left with 12 residues that have a reasonably likely role in $E_2$17βG binding and/or transport: human residues Val-22, Ile-33*, Gly-62*, Val-68, Ala-75, Ala-224, Ala-227*, Val-243, Ile-273, Thr-300*, Thr-338*, Ala-348. Within this list of deduced targets for investigation, there is an over-representation of amino acids which are not conserved between human and mouse, marked with an asterisk (see Figure 3.1). These are an especially good starting point.

Further, five of these residues occur on CL0, making one small segment-swap chimera an efficient first screening strategy. With our knowledge of hABCC4 SNPs that have transport implications (Table 1.3), we might preferentially target residues in CL2 and TM6, giving us 3 most likely choices: human amino acids Ile-273, Thr-300, Ala-348. There is also some evidence from hABCC4 that the residues of NBD1 can have impact on transport.

DMA^V

The transition from analysis of the E217βG binding site to the arsenicals binding sites is a clear analogy. The highest impact future studies will combine our arsenic-transport knowledge with this species differences approach outlined above, to narrow in on DMA^V and $MMA(GS)_2$ binding sites as efficiently as possible.

The existence of overlap between the DMA^V and $E_2$17βG binding sites on hABCC4 is completely unknown, and could be investigated with inhibition studies. Although there are no chimera data for DMA^V transport yet, to make use of our discovered differences between the rat, mouse and human proteins for this arsenical, we might look for residues that are different in all three species. These are listed here with human sequence identified: I33, S44, N118, F143, A227, V345, L402, S465, I580, S676, T684, T722M A723, V747, V749, S769, I876, I878, M958, Q1028, N1148, G1301. We might look instead at residues which are conserved between rat and human (which transport DMA^V) but which differ in mouse (which does not): T338, V376, Q401, T425, T434, P642, V643, N651, V755, V789, I873, I874, D975.

Table A.2.3. Comparing cytotoxicity and transport data for hABCC4, rAbcc4, and mAbcc4.

Behaviour	hABCC4	rAbcc4	mAbcc4
In HEK293 cells protects against:			
As^{III}	No	No	No
As^{V}	Yes	Yes	No
MMA^{III}	Yes	No	No
MMA^{V}	Yes	No	No
DMA^{III}	Yes	No	No
DMA^{V}	Yes	No	No
Vesicle Transport Assay			
Transports DMA^{V}	High	Intermediate	Not found
Transports $E_2$17βG	Low	Not found	High
Transports $MMA(GS)_2$	Yes	Not found	Not found

Summarized data from Banerjee, Carew, et al. 2014 and Chapter 3 of this thesis.

Table A.2.4. All protein sequence differences between mAbcc4 and rAbcc4

Rat:AA#:Mouse	Predicted domain	Rat:AA#:Mouse	Predicted domain
L22V	NT (CL0)	N651K	NBD1
A33T	NT (CL0)	V673A	NBD1
G62R	NT (CL0)	D675E	NBD1
V68L	NT (CL0)	A685V	NBD1
A75S	NT (CL0)	L722M	TM7
I111L	EL1	M723V	TM7
D118E	EL1	R741K	EL4
G224A	TM3	D747N	EL4
I227V	TM3	K749R	EL4
I243V	TM4	V755I	EL4
F273I	CL2	G757E	El4
T300A	CL2	T769A	TM8
T338S	TM5	V789I	TM8
K345E	EL3	I873V	TM10
S348A	TM6	I874V	TM10
V376G	NBD1	V876L	TM10
V380I	NBD1	V958I	TM11
V383I	NBD1	D975N	EL6
E396Q	NBD1	S986A	TM12
Q401H	NBD1	R1028K	NBD2
E402V	NBD1	S1142T	NBD2
T425S	NBD1	K1148R	NBD2
T434I	NBD1	K1194N	NBD2
T465A	NBD1	R1252K	NBD2
R497K	NBD1	A1301T	NBD2
T581A	NBD1	S1303T	NBD2
P642T	NBD1	S1309N	NBD2
V643A	NBD1		

NT: NH_2-terminus; CL: cytosolic loop; NBD: nucleotide binding domain; EL: extracellular loop

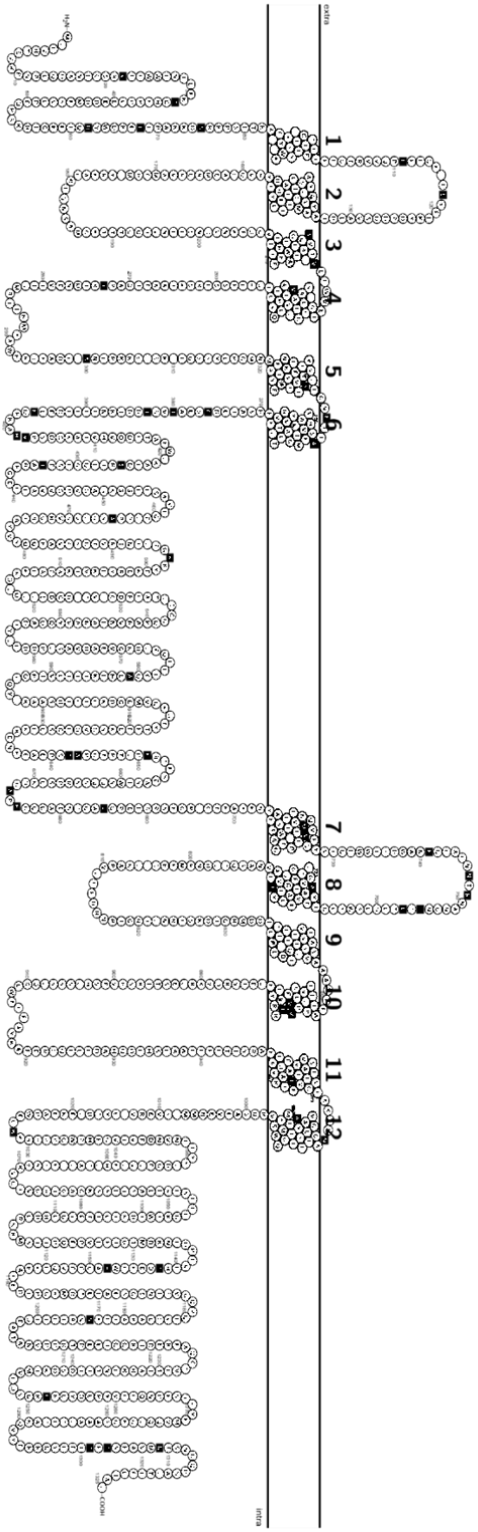

Figure 7.3. Mouse Abcc4 with differences from rAbcc4 marked in black, with topology predicted as in (Omasits, 2013).

Appendix 3: Speciation Data for Section 5.2.2.

The speciation data from section 2.2.13 is included here as three figures. Methods are described in section 2.2.11.

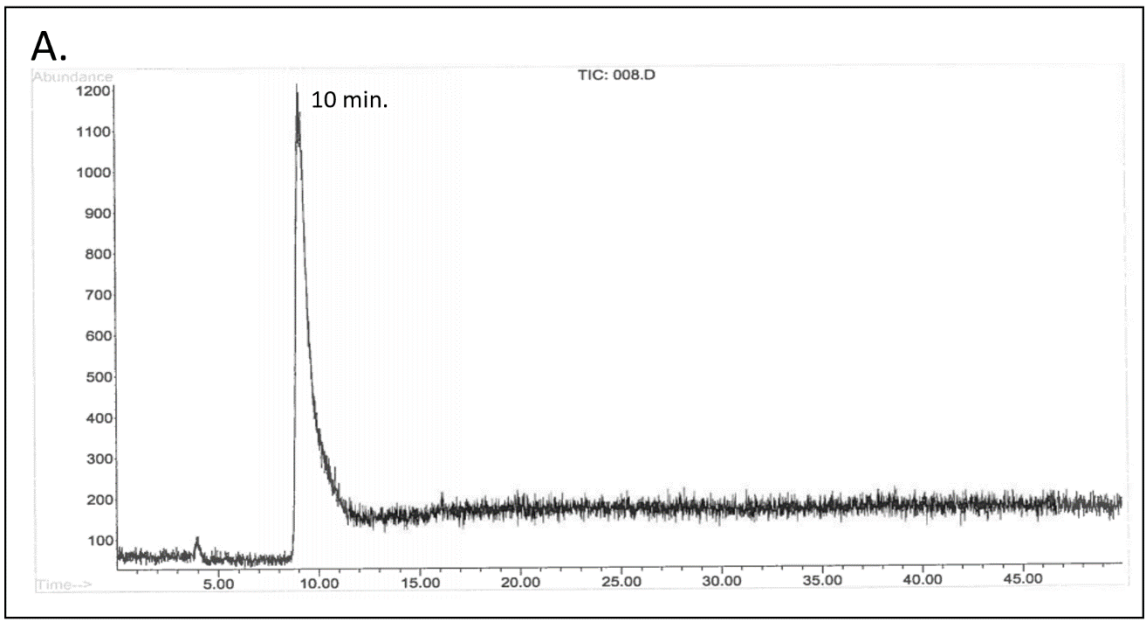

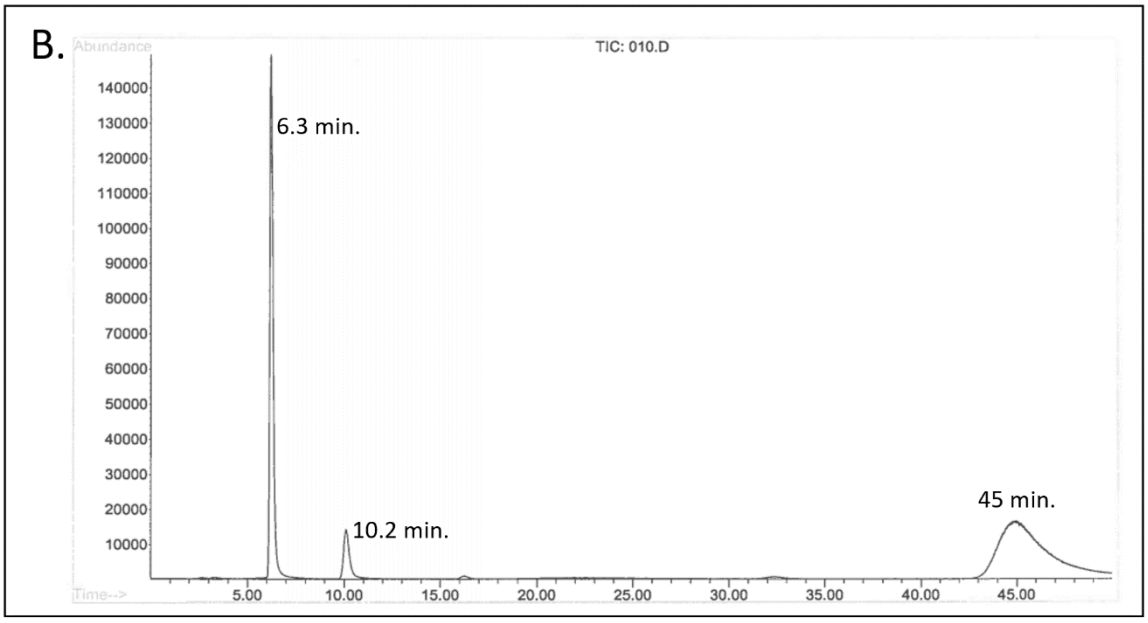

C.

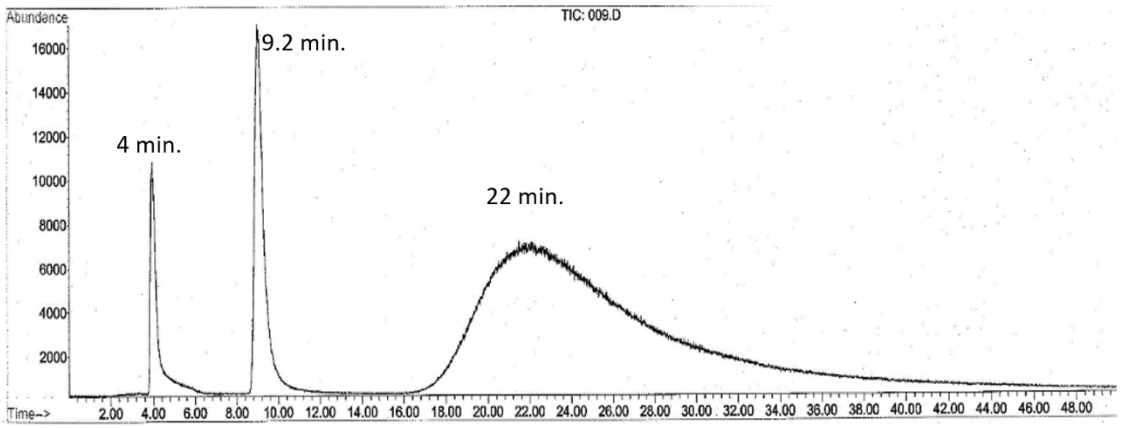
Abundance
TIC: 009.D
16000
14000
12000
10000
8000
6000
4000
2000
4 min.
9.2 min.
22 min.
Time-->
2.00 4.00 6.00 8.00 10.00 12.00 14.00 16.00 18.00 20.00 22.00 24.00 26.00 28.00 30.00 32.00 34.00 36.00 38.00 40.00 42.00 44.00 46.00 48.00

D.

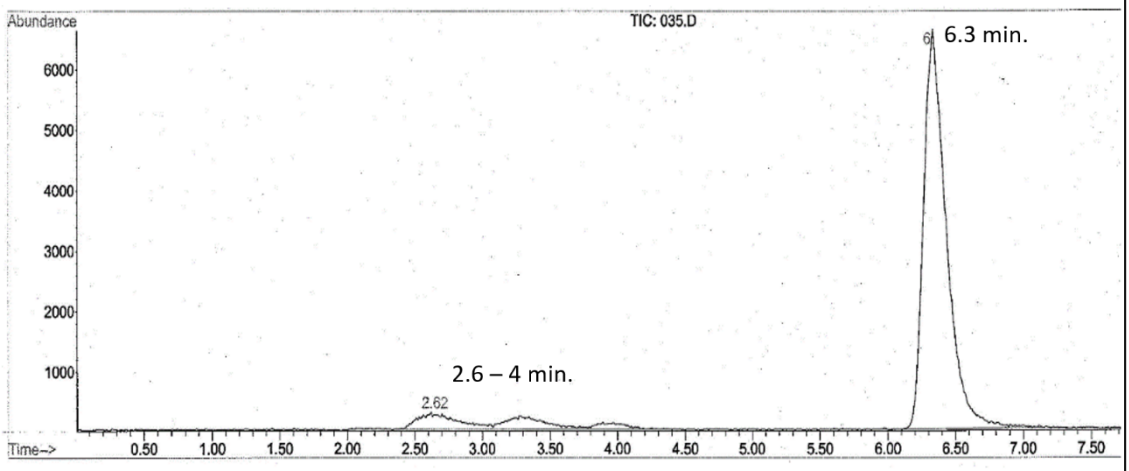
Abundance
TIC: 035.D
6000
5000
4000
3000
2000
1000
6.3 min.
2.6 – 4 min.
2.62
Time-->
0.50 1.00 1.50 2.00 2.50 3.00 3.50 4.00 4.50 5.00 5.50 6.00 6.50 7.00 7.50

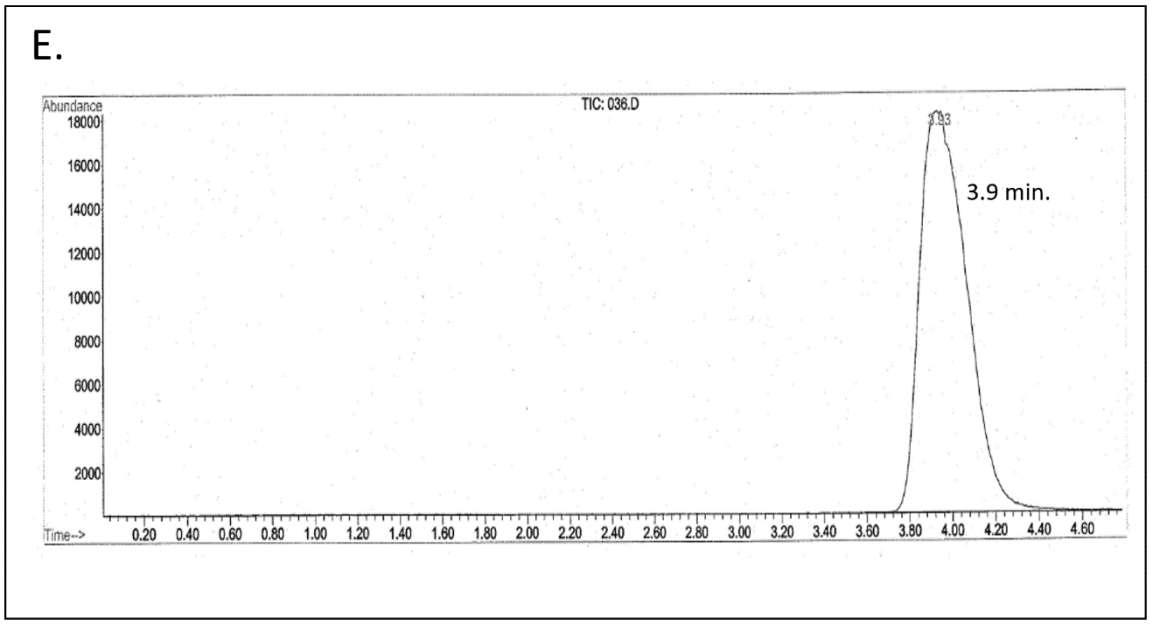

Figure A.3.1. Chromatograms of speciation standards. Chromatograms generated using methods described in section 2.2.11 are shown with retention times of peaks in minutes labelled. A) Dimethyldithioarsinic acid (DMDTA) standard. B) monomethylmonothiol arsinic acid (MMMTA) standard. C) Dimethylmonothioarsinic acid (DMMTA) standard. D) MMA standard. E) DMA standard.

A.

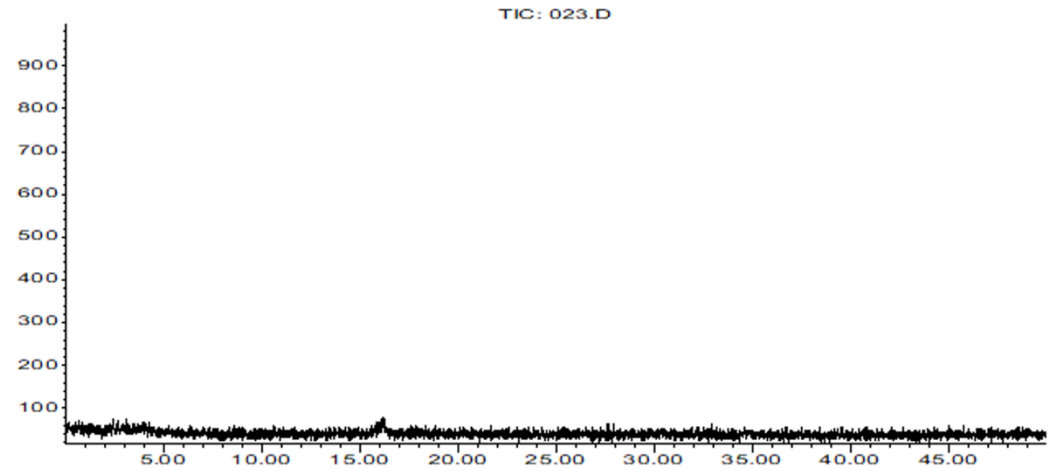
TIC: 023.D
900
800
700
600
500
400
300
200
100
5.00
10.00
15.00
20.00
25.00
30.00
35.00
40.00
45.00

B.

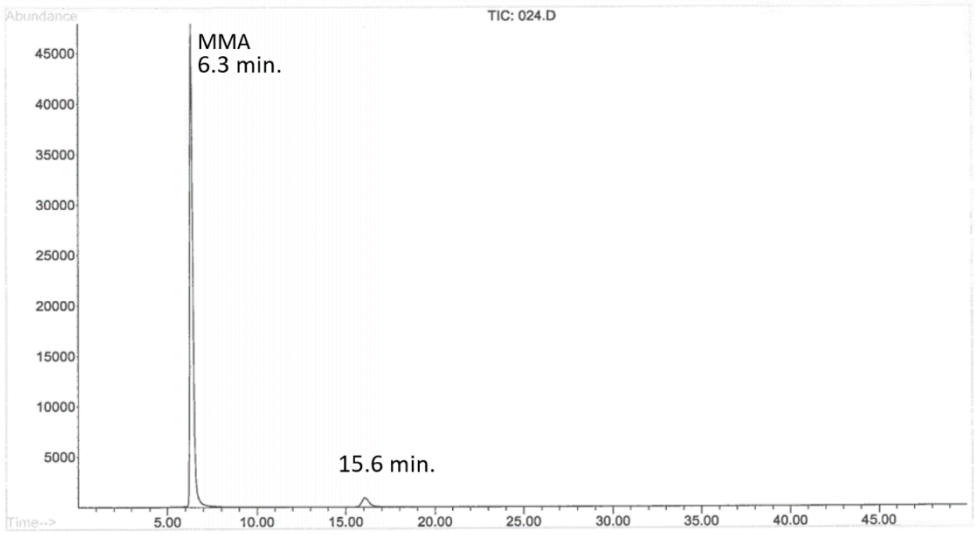
Abundance
TIC: 024.D
MMA
6.3 min.
45000
40000
35000
30000
25000
20000
15000
10000
5000
15.6 min.
Time-->
5.00
10.00
15.00
20.00
25.00
30.00
35.00
40.00
45.00

C.

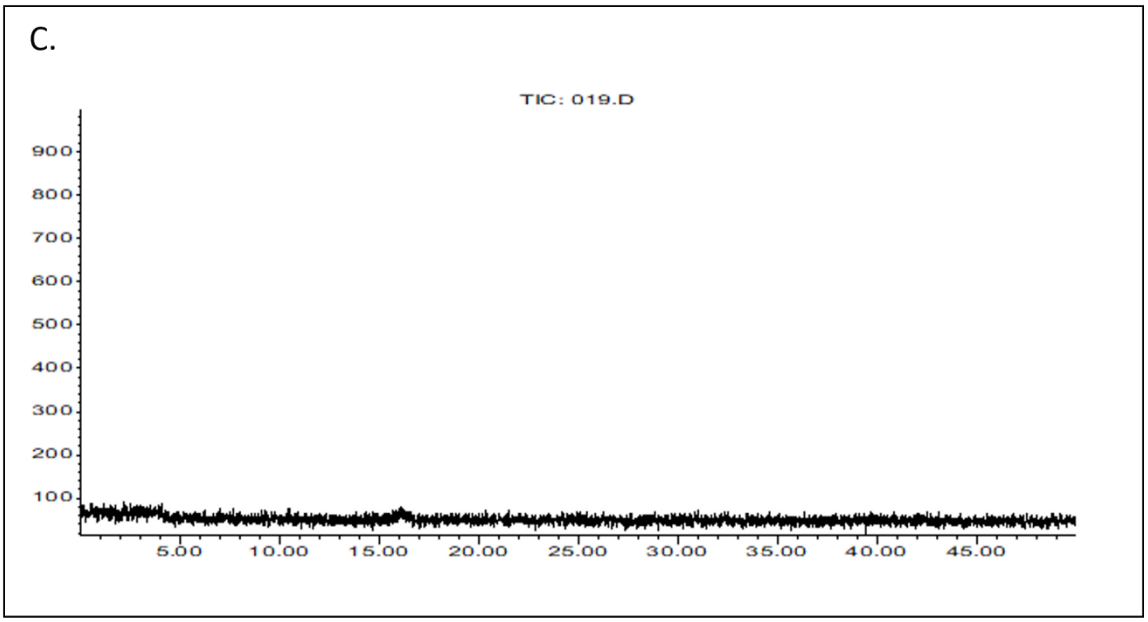
TIC: 019.D
900
800
700
600
500
400
300
200
100
5.00
10.00
15.00
20.00
25.00
30.00
35.00
40.00
45.00

D.

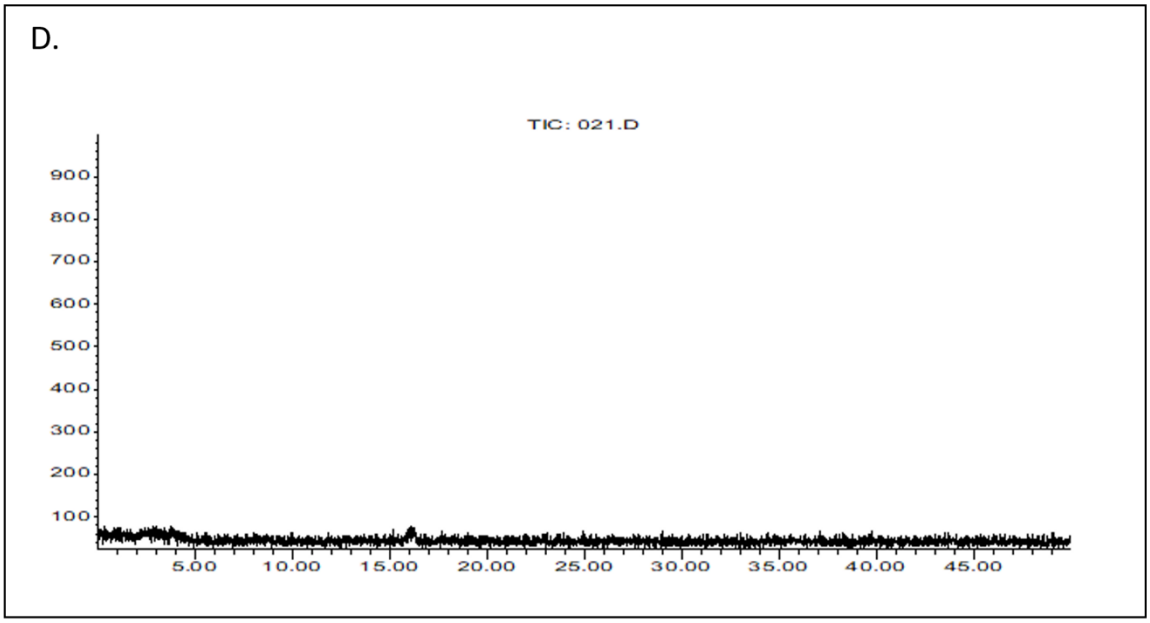
TIC: 021.D
900
800
700
600
500
400
300
200
100
5.00
10.00
15.00
20.00
25.00
30.00
35.00
40.00
45.00

Figure A.3.2. Chromatograms of speciation controls. Chromatograms generated using methods described in section 2.2.11 are shown with retention times of peaks in minutes labelled. A) Fresh HEK293 growth medium, untreated with arsenic, and unused for cell culture. B) The same fresh medium as in (A), but with the same MMA^V used to treat cells added to the medium. C) The same medium as in (A), but after growing HEK-V cells in arsenic-free conditions. D) The same medium as in (A), but after growing HEK-ABCC1 cells in arsenic-free conditions.

A.

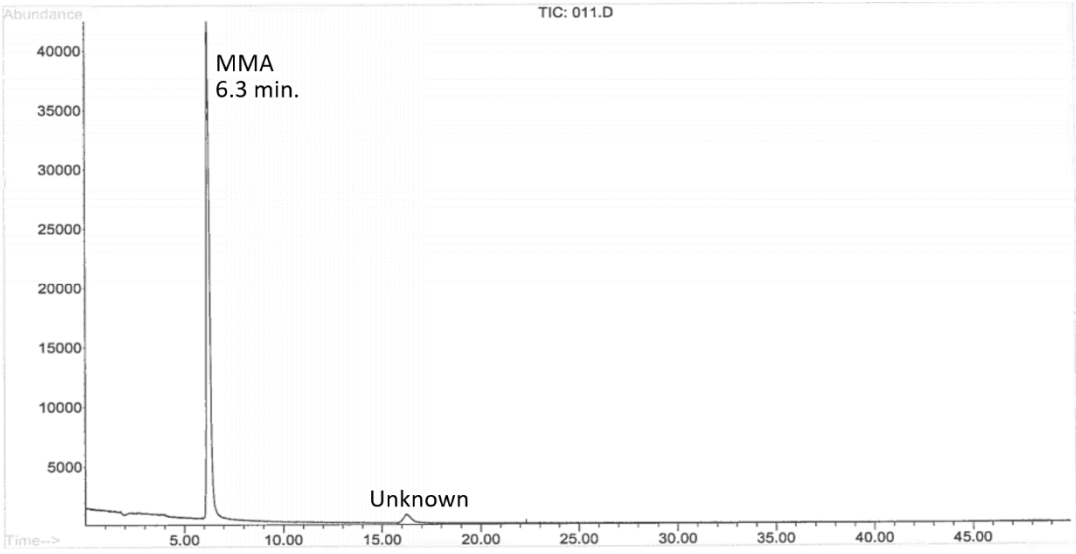
TIC: 011.D
Abundance
40000
35000
30000
25000
20000
15000
10000
5000
MMA
6.3 min.
Unknown
Time-->
5.00
10.00
15.00
20.00
25.00
30.00
35.00
40.00
45.00

B.

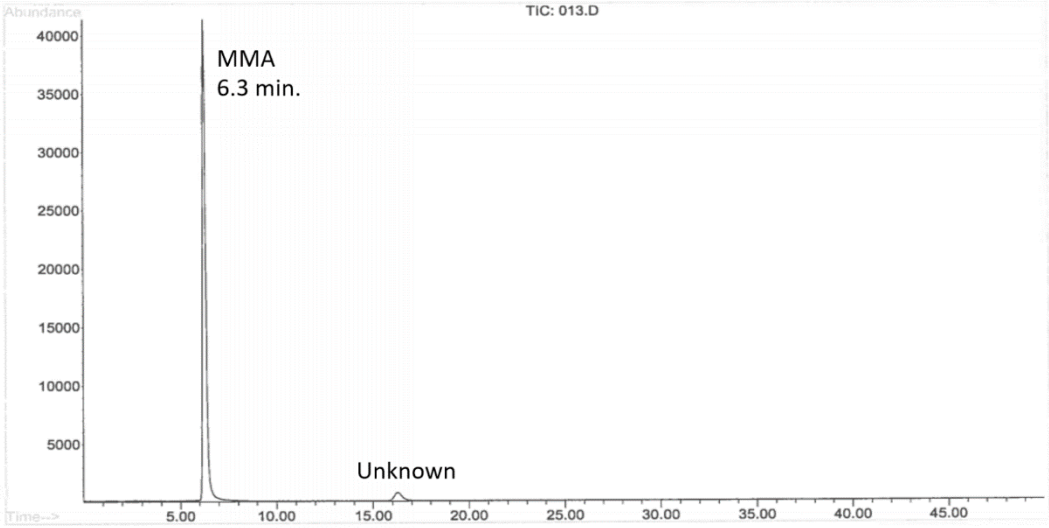
TIC: 013.D
Abundance
40000
35000
30000
25000
20000
15000
10000
5000
MMA
6.3 min.
Unknown
Time-->
5.00
10.00
15.00
20.00
25.00
30.00
35.00
40.00
45.00

C.

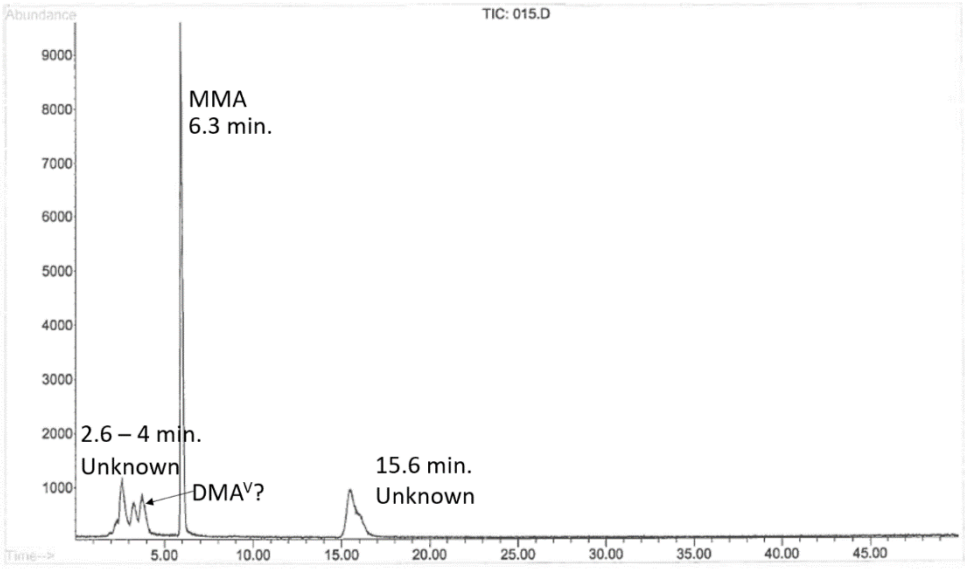
TIC: 015.D
Abundance
9000
8000
7000
6000
5000
4000
3000
2000
1000
MMA
6.3 min.
2.6 – 4 min.
Unknown
DMA^{V}?
15.6 min.
Unknown
Time-->
5.00
10.00
15.00
20.00
25.00
30.00
35.00
40.00
45.00

D.

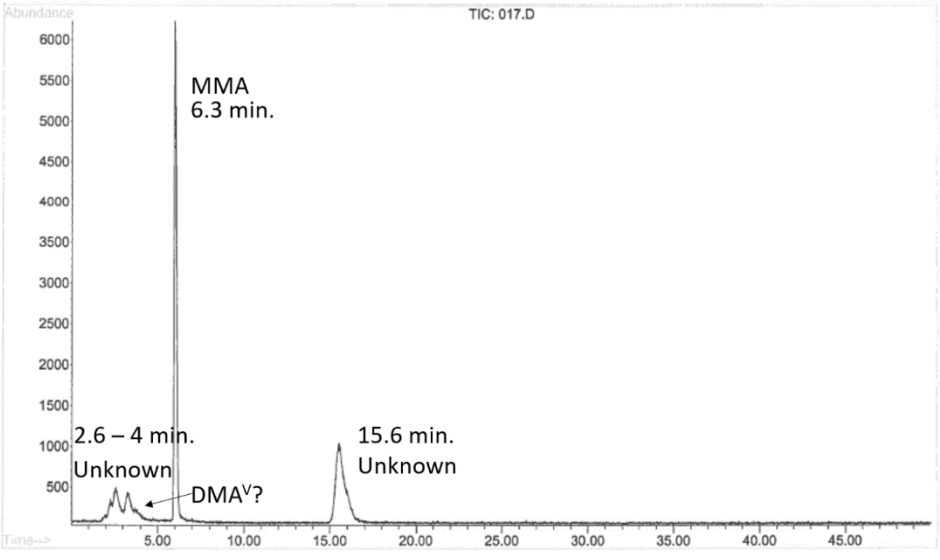
TIC: 017.D
Abundance
6000
5500
5000
4500
4000
3500
3000
2500
2000
1500
1000
500
MMA
6.3 min.
2.6 – 4 min.
Unknown
DMA^{V}?
15.6 min.
Unknown
Time-->
5.00
10.00
15.00
20.00
25.00
30.00
35.00
40.00
45.00

Figure A.3.3. Chromatograms of media from HEK293 cells exposed to MMA^V. A) Medium from HEK-V cells grown in the presence of 200 μM MMA^V for 24 hours. B) Medium from HEK-ABCC1 cells grown in the presence of 200 μM MMA^V for 24 hours. C) HEK-V cells as in (A) were washed and then fresh medium was added for 2 hours and then collected and analyzed. D) HEK-ABCC1 cells as in (B) were washed and then fresh medium was added for 2 hours and then collected and analyzed.